NIST GCR 99-778

EVALUATION OF THE HDR FIRE TEST DATA AND ACCOMPANYING COMPUTATIONAL ACTIVITIES WITH CONCLUSIONS FROM PRESENT CODE CAPABILITIES. VOLUME 3: TEST SERIES DESCRIPTION AND CFAST VALIDATION FOR HDR T51 WOOD CRIB FIRE TEST SERIES

Jason Floyd and Lothar Wolf
Department of Materials and Nuclear Engineering
University of Maryland
College Park, MD 20742

United States Department of Commerce
Technology Administration
National Institute of Standards and Technology

NIST GCR 99-778

EVALUATION OF THE HDR FIRE TEST DATA AND ACCOMPANYING COMPUTATIONAL ACTIVITIES WITH CONCLUSION FROM PRESENT CODE CAPABILITIES. VOLUME 3: TEST SERIES DESCRIPTION AND CFAST VALIDATION FOR HDR T51 WOOD CRIB FIRE TEST SERIES

Prepared for
U.S. Department of Commerce
Building and Fire Research Laboratory
National Institute of Standards and Technology
Gaithersburg, MD 20899

By
Jason Floyd and Lothar Wolf
Department of Materials and Nuclear Engineering
University of Maryland
College Park, MD 20742

July 1999
Issued September 1999

Notice

This report was prepared for the Building and Fire Research Laboratory of the National Institute of Standards and Technology under Contract number 60NANB6D0127. The statement and conclusions contained in this report are those of the authors and do not necessarily reflect the views of the National Institute of Standards and Technology or the Building and Fire Research Laboratory.

Evaluation of the HDR Fire Test Data and Accompanying Computational Activities with Conclusions from Present Code Capabilities

NIST CONTRACT 60NANB6D0127

Volume 3:

Test Series Description and
CFAST Validation for

HDR T51 Wood Crib Fire Test Series

July 1998

Jason Floyd
Lothar Wolf

Nuclear Engineering Program
Department of Materials and Nuclear Engineering
University of Maryland at College Park

Evaluation of the HDR Fire Test Data and Accompanying Computational Activities with Conclusions from Present Code Capabilities

NIST CONTRACT 60NANB6D0127

Volume 2:

Test Series Description and

Nuclear Engineering Program
Department of Materials and Nuclear Engineering
University of Maryland at College Park

EXECUTIVE SUMMARY

Between 1984 and 1992 four major test series were performed in the HDR containment encompassing various fuels and three different axial positions in the high-rise, multi-level, multi-compartment facility. At that time, each HDR fire test series was accompanied by extensive efforts to evaluate the predictive capabilities of a variety of fire models and codes developed in different countries by both blind pre-test and open post-test computations. A quite large number of open issues remained in the area of fire computer code predictive qualities upon completion of the HDR program.

In the meantime, large progress has been made in improving and consolidating fire models and computer codes of all levels of simulations. This progress merits revisiting both experimental results and fire computer code validations. The results of the research efforts for this grant during FY 1997/98 are documented in this volume:

Volume 3: Test Series Description and CFAST Validation for HDR T51 Wood Crib Fire Test Series

Volume 3 by focusing on the HDR T51 wood crib fire experiments covers the following aspects:

- Section 1 provides an overall introduction to the HDR test facility and especially the containment building layout. It provides an overview of all four major HDR fire test groups utilizing a range of fire sources including: propane gas burners, wood cribs, liquid fuel pools and nozzle releases, and prototypical electrical cables. These fires have been set at three different axial elevations within the containment building under natural, forced, and combined ventilation conditions.
- Section 2 gives a detailed account for the compartment layouts for the wood crib experiments. It also lists all fuel and thermophysical material properties involved in the experimental setup.
- Section 3 describes the objectives, requirements, and functional principles of the instrumentation applied during the test series and documents the positions of all sensors used in both tabular and graphical forms.
- Section 4 briefly summarizes the common test procedure used for executing every experiment.
- Section 5 provides an overview of major experimental results of the wood crib tests in two subsections. First, selected transient histories are shown for temperatures, gas concentrations, and velocities in the different connected compartments, including the dome, for the three experiments spanning the range of gas fire powers examined. The second set of experimental results involves the maximum values of the same quantities as a function of the applied fire power.
- Section 6 addresses numerous aspects of potential contributions of the wood crib experiments towards the validation of zone model codes such as CFAST (see Volume 2) and containment system codes such as GOTHIC.
- Section 7 describes the CFAST model developed for the wood crib tests.
- Section 8 discusses the results of computations using the CFAST model described in section 7 for each of the three wood crib tests.

- Section 9 addresses the accomplishments achieved and deficiencies experienced with CFAST while modeling the wood crib tests.
- Appendix A contains the CFAST input files for the model discussed in Section 7.
- Appendix B contains a discussion of the spurious results that are obtained when trying to implement the CFAST O2 card while defining the fuel in an input file..

ACKNOWLEDGMENTS

The work performed in this grant was performed under the auspices of the Building and Fire Research Laboratory at the National Institute of Standards and Technology. It was funded by the Department of Commerce during FY 97/98.

The program was monitored at NIST by Dr. Kevin McGrattan whose continued interest in and support of this work is greatly appreciated.

Also, we would like to thank Dr. Walter Jones, Dr. Richard Peacock, and Dr. Glenn Forney in support of the validation efforts documented in Volume 3 of this report.

TABLE OF CONTENTS

TABLE OF CONTENTS (CONT.)

LIST OF FIGURES

LIST OF FIGURES (CONTINUED)

LIST OF FIGURES (CONTINUED)

LIST OF TABLES

1 INTRODUCTION

1.1 HDR Test Facility and Containment Building

The HDR (Heiss-Dampf Reaktor) facility, shown in Figure 1.1, was the containment building for a decommissioned, experimental reactor in Germany. The building, while smaller in volume than a typical US containment building, contained many features which made it valuable for use in a containment research program. Many of these features also make it extremely valuable as a generic source of test data for industrial facilities. The building was a cylinder approximately 20 m in diameter by 50 m in height topped by a 10 m radius hemispherical dome for a total facility height of 60 m.. Internally the building was divided into eight levels with each level further subdivided into smaller compartments. For a typical HDR test approximately 60-70 compartments were available. Compartments were connected by a variety of flow paths which included doorways, pipe runs, cable trays, hatches, and staircases. Three fixed and two adjustable vertical channels were provided for in the form of an elevator shaft, two staircases, and two sets of equipment hatches running the axial length of the building which could be opened or closed to change the available vertical flow path at each level. Much of the original equipment from the nuclear steam supply system was still present in the facility including the reactor vessel, primary and secondary piping, pumps, electrical connections, and ventilation and exhaust systems. The total free volume of the facility was 11,000 m^3 of which the dome contained 4,800 m^3 above the operating deck. The HDR containment, its compartments, and internal structural materials, vent flow openings and other pertinent data are documented in [1].

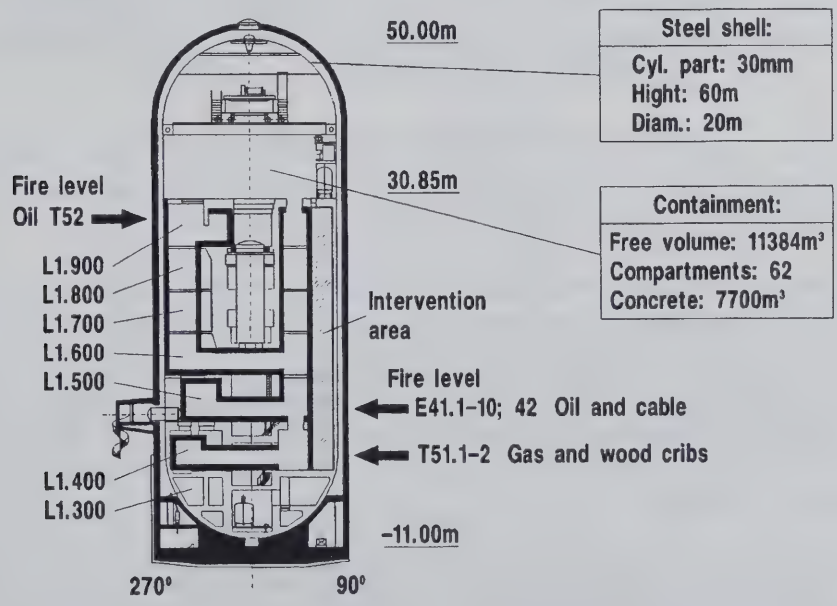

Figure 1.1: HDR Facility and Fire Test Group Locations

1.2 Summary of Fire Test Matrix

From 1984 to 1991 a total of four test series divided into seven fire test groups were performed inside the HDR facility. The fire tests consisted of the T51 series, six propane gas tests, three wood crib tests, and five more propane gas tests; the T52 series, four hydrocarbon oil pool tests; the E41 series, ten hydrocarbon oil pool tests; and the E42 series, three cable fire tests. Figure 1.2 shows the overall test matrix and range of fires powers tested and Figure 1.1 shows the location of the various test series inside the HDR facility. Each test series was performed at a different location inside the containment building as indicated.

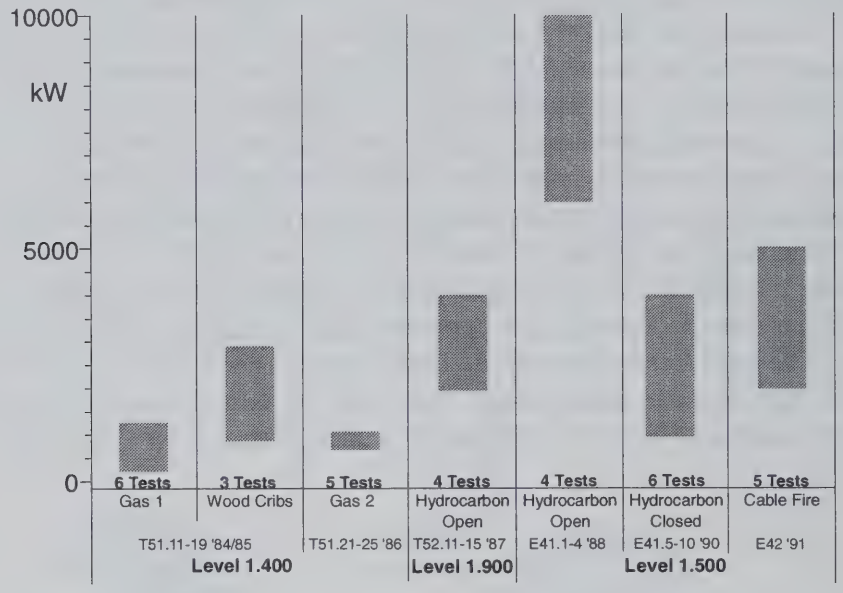

Figure 1.2: Fire Test Group Summary

The fire tests were performed with the following general objectives:

- An improvement in the general understanding of fire phenomena including smoke and aerosol production, distribution, and removal; temperature and pressure changes; and transient combustion in a large scale building.
- A better understanding of the effects of boundary conditions on fire phenomena.
- The creation of a large database for fire model and fire computer code validation.
- An increase in the ability to plan for successful fire fighting and rescue operations inside a burning high-rise structure.

The multi-level, multi-compartment structure of the HDR facility with its vertical shafts, large dome, and concrete and steel construction means that subsets of the fire test database have applications outside the nuclear industry. In general the fire test data can be used to gain insight on many industrial and commercial facilities as most share basic HDR features such as being a multilevel, steel and concrete structure with ventilation systems. More specifically, data from the large dome can be applied to hangars and atrium spaces. Data from the vertical shafts can be applied to any facility containing elevators, large vertical pipe channels, etc.

Each individual test series had its own specific objectives, which have been specified in the respective test series Design Report containing all pertinent geometric data, initial and boundary conditions, instrumentation plan, test procedures, and summary descriptions of the computer codes that participated in the pre-test and post-test computations. Data Reports were issued right after the experiments were performed and contained corrections/modifications of test procedures, qualification of the sensor operability and quality as well as all measured data in plots. All documented data have been stored on the PHDR data bank with the same format and sensor descriptions as used in all other HDR safety research experiments. Quick Look reports present and interpret the data according to the test series objectives and the associated physical phenomena. In addition to the presentation of the data of the individual experiments, results across the test series are documented. Moreover, Quick Look reports contain the comparisons between data and blind pre-test computational results by different models and codes used by the respective group of national and international participants. The Final Evaluation report documents all data assessments from the test series together with final conclusions and open issues. In addition, it contains the comparisons between data and open post-test predictions and identifies the learning effect, model and code improvements observed, lists remaining discrepancies, and open modeling issues. It is the final document for the test series. Section 7 lists all relevant documentation cited above for the respective HDR fire test series. The respective reports will be referenced where applicable in Section 1.3, which summarizes the fire tests.

The T51 test series, performed at the 1.400 level in the lower portion of the containment, was designed to be a relatively low power, exploratory test series in order to determine basic parameters of fire phenomena inside the facility [2-10]. The temperature changes inside of the fire room and the spread of smoke through the building and building ventilation systems was examined to determine safety margins for future, higher powered tests.

The T52 test series, performed just below the operating deck, was designed to simulate a large cable fire through an equivalent oil fire [11-13]. The effects of ventilation systems on smoke movement was examined to assess rescue and fire fighting techniques. One major objective was to measure the plume behavior from the fire into the dome.

The E41 test series, performed in the level above the one for the T51 test series, incorporated experiments that spanned the total range of fire powers examined in the HDR facility [14-20]. Additional parameters examined during this fire test series were the effects of opening and closing doors to the fire room, filter loading rates, and the effects of fire suppression systems.

The final test series, E42, was performed at the same level as the E41 tests. The tests, consisting of cable fires, were to collect data on the burning of prototypical cables in cable trays under natural conditions [21-25]. The fires took place in an completely isolated set of subcompartments to prevent the spread of toxic combustion products, namely dioxin, resulting from the burning of the PVC insulation. A primary objective of these tests was to monitor the propagation of the fire through racks of cable trays in various orientations and to closely examine the spread and impact of combustion products.

Initially, the HDR fire tests were designed, performed, and evaluated solely by the Nuclear Center Kalrsruhe, German universities, industry, and research labs. However, the international nuclear community quickly realized the value of these tests [10]. Which resulted in international support, cooperation, and participation throughout much of the fire testing program at the HDR. Reflecting this is the fact that one of the E42 tests was selected to be a European Commission Standard Problem for the evaluation of computer fire models [24,25].

1.3 Overview of Individual Fire Test Series

With the large variety of fire experiments performed in the HDR over many years, it is important to see where any one particular set of tests fits into the overall database of information. To this end a brief description of each of the fire test groups follows.

1.3.1 Gas Fire Tests (T51.11-T51.15, T51.19, and T51.21-T51.25)

The gas fire tests, the T51 test series [2-10], were the first set of fire experiments performed in the HDR facility, and they are the subject of the remainder of this volume as well as volume 2 [26]. A total of 14 tests were executed between 1984 and 1985. These tests consisted of three subgroups of five gas fires, a single gas fire performed at the end of the wood crib test series [5], and five additional gas fires [6-8,10]. The tests all took place in a specially constructed fire room on the 1.400 level, shown in Figure 1.3, of the HDR facility. This fire room was connected to a hallway which terminated under a vertical shaft formed by open maintenance hatches. Each experiment followed a similar test plan of a short period of pre-fire data collection to record initial conditions, followed by an hour long fire, and ending with approximately half an hour of cool down data collection. The fuel for each of the test was propane gas intended to be premixed with 10% excess air drawn from a vent in room 1.603. For the first group of gas tests no ventilation systems other than the air supply for the gas burners was employed. For the second group of gas tests a vent was constructed which connected the fire room to the 1.600 level. The vent had an adjustable damper which could be controlled during an experiment to change the size of the vent opening.

This first test series had a number of primary objectives. The foremost objective was to demonstrate that fire tests could be performed safely inside the HDR containment building as the integrity of the structure was still regulated as a nuclear facility. Another objective was to determine the extent to which the fire would involve the building in its entirety. A further objective was to examine the ability of the ventilation systems to remove smoke and other fire products. Lastly, data collected during the tests would serve as a initial data for computer code evaluation.

The gas fire tests contain a number of characteristics which pose different of challenges for fire code models. These are:

- The fire room is not a rectangular parallelepiped. The floor cross-section is L-shaped as can be seen in Figure 2.1 of Section 2. This geometric irregularity acts to impede some of the mixing that would otherwise occur in a symmetric compartment.
- The fire source is not a single location on the floor in the center of the room. Rather, there are six gas burners mounted on the wall 0.375 m off the floor along the L-side of the rooms length. Therefor the fire cannot be truly considered a point or local area source for the purpose of evaluating mixing and entrainment using common zone model approaches. Also the presence of the wall that the burners are mounted on prevents the formation of a typical, axi-symmetric plume that is assumed in many fire models.
- The number and selection of burners used varied depending on fire power.
- The doorway of the fire room is located at a corner, rather than at the center of one of the room's walls. As with the shape of the room this affects the mixing that takes place inside the fire compartment.
- The hallway from the fire room terminates in a subcompartment with a narrow vent, 0.5 m high, along the floor and a ceiling vent to a shaft leading to the hemispherical dome. Therefore, a fire model must be capable of handling a large ground level airflow as well as a separate, large buoyant plume in the same compartment.
- The hallway from the fire room is not a rectangular parallelepiped. It is a volume of revolution, a rectangle slowly increasing in width rotated at a fixed distance about an axis.

Table 1.1 on the next page contains a brief summary of the major characteristics of the gas fire tests. Figure 1.3 shows a top view of the fire floor.

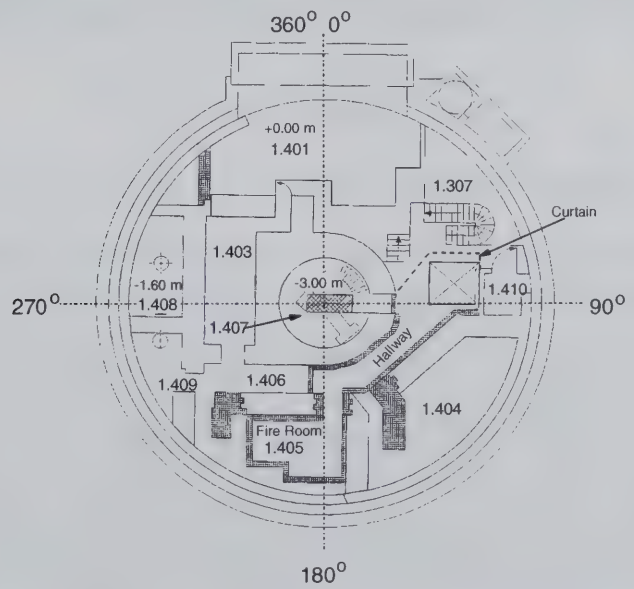

Figure 1.3: Level 1.400, Fire Floor for the T51 Tests

Table 1.1: Gas Fire Test Series Summary

Test	Fire Power (kW)	Gas Consumption (m^3)	Ventilation and Other Test Execution Comments	Burners Used
T51.11	229	8.82	All run with the same configuration with only fire power changing	Burner 3
T51.12	380	14.63		Burners 2,3
T51.13	692	26.62		Burners 2,3,4,5
T51.14	1,025	39.44		Burners 1,2,3,4,5
T51.15	380	14.62	T51.12 with closed vent between 1.600 and 1.700	Burners 2,3
T51.19	1,255	48.30	Increased number of sensors Uses Wood Crib sensor map	Burners 1,2,3,4,5
T51.21	716	27.55	Changes in sensor map Repeat of test T51.13 with vent to 1.600 closed	Burners 1,2,5,6
T51.22	715	27.55	30 minutes with vent 100% open 15 minutes with vent 75% open 15 minutes with vent 25% open	Burners 2,3,4,5
T51.23	1,011	38.98	Repeat of test T51.14 with vent to 1.600 closed	Burners 1,2,3,4,5
T51.24	951	36.58	30 minutes with vent 100% open 15 minutes with vent 75% open 15 minutes with vent 25% open	Burners 1,2,3,4,5
T51.25	985	37.91	30 minutes with vent 100% open 30 minutes with vent closed	Burners 1,2,3,4,5

1.3.2 Wood Crib Fire Tests (T51.16-T51.18)

The wood crib tests were part of the T51 series of experiments [5,8,9]. The wood crib tests, while not a fuel typically available in a nuclear power plant, were added for the benefit of the fire community which does use wood cribs as a standard fire load. Three separate tests of increasing fire power were executed. The tests took place in the same fire room as the gas fire tests. Each test consisted of burning one or more cribs made up of 30 cm x 4 cm x 4 cm beams of pine containing 8% humidity. The beams were nailed together into 15 layers of 4 beams each with adjacent layers having a 90° rotation of the beams, Figure 1.4 shows the construction of a wood crib. A 300 ml reservoir of mineral spirits was used to start the ignition of the wood cribs which were allowed to burn uncontrolled. Electronic scales underneath the wood cribs were used to determine the time-dependent burning rate for use as input functions for the computer code simulations. As compared to propane gas which burns relatively smokeless, these wood crib tests were performed with a main purpose of evaluating the response of the HDR facility and ventilation systems to heavy loadings of smoke in an effort to determine safety margins for

future oil fires. The wood crib fires lasted on the order of 30 minutes. Table 1.2 gives some additional details on the wood crib tests.

The wood crib tests produced large quantities of smoke which were quickly distributed throughout the whole containment. This smoke overloaded the building ventilation system's HEPA filters and resulted in adjusting the testing schedule to accommodate the longer time required to clean the containment atmosphere between tests. The smoke was corrosive to the test equipment of other experiments, and some instrumentation was damaged. The smoke deposits of the HDR surfaces also proved difficult to remove, with success only occurring in cleaning of metal surfaces.

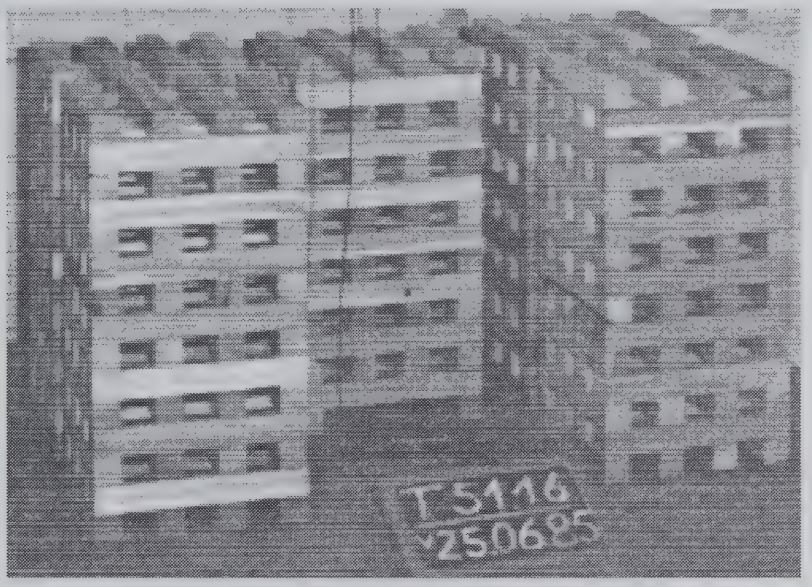

Figure 1.4: Wood Crib Construction

Table 1.2: Wood Crib Fire Test Series Summary

Test	Fire Power (kW)	Wood Consumption (kg)	Ventilation and Other Test Execution Comments
T51.16	1,000	79 (5 cribs)	Start of Wood Crib sensor map. Fires were naturally ventilated and natural convection conditions existed in the containment.
T51.17	1,500	109.8 (7 cribs)	Increase in fire load.
T51.18	2,300	169.1 (11 cribs)	Further increase in fire load.

1.3.3 Oil Fire Test Summary (T52)

The second test series of fire experiments was the T52 oil fire test series which consisted of four oil pool fire tests performed in 1986 [10-14]. The tests ranged in power from two to four megawatts with the fire lasting approximately 30 minutes. Whereas the previous test series, the gas and wood fires, were performed at a level low in the containment building it was decided to position this test series high up in the containment building as shown in Figure 1.1. Thus, the fires were positioned in a special fire compartment constructed on the 1.900 level, the level just below the operating deck. It was anticipated that this would confine smoke and soot to the dome region. The fire compartment, shown in Figure 1.5, was located such that it vented directly into the dome through the maintenance hatch next to the spiral staircase. Fuel for the fires consisted of an initial volume of oil in a pool with a surface area ranging from 1 m^2 to 3 m^2 in size.

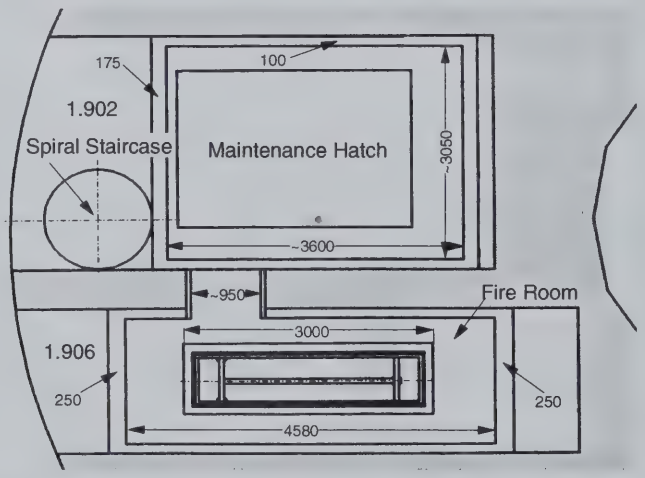

Figure 1.5: T52 Oil Fire Compartment

The initial amount of fuel was augmented by a nozzle feeding a continuous supply of oil once the initial pool was consumed. Each fire lasted approximately 30 minutes. Oxygen for the fires was supplied either by natural convection alone or a combination of forced and natural convection.

For this test series special attention was paid to the buoyant fire plume entering the upper dome. Two-dimensional grids of thermocouples and other sensors were placed at two axial levels within the plume to aid in determining the plume's evolution in the dome.

In addition to the generic purposes of improvements in knowledge about fire dynamics in a complex structure this test series introduced the concept of selective pressurization of test compartments for the prevention of smoke entry in rescue/intervetion areas. For this test series the elevator shaft next to the main staircase, see Figure 1.1, was pressurized and monitored to determine if selective pressurization was indeed capable of maintaining the entire shaft as a relatively smoke free area for the purpose of evacuation or for the staging of emergency personnel.

Some of the significant results are noted below:

- The fires quickly reached flashover conditions, turning the fire room into a large fire ball with heavy soot production.
- As the fire vented directly into the upper dome a large buoyant plume formed whose basic characteristics were measured.
- The large buoyancy forces of the plume rising through the maintenance hatch behaved like a jet pump; that is large quantities of air were entrained into the plume which resulted in a large global circulation inside of the entire facility which widely spread the soot throughout the whole building.
- Provided a sufficient air flow rate was used, the selective pressurization strategy was successful in keeping the elevator shaft free of smoke.
- Due to the high entrainment, fire plume temperatures impinging on the containment steel shell were rather low.

Table 1.3 below summarizes some details on the T52 tests.

Table 1.3: T52 Oil Fire Test Series Summary

Test	Peak Fire Power (kW)	Pool Size (m^2)	Initial Fuel Volume (liters)	Fuel Delivery Rate (liter/min)
T52.11	2,000	1	25	3.72
T52.12	3,000	1	50	5.57
T52.13	4,000	3	75	7.43
T52.14	3,500	3	50	5.57

1.3.4 Oil Fire Test Summary (E41)

The T52 test group indicated that both higher power and longer duration tests could be withstood by the HDR facility. A further set of oil fires, the E41 test group [14-20], was performed to take advantage of this. This test group, which consisted of ten tests ranging in power from six to ten megawatts, took place on the 1.500 level of the containment building. As with the other test groups a specially prepared fire compartment was used for this series. This compartment, shown in Figure 1.6, was significantly larger than compartments for the other tests and included sprinkler systems, ventilation systems, and a remotely operated doorway. For this test series the building ventilation systems were equipped with different types of filter setups. Furthermore, autonomous, aerosol measurement devices were added to the sensor equipment.

The addition of extra features to the fire room and ventilation system allowed the examination of some additional fire phenomena. Filter loading and clogging was examined through the use of the different filter systems. The effects of steam release into the fire room was examined. The interrelationships of doorway openings and mechanical ventilation were explored. The selective pressurization strategy was examined further. Tables 1.4 and 1.5 provide details on this test group. Note that each test in the latter portion of this test series actually consists of a series of individual subtests.

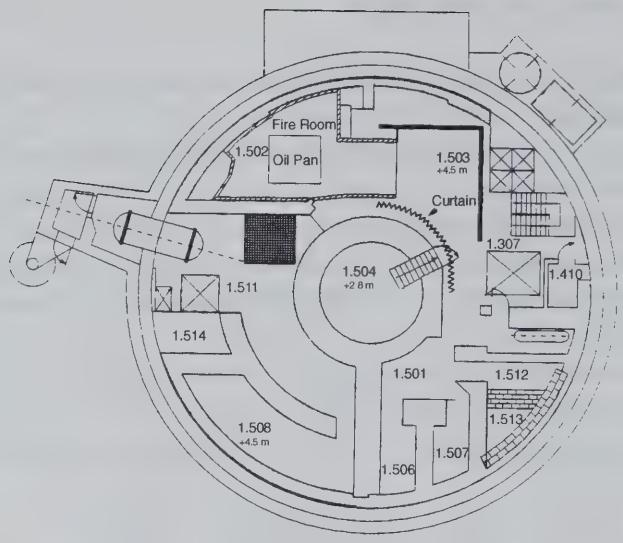

Figure 1.6: E41 Oil Fire Compartment

Some of the significant results of this test group are given below:

- Fire extinguishing systems were tested under extreme conditions of fire power and temperature due to the high fire powers, as high as 10 MW, in the fire compartment.
- Spatial and temporal distributions of aerosols were measured at different locations.
- Depending on the ventilation system settings a variety of flow circulation modes were observed inside the containment building.
- Selective pressurization of the elevator shaft was again successful in preventing smoke from entering this rescue shaft.
- Filters continued to become overloaded with soot even when a prefiltered bank consisting of coarse filters was added to the filtration system.

Table 1.4: E41.1-10 Oil Fire Test Series Summary

Test	Pool Size (m^2) and Pool Wall Material	Fuel Volume* (l)	Max Power (kW)	Fire Duration (min)
E41.1	3 (steel)	224	7,055	17
E41.2	2 (steel)	150	4,016	20
E41.3	2 (steel)	224	4,798	25
E41.4	2 (steel)	224	5,452	22
E41.5	2 (steel)	20	850	78
E41.6	2 (steel)	60	4,250	68
E41.7	2 (steel)	40	5,100	65
E41.8	2 (steel)	40	3,400	74
E41.9	1.7 (concrete)	48	4,250	43
E41.10	1.7 (concrete)	40	2,550	50

*For tests E41.5-10 the fuel volume represents the initial pool volume.

Table 1.5: E41.5-10 Oil Fire Test Subsection Summary

Test	Subsection	End Time (min)	Fuel Addition (kg/s)	Door
E41.5	E41.51a	5	Initial Volume	Closed
	E41.51b	20	0.01	Closed
	E41.52	35	0.01	Closed
	E41.53	50	0.02	Closed
	E41.54	65	0.05-0.07	Closed
	E41.55	90	0.07	Door 1,45°
E41.6	E41.61	15	Initial Volume	Closed
	E41.62	30	0.01	Door 1,45°
	E41.63	45	0.02	Door 1,45°
	E41.64	60	0.02	Door 1 Open
	E41.65	75	0.01	Both Open
	E41.66	80	None	Both Open
E41.7	E41.71	15	Initial Volume	Closed
	E41.72	30	0.1	Door 1 Open
	E41.73	45	0.02	Closed
	E41.74	60	0.1	Both Open
	E41.75	75	.03-.05	Door 1 Open
	E41.76	90	.03-.05	Door 1, 45°
E41.8	E41.81	15	Initial Volume	Both Open
	E41.82	30	0.1	Both Open
	E41.84	45	0.1	Door 1 Open
	E41.84	60	0.03-0.05	Door 1 Open
	E41.85	75	0.03-0.05	Door 1 Open
	E41.86	90	None	Closed
E41.9	E41.91	15	Initial Volume	Both Open
	E41.92	30	0.1	Both Open
	E41.93	45	0.1	Door 1 Open
	E41.94	60	0.05-0.07	Closed
	E41.95	75	0.01	Closed
	E41.96	90	None	Closed
E41.10	E41.101	15	Initial Volume	Closed
	E41.102	30	0.05	Door 1 Open
	E41.103	45	0.03	Closed
	E41.104	60	0.05	Door 1, 90°
	E41.105	75	0.05	Closed

1.3.5 Cable Fire Test Summary (E42)

The cable fire test group was the last set of fire experiments performed in the HDR and had the primary purpose of evaluating the effects of a prototypical fire using real fuel sources, e.g. the electric power and instrumentation cables used in power plants [21-25]. Due to concerns of dioxin production from the PVC cable insulation, this test group was performed in an isolated subset of compartments on the 1.500 level which is shown in Figure 1.7. Additional partitions and ventilation and fire extinguishing systems were constructed on this level to prevent the spread of toxic combustion products through the rest of the facility and into the local environment. Three tests involving different amounts and types of cables were performed. It is important to note that the fire compartments were completely sealed for the duration of this test series which created problems in determining the exact fuel source available or consumed during any given test. As shown in Figure 1.8, before the first test, E42.1, many of the cable trays were wrapped in Alsiflex mats in an attempt to prevent the combustion of those cables during the first test. Attempts were made to isolate specific cable trays from burning by covering some of the cable trays in Alsiflex blankets which could be removed for other tests. The blankets did not completely prevent combustion of the protected cables; that plus a lack of information on the fraction of exposed cables which completely burned results in an uncertainty in specifying the exact fuel source available and consumed during each test.

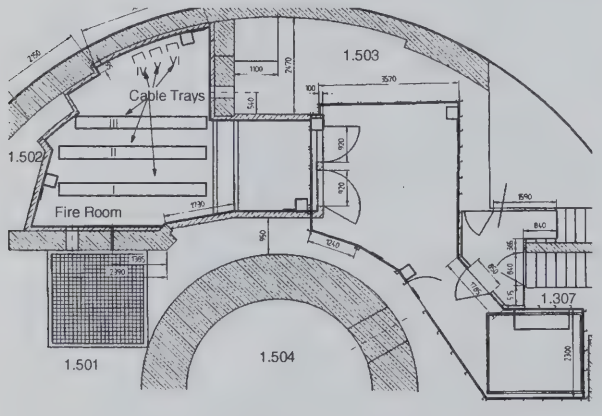

Figure 1.7: E42 Cable Fire Room

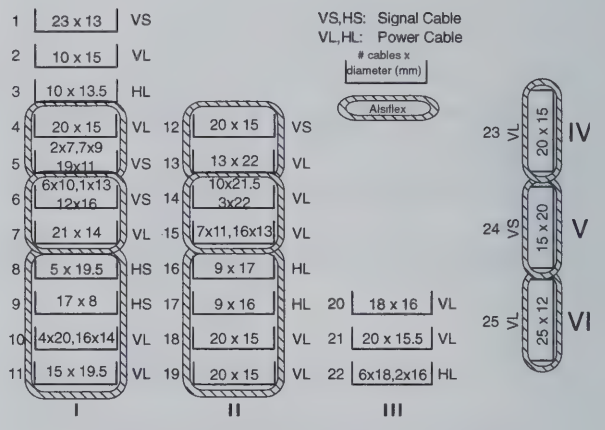

Figure 1.8: Cable Tray Layout

Some of the important results from the E42 test series are given below:

- Depending on the particular configuration of available cables the cables fires were either self sustaining to the point of flashover or burned out after a short period of time.
- Dioxin production from the PVC insulation was not detectable/measureable.
- The fires were capable of becoming intense enough to burn the cables underneath the Alsiflex blankets.
- The presence of the blankets actually acted to prolong fires as they prevented water from the sprinklers from reaching the cables under the blankets.

2 FACILITY DESCRIPTION

2.1 Compartment Layouts for the T51 Wood Fire Tests

2.1.1 Fire Floor (Level 1.400)

To avoid damaging the structure of the HDR facility, as the building was still considered a nuclear facility, a special set of fire test rooms was prepared at the 1.400 level of the containment building, see Figure 1.1 for the location of the 1.400 level. These rooms also served to control the flow of gases in and out of the fire room. Figure 2.1 shows a cross section view of the 1.400 level and indicates the location of these rooms which consisted of the fire room with a narrow doorway, a long hallway wrapping around the reactor vessel shield wall, and a curtained area centered beneath the maintenance hatch next to the main staircase. For the remainder of the facility no special precautions were undertaken with respect to insulation as gas temperatures outside the fire floor were anticipated to be below damage causing levels. Table 2.1 below gives the geometric data of the prepared compartments [2]. These compartments are the same compartments that were used for the gas fire tests T51.11-15, T51.19, and T51.21-25.

Table 2.1: Fire Compartment Dimensions

Compartment	Height (m)	Area (m2)	Volume (m3)	Doorway (m wide x m tall)	Hatch (m x m)
Fire Room	2.750	9.66	26.58	1.01x1.975	N/A
Doorway	1.975	1.51	2.99	1.01x1.975	N/A
Hallway	2.485	11.16	22.15	1.80x2.485	N/A
Curtained	5.350	11.83	63.29	7.40x0.50	2.3x2.0

The fire room, its vertical cross section through the 0-180° plane and horizontal cross section at the +0.0 m elevation are shown in Figure 2.2, was constructed inside of room 1.405. The floor, walls, and ceiling of the fire room were lined with 25 cm of Ytong fire brick. The ceiling, which would be exposed directly to the fire plume, had additional protection in the form of a 3 cm thick layer of Alsiflex fireproof matting. Alsiflex is a ceramic fabric. Due to damage from the first series of gas fire tests, T51.11-15, this layer was replaced before the start of the wood crib tests. The floor of room 1.405 below the Ytong fire bricks consisted of a 1 m thick layer of concrete coated with a 1.5 mm thick coating of paint. The wood cribs were placed in the larger open area just inside the fire room doorway, see Figure 2.2. The wood cribs were placed on top of a 0.281 m high platform in the manner indicated in Figure 2.2. Lastly, on the ceiling of the fire room, over the wood crib platform, a fire suppression steel pipe was installed. This pipe would inject coolant water to extinguish the wood crib fires in the event that unsafe conditions developed during a wood crib test.

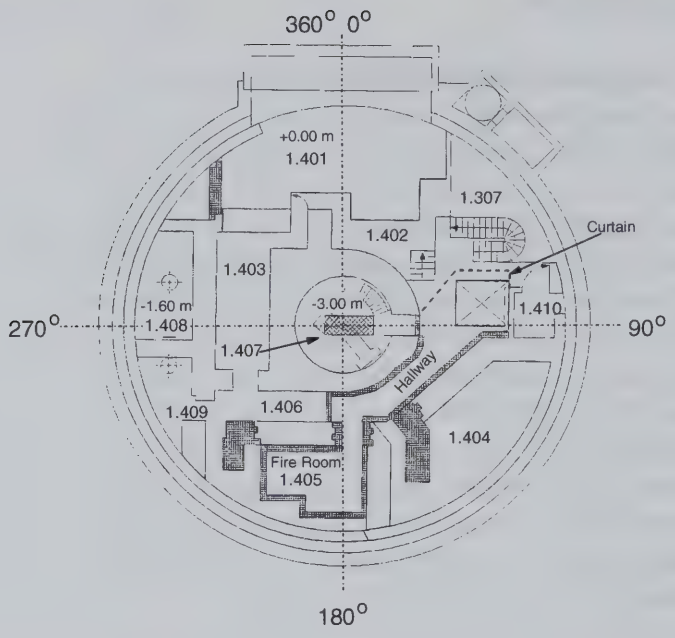

Figure 2.1: Fire Floor at Level 1.400 for T51 Wood Crib Tests

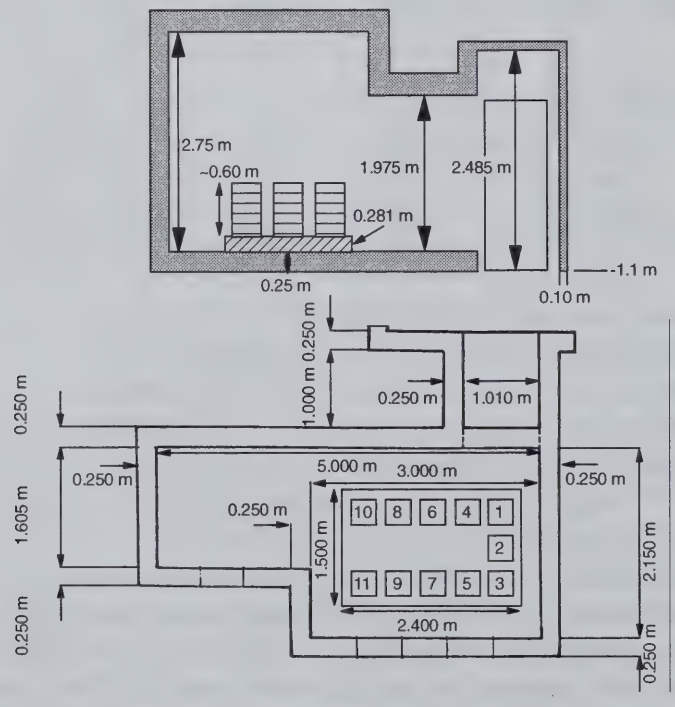

Figure 2.2: Fire Room and Doorway

The wood crib platform was designed to allow the measuring of the wood's combustion rate by the use of three digital scales. The platform consisted of a scale plate with three layers of insulation to protect the digital scales from the high temperatures of the fire. Two layers of Promalan HT 400 with an intermediate layer of Promasil 1060 where used to protect the surface

of the scale plate, see Figure 2.3. The sides of the platform were protected by a wall of Ytong firebrick. On the fire room floor beneath the scale plate, two flat coolers (0.800 m x 0.826 m) were installed for further protection of the scales, see Figure 2.4. These coolers were cooled by chilled water. The whole platform rested on top of three digital scales which were used to determine the burning rate.

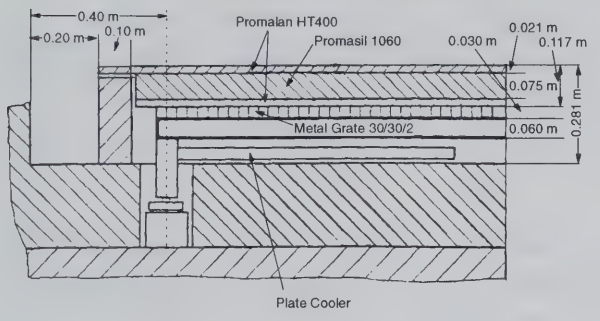

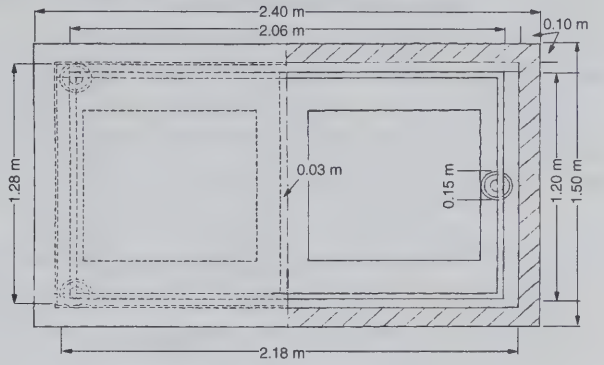

Figure 2.3: Wood Platform Cross-Sectional View **Figure 2.4: Wood Platform Top View**

The doorway to the fire room had the same construction as the fire room itself. The doorway's height was less than both that of the fire room and the hallway as depicted in Figure 2.2.

The hallway, its top view shown in Figure 2.5, was constructed inside of room 1.406. This compartment wrapped around the reactor vessel shield wall, thus, the walls along the length are not parallel planes, but instead are concentric arcs. The doorway from the fire room enters the hallway slightly offset from the end of the hall. The walls and ceiling of the hallway were constructed of a 10 cm thick layer of Ytong fire brick. The floor of the hallway was not insulated and was of the same concrete and paint as in the fire room. This results in the floor of the hallway being 25 cm below the floor of the fire room and doorway. The hallway had a constant ceiling height, and its width varied from 1.14 m at the door to the fire room to 1.8 m at the entrance to the curtained area. This variation results from the curvature of the hallway and the general layout of neighboring compartments as depicted in Figure 2.5..

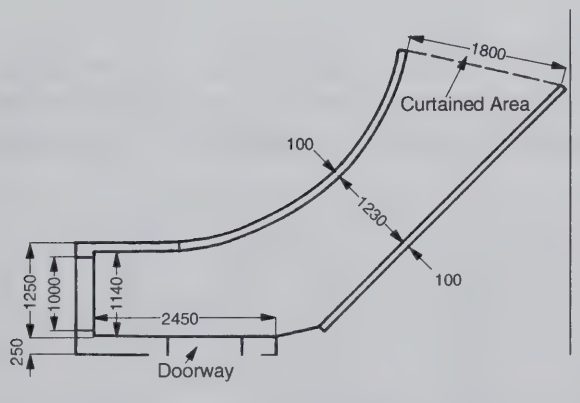

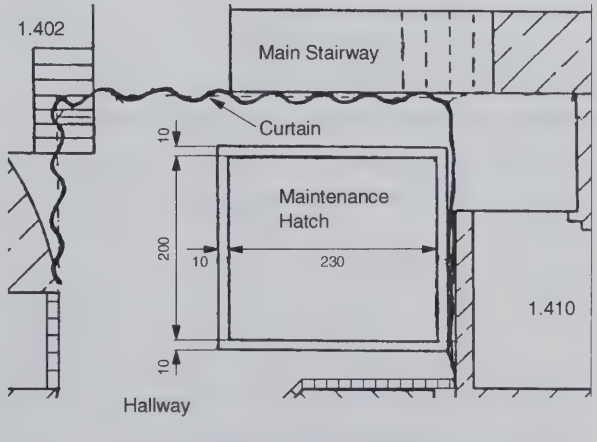

Figure 2.5: Fire Level Hallway **Figure 2.6: Curtained Area**

The curtained area, shown in Figure 2.6, was constructed next to the main staircase under an open maintenance hatch and was created primarily to force flue gasses from the fire away from the inside steel shell and up through the vertical shaft of the open maintenance hatches by buoyancy. This area was created by draping Alsiflex mats from the ceiling down to 0.5 m above the floor. This 0.5 m gap served to enhance the cold air return flow through the hallway to the fire room and to force a separation of the hot and cold gas streams. It is important to note that the gap below the curtain opened up towards both the main staircase and towards compartment 1.403 which had a floor elevation that was 1.1 m above the floor of the fire hallway or 0.6 m above the top edge of the gap beneath the curtain. The floor of the compartment below the hatch consisted of a 0.6 m thick layer of concrete protected by a 1.5 mm thick paint coating. The ceiling around the open maintenance hatch consisted of a 0.25 m thick layer of concrete protected with a 1.5 mm thick paint coating.

Figure 2.7 shows a perspective view of all the added enclosures indicating (1) the fire room, (2) the doorway, (3) the hallway, (4) the area inside the curtain, (5), the curtain, (6) the maintenance hatch, and (8) a window for viewing the fire with a video camera.

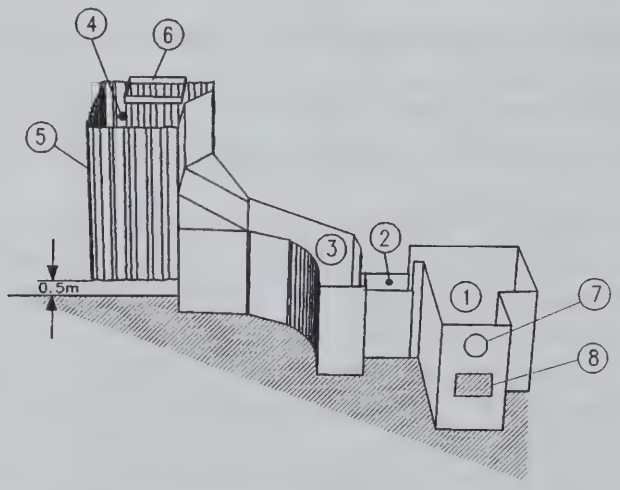

Figure 2.7: Perspective View of Level 1.400 Fire Compartments

2.1.2 Facility Remainder

The following two tables, Tables 2.2 [1,26-27] and 2.3 [1,26-28], document the volumes of the different compartments in the HDR facility as well as the sizes of the major room interconnections available during the gas fire tests. Details of the layout of the HDR compartments can be located on the instrumentation maps shown in Section 3.

Table 2.2: HDR Compartment Volumes

Compartment Number	Volume (m^3)	Elevation (m)	Height (m)	Comments
1.201	152	-8.50	1.80	
1.202 1.203 1.303	78	-9.20	5.80	Separate volume information not given for these compartments.
1.301	206	-5.80	5.30	
1.302	93	-5.80	3.60	
1.304	39	-5.80	3.60	
1.305 1.311	63	-4.80	4.60	Separate volume information not given for these compartments.
1.307	58	-5.80	4.10	Main staircase level 1.300
1.308	102	-5.80	3.60	
1.317	63	-1.10	5.45	Main staircase level 1.400
1.327	61	4.50	5.25	Main staircase level 1.500
1.337	40	10.00	4.80	Main staircase level 1.600
1.347	83	15.05	4.70	Main staircase level 1.700
1.357	40	20.60	4.65	Main staircase level 1.800
1.367	82	25.30	5.30	Main staircase level 1.900
1.401	296	0.00	4.10	Not open during wood crib tests.
1.402	40	0.00	3.50	No volume found, estimated from floor area.
1.403	76	-1.10	4.60	
1.404	116	-1.10	4.60	.
1.405	95	-1.10	4.60	Includes volume of fire room
1.406	266	-1.10	4.60	Includes volume of fire hallway and curtained area.
1.407	84	-3.00	5.00	
1.408	59	-1.60	4.60	
1.409	37	-1.10	4.60	
1.410	113	-2.60	39.90	Elevator shaft. Not open for T51
1.501 1.506 1.507 1.512	158	4.50	4.50	Separate volume information not given for these compartments.
1.502	107	4.50	4.50	
1.503	304	4.50	5.25	
1.504	57	2.80	3.40	
1.505	10	4.50	4.50	
1.508	57	4.50	4.50	
1.511	222	4.50	5.00	
1.513	8	3.50	8.80	Not open during wood crib tests.

Compartment Number	Volume (m^3)	Elevation (m)	Height (m)	Comments
1.514	13	4.50	5.00	
1.602	61	10.00	4.75	Not open during wood crib tests.
1.603	280	8.70	7.70	
1.604	25	10.00	3.25	
1.605	78	7.40	4.70	
1.606	183	10.00	4.60	
1.607 1.608	87	10.00	3.40	Separate volume information not given for these compartments.
1.609	59	10.00	4.75	Not open during wood crib tests.
1.611	192	10.00	4.75	
1.701u	64	13.85	3.90	
1.701o	44	20.60	2.50	
1.702	54	15.05	4.20	Not open during wood crib tests.
1.703	83	15.05	4.20	
1.704 1.901	805	14.25	15.60	Separate volume information not given for these compartments.
1.706	19	15.05	4.20	Not open during wood crib tests.
1.707	119	15.05	4.20	
1.708	90	15.05	5.35	
1.801	343	21.05	9.80	
1.802	125	20.60	7.10	
1.804	79	20.60	5.00	
1.805	58	20.60	5.00	
1.902	90	25.30	4.50	
1.903	71	25.30	4.50	
1.904 1.905 1.803	164	20.60	4.60	Separate volume information not given for these compartments.
1.906	62	25.30	4.50	
Lower Dome	2,153	30.85	9.15	Cylindrical portion of dome
Upper Dome	2,660	40.00	10.00	Hemispherical portion of dome

Table 2.3: HDR Room Interconnections for the T51 Wood Crib Fire Tests

Connects		Type	Width	Height	Depth	Comment	Connects		Type	Width	Height	Depth	Comment
Room 1	Room 2		(m)	(m)	(m)		Room 1	Room 2		(m)	(m)	(m)	
1.201	1.202	C	0.2	0.2	1		1.201	1.203	C	0.2	0.2	1	
1.201	1.308	P	1	0.5	0.82	2 of these	1.201	1.301	P	0.45		0.7	Width is diam.
1.201	1.301	P	0.35		0.8	Width is diam.	1.201	1.301	W	0.1	0.9	0.1	
1.202	1.302	P	0.28	0.51	4	Min. opening	1.203	1.305	P	0.28	0.56	4	Min. opening
1.301	1.302	W	0.1	0.15	0.5		1.301	1.302	P	0.3	1	11.9	Min. opening
1.301	1.302	P	0.1	0.4	5.2		1.301	1.303	P	0.5	0.5	1.2	2 of these
1.301	1.308	W	1.27	1.77	1.15		1.301	1.408	W	1.2	1	0.35	
1.302	1.308	B	0.1		0.5	Width is diam. 22 of these	1.302	1.308	D	0.66	1.97	0.6	Min. opening
1.302	1.408	P	1.1	0.6	0.54	2 of these	1.302	1.408	P	0.7	0.6	0.54	
1.302	1.408	P	1.3	0.6	0.54		1.302	1.409	B	0.13		0.6	Width is diam. 2 of these
1.302	1.502	P	0.93		5	Width is area (m^2)	1.303	1.308	B	0.1		1.29	Width is diam. 22 of these
1.303	1.308	D	1.9	0.96	1.02	Min. opening	1.303	1.407	P	0.9	0.55	0.81	Min. opening
1.303	1.407	P	0.3	1.45	0.8		1.304	1.305	P	0.32	0.54	0.4	
1.304	1.305	W	2.5	3.73	0.43		1.304	1.308	D	0.56	1.9	1	Min. opening
1.304	1.308	O	1.2	2	0.4	Min. opening	1.305	1.308	W	1.52	2	0.4	Min. opening
1.305	1.308	D	0.55	1.98	0.48	Min. opening	1.308	1.404	P	2.1	0.7	1.05	
1.307	1.317	S	1.8			Width is area (m^2)	1.402	1.403	D	0.54	1.82	2.8	Min. opening
1.403	1.406	W	0.5	1.21	1.05	1.4	1.403	1.406	P	1	1.2	2.18	
1.403	1.511	W	2.3	2.3	1	1.4	1.403	1.406	C	0.4	0.25	0.8	
1.404	1.507	0.07			1.05	Width is area (m^2)	1.405	1.406	W	2.72	1.9	1.05	
1.406	1.409	D	0.56	1.9	1		1.406	1.501	P	3.35			Width is area (m^2)
1.407	1.504	C	0.19		1.89	Width is diam. 6 of these	1.408	1.502	P	0.4	0.84	1	
1.317	1.327	S	3.61			Width is area (m^2)	Fire Room	Hallway	D	1.01	1.98	1.5	Fire room doorway
Hallway	Curtained Area	D	1.8	2.485			Curtained Area	1.501	M	4.54		0.57	Width is area (m^2)

Table 2.3: HDR Room Interconnections for the T51 Wood Crib Fire Tests (continued)

Connects		Type	Width (m)	Height (m)	Depth (m)	Comment	Connects		Type	Width (m)	Height (m)	Depth (m)	Comment
Room 1	Room 2						Room 1	Room 2					
Curtained Area	Main Staircase	O	4.3	0.5		Gap under curtain	Curtained Area	1.402	O	2	0.5		Gap under curtain
1.501	1.511	B	0.06		1.2	Width is diam.	1.501	1.606	P	2.55			Width is area (m^2)
1.502	1.503	B	0.08		0.5	Width is diam. 4 of these	1.502	1.503	D	0.5	1.95	1.58	Min. opening
1.502	1.511	B	0.08		0.5	Width is diam. 7 of these	1.502	1.511	C	0.47	0.42	0.5	
1.502	1.511	C	0.66	0.15	0.5		1.502	1.603	P	0.8	0.7	5	Min. opening
1.502	1.611	P	0.7	2.2	0.5		1.503	1.504	D	0.96	2	1.15	Min. opening
1.503	1.511	W	1.08	3.67			1.503	1.603	C	0.27		2.9	Width is diam.
1.503	1.605	C	0.27		2.9	Width is diam.	1.503	1.605	C	0.16			Width is area (m^2)
1.504	1.605	W	0.08		1.2	Width is area (m^2)	1.505	1.607	W	0.12		1.06	Width is area (m^2)
1.506	1.508	W	0.95	1.5	1.22		1.507	1.608	P	0.41	1	1.05	
1.508	1.511	D	0.55	1.92	0.1		1.501	1.606	M	4.54		0.57	Width is area (m^2)
1.511	1.611	C	0.14		0.57	Width is area (m^2) 2 of these	1.603	1.605	W	0.3	0.67	1.3	
1.327	1.337	S	3.2				1.603	1.606	D/S	1.6	0.69	2.8	Min. opening
1.603	1.606	W	5.5		1.2	Width is area (m^2)	1.603	1.608	W	0.6	0.47	1.2	
1.603	1.608	W	1	1	1.2		1.603	1.704	W	1.64		0.15	Width is area (m^2)
1.603	1.704	C	1.7	0.5	1.4		1.603	1.704	C	0.39	0.4	1.9	Min. opening 3 of these
1.603	1.704	W	1.8	2	4		1.605	1.606	C	0.3		2.3	Width is diam. 5 of these
1.603	1.708	O	2	1.64	1.2	Min. opening	1.605	1.701u	B	1.37		2	Width is area (m^2) 2 of these

Table 2.3: HDR Room Interconnections for the T51 Wood Crib Fire Tests (continued)

Connects		Type	Width	Height	Depth	Comment	Connects		Type	Width	Height	Depth	Comment
Room 1	Room 2		(m)	(m)	(m)		Room 1	Room 2		(m)	(m)	(m)	
1.606	1.704	P	0.5	0.5	3	Width is diam. 5 of these	1.606	1.707	P	3.58			Width is area (m^2)
1.606	1.707	M	4.54		0.5	Width is area (m^2)	1.606	1.708	M	4.81		0.6	Width is area (m^2) Spiral stair
1.606	1.708	S	0.74		0.42	Width is area (m^2) Spiral stair	1.607	1.704	P	0.5	0.5	1.06	
1.608	1.704	W	0.3	0.14	1.3		1.608	1.704	C	0.4	0.4	1.9	
1.611	1.703	C	0.25	1.74	0.56		1.337	1.347	S	3.39			Width is area (m^2)
1.701u	1.701o	W	1.7		3	Width is area (m^2)	1.701o	1.704	P	0.7	0.48	1.75	Min. opening 2 of these
1.701o	1.704	W	1.3	1.8	1.6	Min. opening	1.701o	1.704	B	0.52		1.75	Width is diam.
1.701o	1.704	C	0.6	0.6	1.6	2 of these	1.701o	1.707	B	0.3		3	Width is diam.
1.701o	1.804	C	0.4	0.6		Min. opening	1.701o	1.805	B	0.08		2	Width is area (m^2) 3 of these
1.703	1.707	D	0.84	2.01	0.28	Min. opening	1.704	1.707	D	2.09	0.62	2.37	Min. opening
1.704	1.804	P	0.79	0.6	2.27		1.704	1.805	B	0.25		1.24	Width is diam. 2 of these
1.704	1.901	W	0.8	0.6	0.8		1.704	1.903	W	1.64		0.15	Width is area (m^2)
1.704	1.904	B	0.55		1.25	Width is diam.	1.704	1.906	W	1.6		1.3	Width is area (m^2)
1.707	1.805	P	2.32			Width is area (m^2)	1.707	1.805	M	4.54		0.5	Width is area (m^2)
1.708	1.804	M	4.81		0.6	Width is area (m^2) Spiral stair	1.708	1.804	S	0.74		0.42	Width is area (m^2) Spiral stair
1.347	1.357	S	3.24			Width is area (m^2)	1.801	1.905	W	4.5			Width is area (m^2)
1.802	1.804	D	0.63	0.2	0.4		1.802	1.902	D	0.94	1.87	0.4	

Table 2.3: HDR Room Interconnections for the T51 Wood Crib Fire Tests (continued)

Connects		Type	Width (m)	Height (m)	Depth (m)	Comment	Connects		Type	Width (m)	Height (m)	Depth (m)	Comment
Room 1	Room 2						Room 1	Room 2					
1.802	1.902	W	0.4	0.23	0.4		1.802	Dome	W	0.4	1.2	1.52	
1.804	1.902	M	4.81		0.6	Width is area (m^2) Spiral stair	1.804	1.902	S	0.74		0.42	Width is area (m^2) Spiral stair
1.805	1.903	P	2.32			Width is area (m^2)	1.805	1.903	M	4.54		0.5	Width is area (m^2)
1.357	1.367	S	3.24			Width is area (m^2)	1.902	1.906	P	0.3	0.5	0.5	2 of these
1.902	Dome	W	0.4	0.2	0.4	2 of these	1.902	Dome	W	0.45	2.65	0.4	
1.902	Dome	M	4.81		0.6	Width is area (m^2) Spiral stair	1.902	Dome	S	2.06		0.42	Width is area (m^2) Spiral stair
1.903	Dome	P	2.32			Width is area (m^2)	1.903	Dome	M	4.54		0.5	Width is area (m^2)
1.906	Dome	C	0.2	1.3		Width is diam.	1.367	Dome	S	3.25			Width is area (m^2)

2.2 Thermophysical Material Properties

2.2.1 Thermophysical Wall Surfaces Properties

There were five different materials which were used as compartment surfaces within the HDR facility. Alsiflex mats and Ytong firebrick were used to create the fire room and hallway on the 1.400 level. In general, rooms in the HDR facility had painted concrete for the room surfaces with a different paint used for the floor than was used on the other room surfaces. Tables 2.4 and 2.5 provides the thermophysical properties for these materials [16,20,35]

Table 2.4 :Material Properties for Room Surfaces

Material	Density (kg/m^3)	Specific Heat (kJ/kg K)	Thermal Conductivity (W/m K)
Alsiflex Mats	130	1,000	See Table 2.5
HDR Concrete	2,225	879	2.10
HDR Floor Paint	1,540	1,280	0.29
HDR Wall Paint	1,250	1,550	0.20
Ytong Fire Brick	340	950	See Table 2.5

Table 2.5 :Thermal Conductivities for Room Surfaces

Material	Thermal Conductivity (W/m K)				
	100 °C	300 °C	500 °C	800 °C	1000 °C
Alsiflex Mats	0.05	0.05	0.10	0.18	0.25
Ytong Fire Brick	0.09	0.15	0.19	0.23	0.24

2.2.2 Thermophysical Fuel Properties

The fuel for this fire consisted of either five, seven, or eleven wood cribs constructed of pine with an initial humidity of 8%. Each crib had fifteen layers of four 30 cm x 4 cm x 4 cm boards. Each layer was nailed crosswise to the layer below it, see Figure 2.8. The lowest layer of the wood cribs contained only the two side boards. The cribs were arranged on the raised platform as indicated in Figure 2.9. The crib designated number 2 was the ignition point, by means of a metallic can filled with 300 ml of alcohol, which was manually ignited for each of the three wood crib tests. Posttest data analysis used a heat of combustion value of 12600 kJ/kg to determine the maximum fire powers achieved [10].

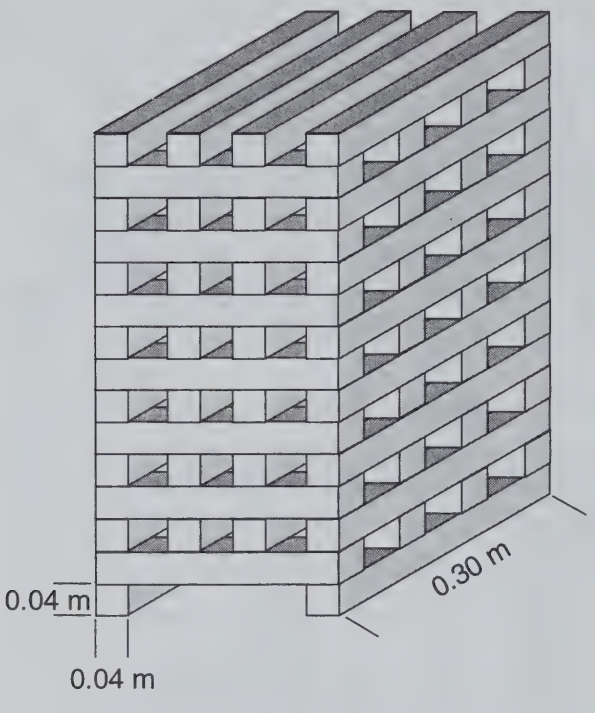

Figure 2.8: Wood Crib Construction

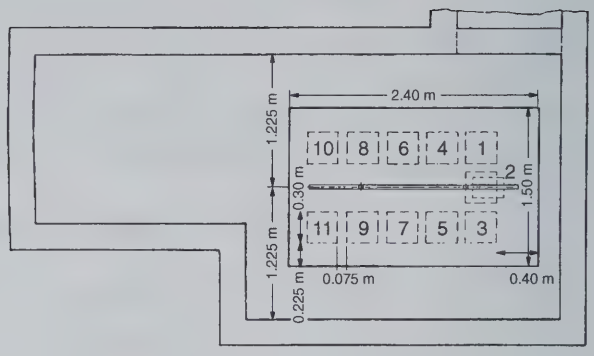

Figure 2.9: Wood Crib Placement

3 INSTRUMENTATION LAYOUT

3.1 Introduction

Because the fire research experiments were added to the HDR Safety Program about midway in the course of numerous safety experiments, the development of an instrumentation plan and the selection of the sensor types rested upon tested and proven measurement technologies. Most of these technologies were successfully applied during the previous HDR containment experiments. This proved to hold for the majority of typical pressure and temperature sensors. However, it was apparent from the outset that the fire experiments had somewhat different instrumentation criteria owing to the high temperature, low flow, and corrosive environment that the sensors would be exposed to.

Therefore, the T51.1 experiments opened up new challenges for the instrumentation, especially because all previous expertise resulted from high-momentum driven flows only. On the other hand, the fire experiments required reliable instrumentation for buoyancy driven flows with much lower velocities and much higher temperatures.

Given all these circumstances, test series T51.1 served as an exploratory test bed for advanced instrumentation such as velocity sensors, gas concentration sensors, smoke detection sensors, and other fire related sensors.
In addition to the sensor qualification issues, numerous questions arose regarding:

- safety procedures (injecting explosive gases in the building and the effects of high temperature loads on the structure)
- the optimal placement of a limited number of sensors and sensor types.

Answers and resolution guidance for both issues for all previous HDR experiments commonly rested on so-called design computations representing a broad spectrum of different approaches and models plus compliance with industrial codes and regulatory standards.

In the case of the T51 fire experiments, all analytical and computational methods at that time were limited to treat only single compartment, single burning object and single vent flow opening. The resultant predictions were naturally overly conservative because they did not account for multi-compartment geometry, counter-current flows of hot and cold gas streams and associated mixing as well as heat transfer to structures.

Therefore, safety measures and experimental procedures were extremely stringent and conservative, such as the installation of the curtain at the end of the hallway in order to keep the hot flue gas layer away from the inside surface of the containment steel shell.

Equally, the instrumentation plan for T51.1 was primarily geared towards safety rather than towards physical phenomena in the first place. These details should be kept in mind when reading the subjects about sensor types described in Section 3.3 and the instrumentation map described in Tables 3.1 with its accompanying figures of facility cross-sections and instrument positions.

3.2 Objectives and Requirements

With the background knowledge from the previous section, the instrumentation for the T51.1 wood crib tests was designed to encompass the following elements:

1. Instrumentation in the Fire Room:
   - 20 thermocouples in the fire room and door vent opening
   - 10 thermocouples at/in the structures
   - pressure sensor in the fire room
   - heat transfer instrumentation in the fire room and neighboring compartments
   - digital scales for measuring the combustion rate

2. Instrumentation in the Containment:
   - thermocouples and pressure sensor from previous containment blowdown experiments
   - several flue gas analysis sensors
   - heat transfer blocks from previous containment blowdown experiments
   - pitot tube sensors
   - determination of smoke density
   - miscellaneous special sensors as describe in Section 3.3

3. Instrumentation of Exhaust
   - thermocouples and velocity sensors

4. Safety Instrumentation for Protection of the Containment's Steel Shell Integrity
   - thermocouples along the height of the vertical staircase/maintenance shafts
   - thermocouples in the reactor dome above the operating deck
   - thermocouples at inside and outside steel surfaces
   - gas concentration sensors in the dome and lower containment regions

Whereas the instrumentation in the fire room needs to satisfy the special fire requirements, the rest of the containment instrumentation relied upon the available, proven containment measurement sensors. All data acquisition needs were accomplished by the central HDR computer and data acquisition storage system.

3.3 Instrumentation Descriptions

3.3.1 Temperature Measurement

NiCr-Ni, sheathed thermocouples were used for temperature measurements in accordance with German DIN 43710. The thermocouple sheath had a 3 mm diameter and an insulated tip. The signal wires did not require special treatment as long as they remained outside of the hot flue gasses. Depending on the thermocouples physical location in the facility, the signal wires were up to 20 m in length. As high frequency temperature changes were not anticipated, thermocouples with standard response characteristics were chosen; e.g. for temperature an error of ±1% of the measured value and for strong thermal radiation conditions an error of ±5%.

3.3.2 Pressure Measurement

Figure 3.1 shows schematically the major elements of determining the pressure difference with the TELEPERM measurement converter. The difference between containment inside and outside pressures acts on the bellow and is transmitted through a lever to the flexible beam tube which in turn transmits to a differential capacitor providing an analog signal. The TELEPERM converter works for a pressure difference of up to 5 mbar with a response time of 0.3 s and a measurement accuracy of ±1%. This device had to be protected from high temperatures; hence, its placement on Level 1.6 of the facility.

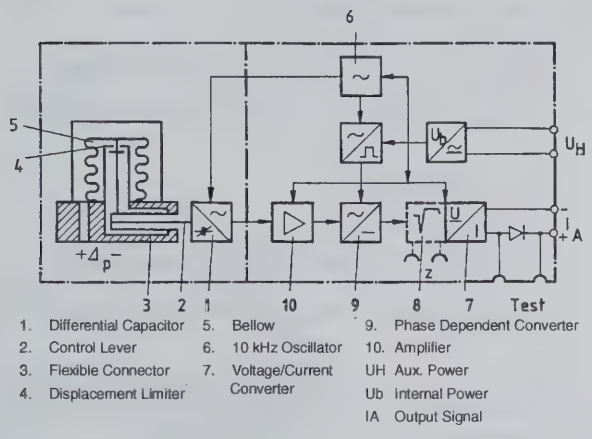

Figure 3.1: TELEPERM Transmitter

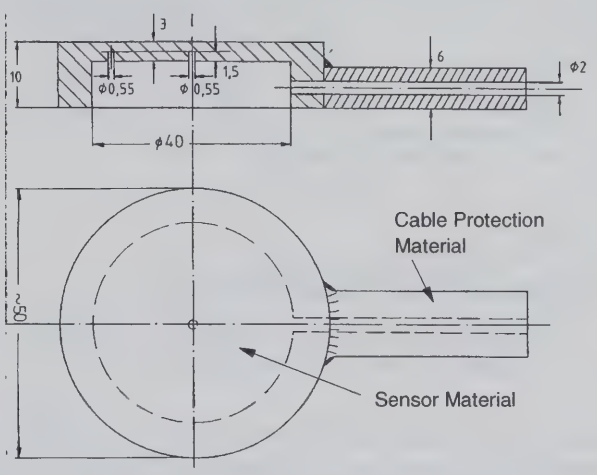

Figure 3.2: Local Heat Transfer Measurement

3.3.3 Heat Transfer Measurement

The local heat transfer at the containment steel shell was determined using the sensor depicted in Figure 3.2. The sensor used a 40 mm diameter annular control volume with a thin disk bottom of known material properties. Two NiCr-Ni sheathed thermocouples with a 0.5 diameter measured the disk temperature.

Additionally, large concrete blocks were devised and equipped with thermocouples as schematically shown in Figure 3.3. The type of concrete chosen was the same as used for the construction of the HDR containment Except for the front surface of the block all other surfaces were insulated. These massive concrete blocks were positioned at location where high convective flows, such as in the staircases, could be anticipated.

As the determination of the heat flux and subsequently the heat transfer coefficient at the measurement block's front surface rests on the solution of the inverse heat conduction problem, errors in these quantities became larger when temperature differences between thermocouples became smaller. Therefore, the expected accuracy of these blocks was only ±20%.

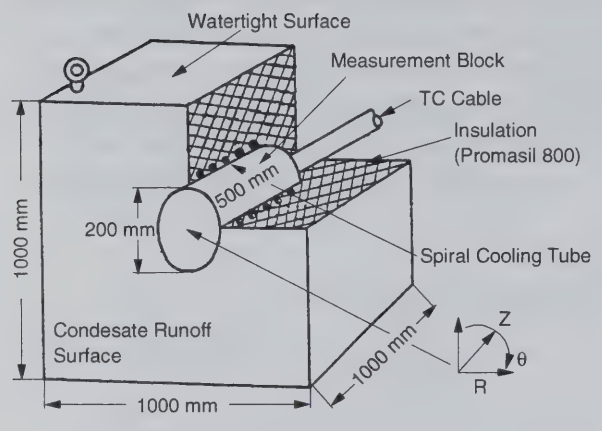

Figure 3.3: Heat Transfer Block

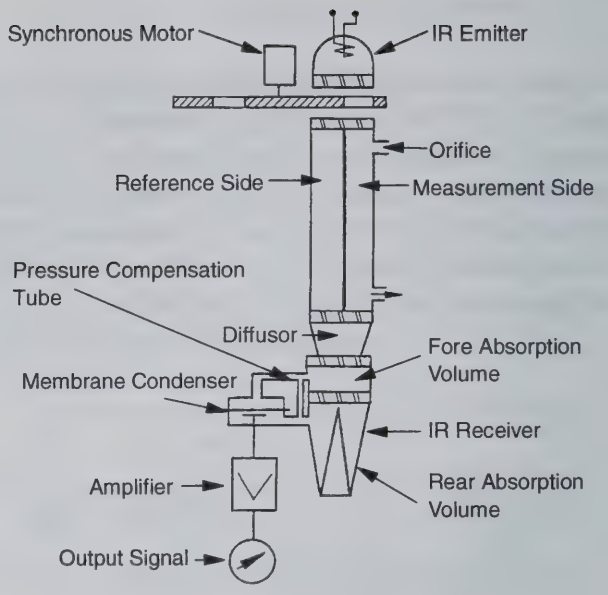

Figure 3.4: Gas Volume Analyzer

3.3.4 Smoke/Flue Gas Analysis

One of the major overall objectives of the HDR fire test series was the evaluation of the hazard potential to personnel, fire fighting, and rescue teams dependent on the type of burning substance, ventilating conditions, and fire location within the high-rise, containment building. Aside from direct exposure to heat, it is the smoke and flue gas mixture (O_2, CO, CO_2, C_nH_m, NO_x, SO_x) as well as the production of HCl and potentially dioxin in the case of burning PVC cables which determines the hazard level. Therefore, instrumentation measuring the concentrations of these individual components had to be in place. Fortunately, as the majority of the experiments of the T51 test series used non-sooting gas flames, the requirements for smoke and gas analysis largely reduced to measuring O_2, CO, and CO_2 concentrations.

Figure 3.4 shows a schematic of the non-dispersive infrared photometer which worked with a modulated, single beam. This instrument allowed for continuos operation using a suction pump in the range of 10-100 l/h volumetric flow. The device outputs a 0-10 VDC signal proportional to the volumetric concentration in terms of vol. % or ppm.

Prior to the start of each experiment, these sensors were calibrated with a calibration gas. The measurement accuracy of these sensors was expected to be ±2%.

3.3.5 Optical Smoke Density (Extinction Coefficient)

In order to follow the distribution and propagation of the flue gases inside the containment, an optical smoke densitometer, type ME82 made by Maurer, was positioned throughout the containment. A schematic of this sensor is shown in Figure 3.5, This sensor was used to determine the optical gas density in the rescue paths as well as the smoke density according to

German Standard DIN 4102 Pt. 1. The output from this device was converted to an extinction coefficient prior to data recording.

As shown in Figure 3.5, a standardized light source in accordance with DIN 5033 emits a beam of light which passes through a control volume containing the gas to be analyzed. The control volume size can be modified. The amount of light passing through the volume is converted to an analog signal from 0-10 VDC corresponding to 100-0% transmittance. The measured values had an accuracy of ±2%.

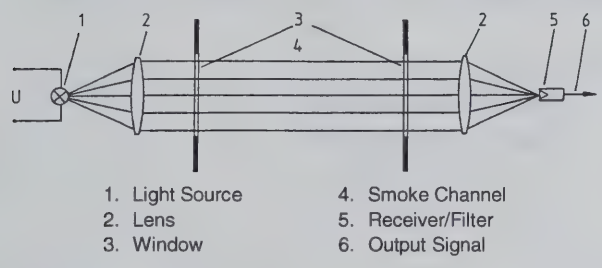

Figure 3.5: Smoke/Gas Density Sensor

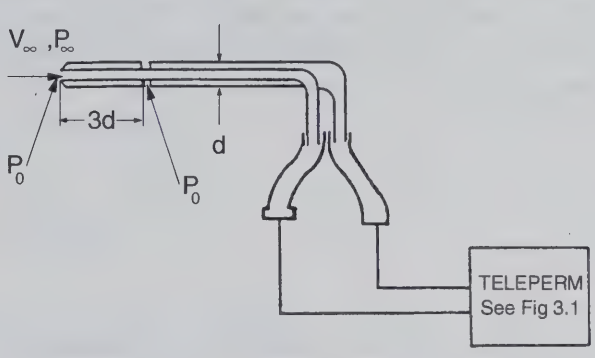

Figure 3.6: Pitot Tube Velocity Sensor

3.3.6 Velocity Measurement

In order to measure the flow velocities in different regions inside the containment, pitot tube type sensors, shown in Figure 3.6, were used. These sensors determine the pressure difference relative to stagnation pressure and use that to calculate the velocity. Hence, they used to same TELEPERM transmitter as discussed in Section 3.3.1, Figure 3.1. To obtain the velocity, the gas density must be measured simultaneously. For this purpose a thermocouple close to the pitot tube was used to determine density by application of the real gas law. The pitot tubes were capable of operating in temperatures as high as 800 °C. As before, the TELEPERM transmitter was shielded to protect it from high temperatures.

3.3.7 Video System

3.3.7.1 Introduction

The HDR facility was equipped with a color video system consisting of cameras, monitors, and tape machines. This system was used for monitoring the fire behavior in the fire compartments. The camera position for the T51 test series is shown in Figure 2.5.

In addition, a black and white video network consisting of 20 cameras with a switching board was installed. This system was developed by the Technical University of Karlsruhe, Germany, for use in monitoring the evacuation of personnel from high-rise buildings during fire exercises.

3.3.7.2 Black & White Video System Network

Figure 3.7 shows the black and white video network which was used to monitor smoke movement at up to 20 locations under low lighting conditions, 20 lux. The cameras are connected with 50 m long cables to a video switching board. This device switches to next camera after three half pictures are taken. With a camera frequency of 50 frames per second, the switching board could rotate through the cameras in 1.2 s. This results in a nearly simultaneous observation of the smoke throughout the building. The other elements shown in the Figure are self-explanatory. During test T51.18, the underventilated nature of the fire resulted in such high levels of smoke, that the video system optics quickly became coated in soot, rendering the test footage for T51.18 useless.

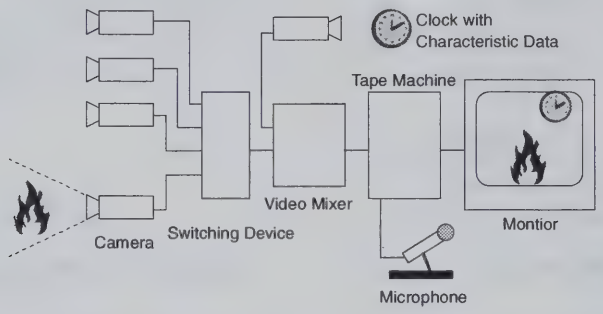

Figure 3.7: B&W Video System

3.3.8 Digital Scales

The wood crib platform was supported by three digital scales, see Figures 2.3 and 2.4 in Section 2.1. The scales were tared with the weight of the platform. Each of the three scales measured the force in Newtons exterted by the wood on the platform. To generate the burning rate the total of the three scales was taken and converted to kilograms of mass.

3.3.9 Safety Measures

In addition to the thermal insulations listed in Section 3.1, the measures described below were implemented for safety purposes:

- The color video system monitoring the fire compartment was continuously operated.
- A number of gas detectors were positioned at Levels 1.4 and 1.6 for safety reasons.
- All other containment regions including the steel shell were monitored with thermocouples.
- A fire suppression system was installed along the ceiling of the fire compartment.

3.4 Instrumentation Layout for T51 Wood Crib Tests

This subsection describes the instrumentation mapping for the T51 wood crib tests. A complete listing of all instruments as well as diagrams showing their locations within the facility are documented in the tables following. To aid in reading the tables and diagrams the following nomenclature, standard for all HDR tests, is used for the instrumentation:

CA:	Force Sensor
CF:	Velocity Sensor
CG:	Gas Concentration Sensor
CP:	Pressure
CQ:	Heat Transfer Measurement Block Sensor
CS:	Temperature Sensor
CT:	Temperature Sensor
CV:	Velocity Sensor
OA:	Steel Shell Expansion

In addition to the directly measured quantities, post processing was performed for some of the tests to yield indirectly measured parameters such as density and mass flow rate. These indirect measurements were not performed consistently throughout the test series. These measurements used the following nomenclature:

CD:	Calculated Density
CM:	Calculated Mass Flow Rate
CQ:	Calculated Heat Flux or Heat Transfer Coefficient

In the table that follows sensor location refers to one of two coordinate systems. For heat transfer measurement blocks the location uses the front, center of the measurement block for the reference location with the position given in Cartesian coordinates [9]. All other sensors use the HDR center line at the +0.0 m elevation, see Figure 1.1, for the reference location with the position given in cylindrical coordinates [1].

Table 3.1 lists all sensors in place for tests T51.16-T51.18. The table shows the quantity/parameter measured, the sampling frequency, and the location for each sensor relative to the appropriate coordinate system. Any special comments about the sensor's performance is also given. Figures 3.1 through 3.14 schematically depict the sensors' locations level by level in the HDR facility for Table 3.1.

Table 3.1: T51.16-18 Instrument Network

Sensor	Parameter	Frequency (Hz)	Location			Comments
			R (cm)	θ (deg)	Z (cm)	
CA4500	kg/s	0.17				Calculated burning rate
CA4510	N	0.17	660	174	-100	Wood crib force sensor
CA4511	N	0.17	740	176	-100	Wood crib force sensor
CA4512	N	0.17	700	189	-100	Wood crib force sensor
CA4513	N	0.17				Wood crib force sensor total
CD1045	kg/m^3	0.17	540	168	96	Calculated density
CF3712	m/s	0.17	540	62	-90	
CF3721	m/s	0.17	840	48	100	
CF3723	m/s	0.17	925	52	1200	
CF3724	m/s	0.17	910	45	2300	
CF4311	m/s	0.17	500	321	100	
CF4612	m/s	0.17	460	124	-90	Failed T51.16
CF5324	m/s	0.17	600	76	500	
CF6611	m/s	0.17	490	0	1200	
CF7701	m/s	0.17	730	85	1700	
CF7821	m/s	0.17	650	273	1700	
CF8521	m/s	0.17	630	83	2300	
CG 401	CO_2 v/o	0.17	0	0	0	Failed
CG1104	CO_2 v/o	0.01	670	85	3100	
CG1145	CO_2 v/o	0.01	590	177	-80	
CG1146	CO_2 v/o	0.01	610	90	-80	
CG1153	CO_2 v/o	0.01	670	85	600	
CG1166	CO_2 v/o	0.01	670	85	1020	
CG1177	CO_2 v/o	0.01	670	85	1700	
CG1178	CO_2 v/o	0.01	670	275	1900	
CG1185	CO_2 v/o	0.01	670	85	2300	
CG1204	CO_2 v/o	0.01	195	50	4000	
CG1266	CO_2 v/o	0.01	670	275	1200	
CG1304	CO_2 v/o	0.01	670	275	3100	
CG1366	CO_2 v/o	0.01	480	20	1270	
CG2104	1/m	0.17	670	85	3100	Extinction coefficient
CG2166	1/m	0.17	670	85	1020	Extinction coefficient
CG2266	1/m	0.17	450	20	1450	Extinction coefficient
CG2366	1/m	0.17	450	20	1360	Extinction coefficient

Table 3.1: T51.16-18 Instrument Network (continued)

Sensor	Parameter	Frequency (Hz)	Location			Comments
			R (cm)	θ (deg)	Z (cm)	
CG2466	1/m	0.17	450	20	1270	Extinction coefficient
CG2566	1/m	0.17	450	20	1180	Extinction coefficient
CG2666	1/m	0.17	450	20	1090	Extinction coefficient
CG4641	CO v/o	0.17	445	175	100	Failed T51.17
CG4642	O_2 v/o	0.17	445	175	100	
CG4643	CO_2 v/o	0.17	445	175	100	
CG4644	C_nH_m ppm	0.17	445	175	100	Failed
CG5301	kg/m^3	0.17	630	88	470	Failed T51.17
CG5302	kg/m^3	0.17	630	88	470	Failed T51.17
CG6601	CO_2 v/o	0.17	0	0	0	Failed
CG6604	CO_2 v/o	0.17	0	0	0	Failed
CG6611	CO_2 v/o	0.17	760	80	1000	Failed
CG6621	CO_2 v/o	0.17	0	0	0	Failed
CG6622	CO_2 v/o	0.17	0	0	0	Failed
CG6623	CO_2 v/o	0.17	0	0	0	Failed
CG6624	CO_2 v/o	0.17	0	0	0	Failed
CG6625	CO_2 v/o	0.17	0	0	0	Failed
CM1045	kg/s	0.17	540	168	96	Calculated mass flow rate
CP4640	ΔP mbar	0.17	500	170	100	
CP6201	ΔP mbar	0.17	1005	0	1100	Staircase stepping in data but follows overall transient
CQ1153	W/m^2 K	0.17	0	0	0	Calculated heat transfer coef.
CQ1185	W/m^2 K	0.17	0	0	0	Calculated heat transfer coef.
CQ2153	W/m^2	0.17	0	0	0	Calculated heat flux
CQ2185	W/m^2	0.17	0	0	0	Calculated heat flux
CQ2353	W/m^2	0.17	0	0	0	Calculated heat flux
CQ3153	°C	0.17	0	0	0	
CQ3185	°C	0.17	0	0	0	
CQ5310	°C	0.17	0	0	5	Steel measurement block
CQ5311	°C	0.17	20	180	5	Steel measurement block
CQ5312	°C	0.17	0	0	30	Steel measurement block
CQ5313	°C	0.17	90	180	355	Steel measurement block
CQ5314	°C	0.17	0	0	395	Steel measurement block
CQ5320	°C	0.17	0	0	10	Concrete measurement block
CQ5321	°C	0.17	0	0	20	Concrete measurement block
CQ5322	°C	0.17	0	0	30	Concrete measurement block
CQ5323	°C	0.17	0	0	40	Concrete measurement block
CQ5324	°C	0.17	0	0	50	Concrete measurement block
CQ5325	°C	0.17	0	0	200	Concrete measurement block

Table 3.1: T51.16-18 Instrument Network (continued)

Sensor	Parameter	Frequency (Hz)	Location			Comments
			R (cm)	θ (deg)	Z (cm)	
CQ5326	°C	0.17	0	0	300	Concrete measurement block
CQ5327	°C	0.17	75	180	400	Concrete measurement block
CQ8510	°C	0.17	0	0	2	Steel measurement block
CQ8511	°C	0.17	20	180	2	Steel measurement block
CQ8512	°C	0.17	0	0	30	Steel measurement block
CQ8513	°C	0.17	90	180	355	Steel measurement block
CQ8514	°C	0.17	0	0	395	Steel measurement block
CS3301	°C	0.17	220	90	-650	
CS3705	°C	0.17	1000	60	600	
CS3710	°C	0.17	1000	65	550	
CS3720	°C	0.17	1000	65	800	
CS4531	°C	0.17	605	185	110	
CS6601	°C	0.17	924	265	1200	Failed
CT 403	°C	0.17	0	270	5000	
CT 404	°C	0.17	195	50	4000	
CT 405	°C	0.17	900	160	4000	
CT 406	°C	0.17	110	50	4500	
CT 410	°C	0.17	310	50	3400	
CT 411	°C	0.17	900	45	3400	
CT 412	°C	0.17	900	270	3400	
CT 413	°C	0.17	635	270	3900	
CT 414	°C	0.17	310	270	4600	
CT 420	°C	0.17	600	90	3900	
CT 421	°C	0.17	600	270	3900	
CT 422	°C	0.17	950	55	3400	
CT 423	°C	0.17	570	80	3400	
CT 424	°C	0.17	550	275	3100	
CT 425	°C	0.17	550	275	3500	
CT3702	°C	0.17	950	70	550	
CT3706	°C	0.17	950	70	1700	
CT4511	°C	0.17	530	175	-70	
CT4512	°C	0.17	685	175	-70	
CT4513	°C	0.17	690	187	-70	
CT4514	°C	0.17	750	205	-70	
CT4521	°C	0.17	530	175	20	
CT4522	°C	0.17	685	175	20	
CT4523	°C	0.17	750	205	20	
CT4531	°C	0.17	530	175	110	
CT4532	°C	0.17	645	172	110	

Table 3.1: T51.16-18 Instrument Network (continued)

Sensor	Parameter	Frequency (Hz)	Location			Comments
			R (cm)	θ (deg)	Z (cm)	
CT4533	°C	0.17	730	185	110	
CT4534	°C	0.17	810	205	110	
CT4541	°C	0.17	690	187	170	Failed T51.17 and T51.18
CT4543	°C	0.17	750	205	170	
CT4542	°C	0.17	685	175	170	
CT4544	°C	0.17	815	181	170	
CT4545	°C	0.17	815	181	170	
CT4551	°C	0.17	590	177	80	Failed
CT4552	°C	0.17	750	190	300	
CT4553	°C	0.17	590	177	50	
CT4554	°C	0.17	590	177	-10	Failed
CT4555	°C	0.17	590	177	-80	
CT4556	°C	0.17	590	177	100	
CT4653	°C	0.17	500	215	0	
CT4654	°C	0.17	410	65	0	Failed
CT4655	°C	0.17	680	60	0	
CT4660	°C	0.17	610	82	-50	
CT4661	°C	0.17	430	105	-50	
CT4662	°C	0.17	390	125	-50	
CT4663	°C	0.17	400	145	-50	
CT4664	°C	0.17	400	165	-50	
CT4671	°C	0.17	430	105	100	
CT4672	°C	0.17	390	125	100	
CT4673	°C	0.17	400	145	100	
CT4674	°C	0.17	400	165	100	
CT4682	°C	0.17	390	125	130	
CT4684	°C	0.17	400	165	130	
CT5101	°C	0.17	410	110	600	
CT5301	°C	0.17	417	25	650	
CT5302	°C	0.17	980	55	600	
CT5303	°C	0.17	740	85	600	
CT5310	°C	0.17	600	75	470	
CT6309	°C	0.17	820	235	800	
CT6402	°C	0.17	450	110	1200	
CT6606	°C	0.17	510	20	1200	
CT6607	°C	0.17	640	280	1200	
CT6609	°C	0.17	720	75	1200	
CT7702	°C	0.17	950	55	1700	
CT7703	°C	0.17	670	80	1700	

Table 3.1: T51.16-18 Instrument Network (continued)

Sensor	Parameter	Frequency (Hz)	Location			Comments
			R (cm)	θ (deg)	Z (cm)	
CT7802	°C	0.17	500	270	1900	
CT8402	°C	0.17	457	270	2257	
CT8502	°C	0.17	700	80	2300	
CT8503	°C	0.17	600	65	2300	
CT8510	°C	0.17	600	73	1520	
CV4640	m/s	0.17	540	168	96	
CV6601	m/s	0.17	490	0	1180	Failed
CV6602	m/s	0.17	490	0	1180	Failed
CV6604	m/s	0.17	490	0	1180	Failed
CV7701	m/s	0.17	650	85	1700	Failed
CV7702	m/s	0.17	650	85	1700	Failed
CV7704	m/s	0.17	730	85	1700	
OA2010	Shell Expansion	0.17	1003	270	4000	
OA2015	Shell Expansion	0.17	1003	270	0	
OA3010	Shell Expansion	0.17	1003	270	4000	
OA3015	Shell Expansion	0.17	1003	270	0	
OA3016	Shell Expansion	0.17	1003	270	-100	

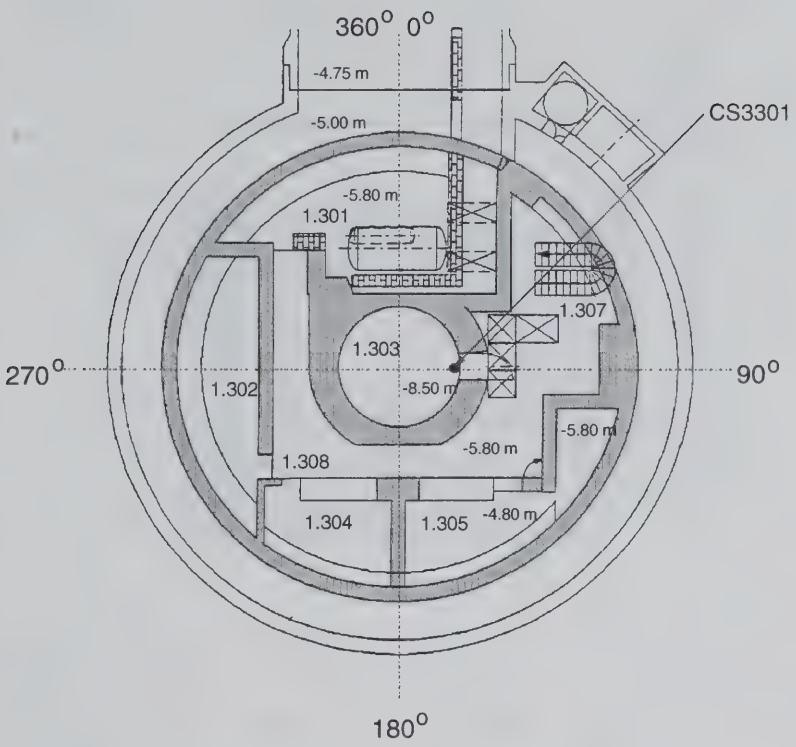

Figure 3.8: Level 1.200 and 1.300 at the -6.5 m Elevation

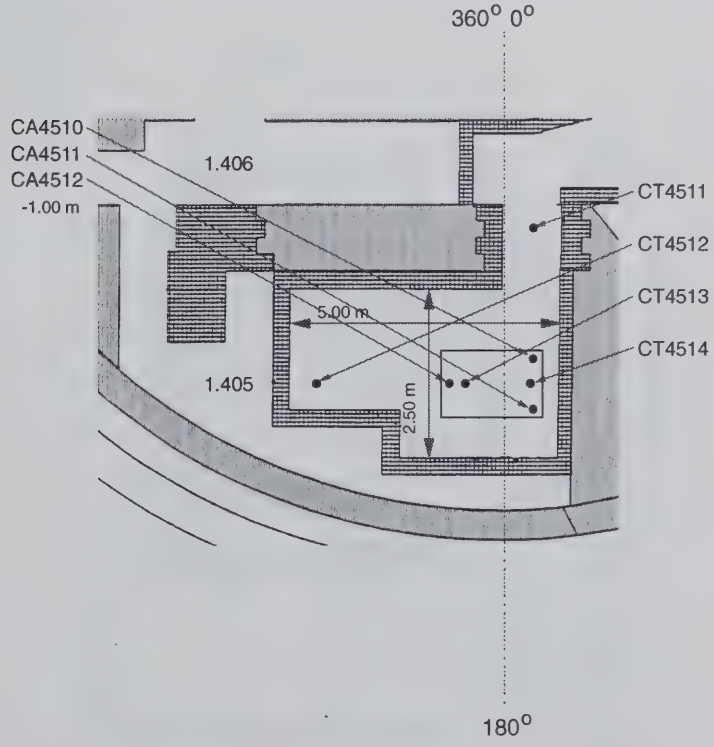

Figure 3.9: Fire Room at the -0.7 m Elevation

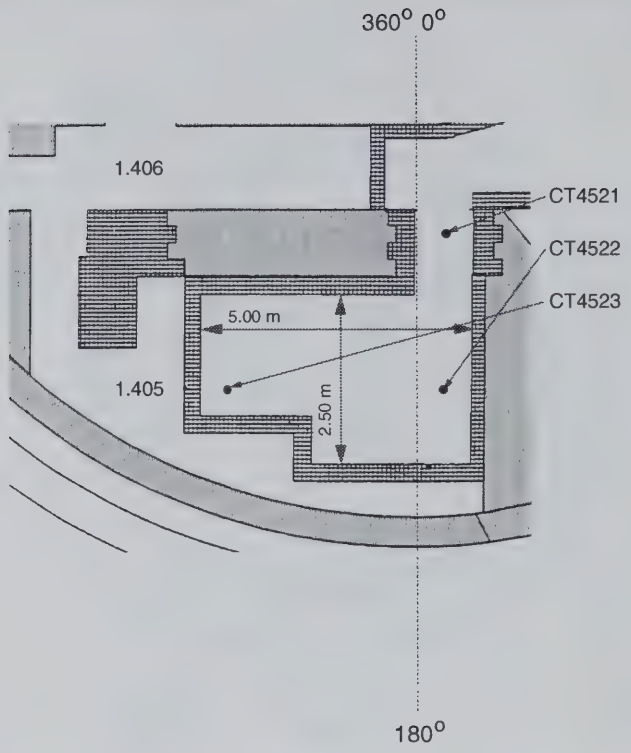

Figure 3.10: Fire Room at the +0.2 m Elevation

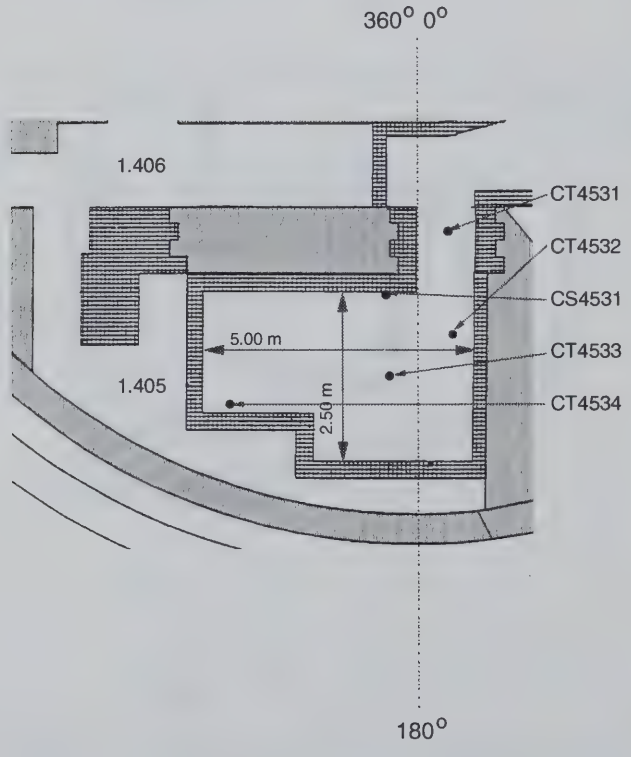

Figure 3.11: Fire Room at the +1.1 m Elevation

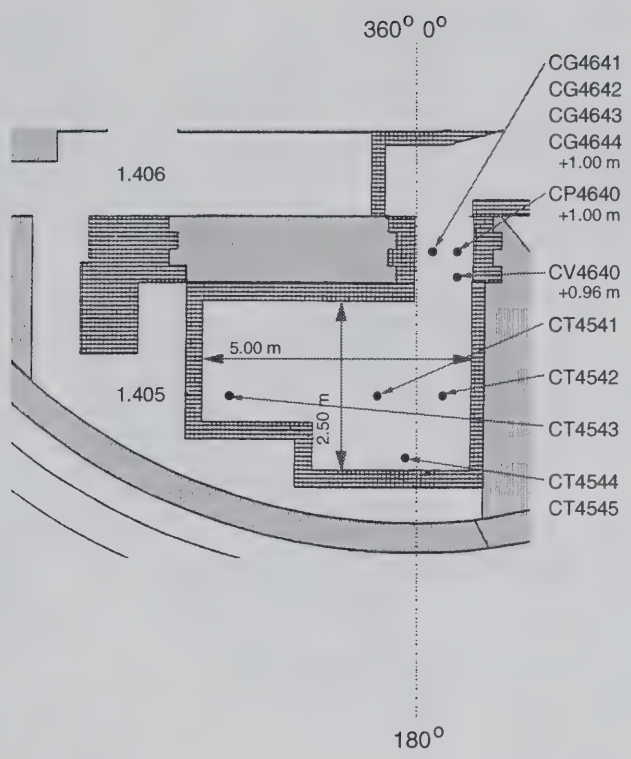

Figure 3.12: Fire Room at the +1.7 m Elevation

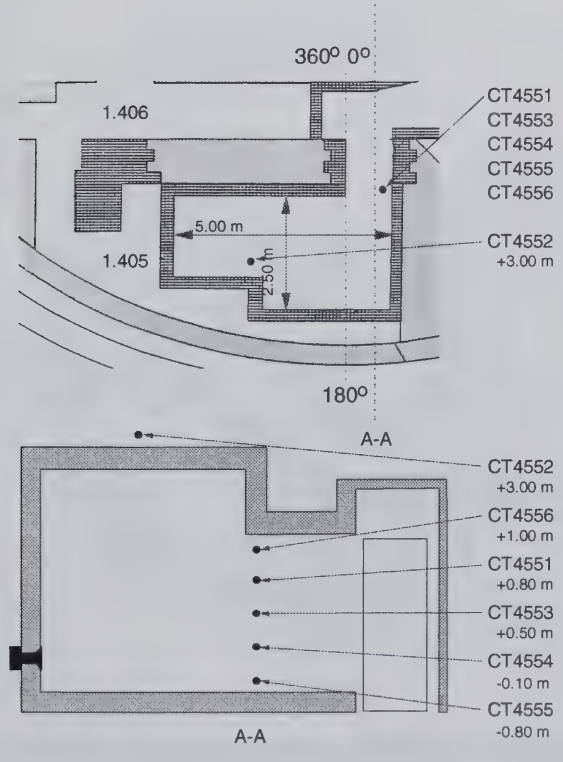

Figure 3.13: Fire Room Vertical Cross-Section

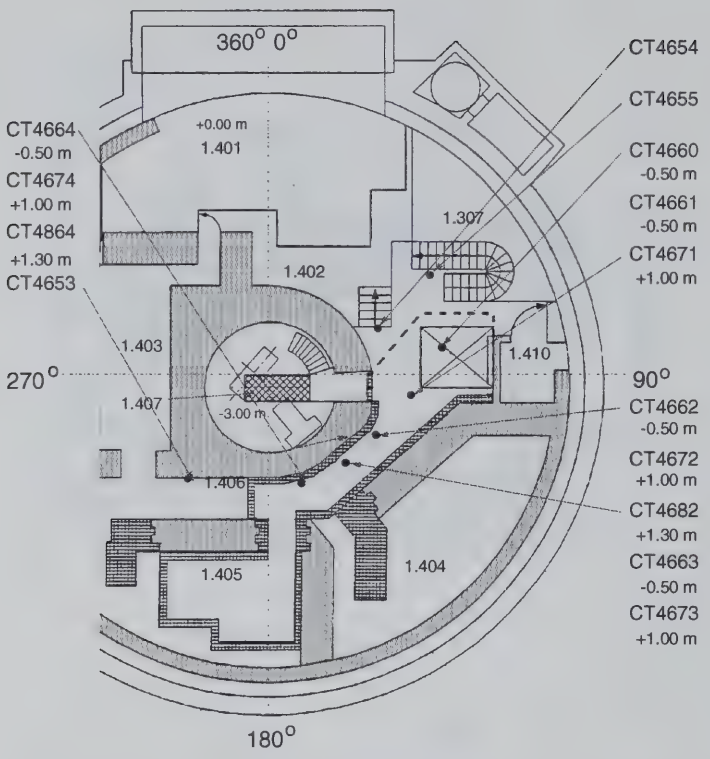

Figure 3.14: Level 1.400 TC's at the +0.0 m Elevation

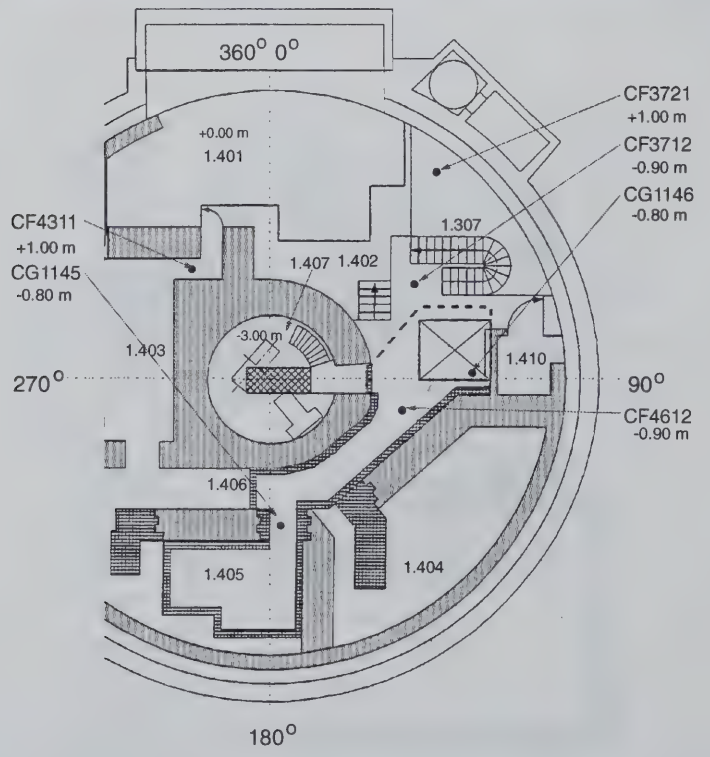

Figure 3.15: Level 1.400 Velocity Sensors and Gas Sensors at the +0.0 m Elevation

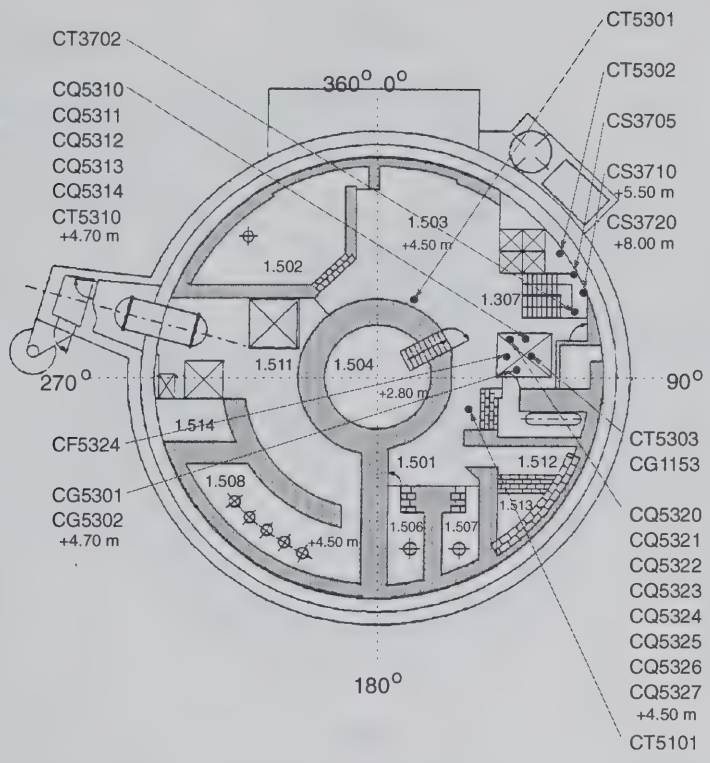

Figure 3.16: Level 1.500 at the +6.0 m Elevation

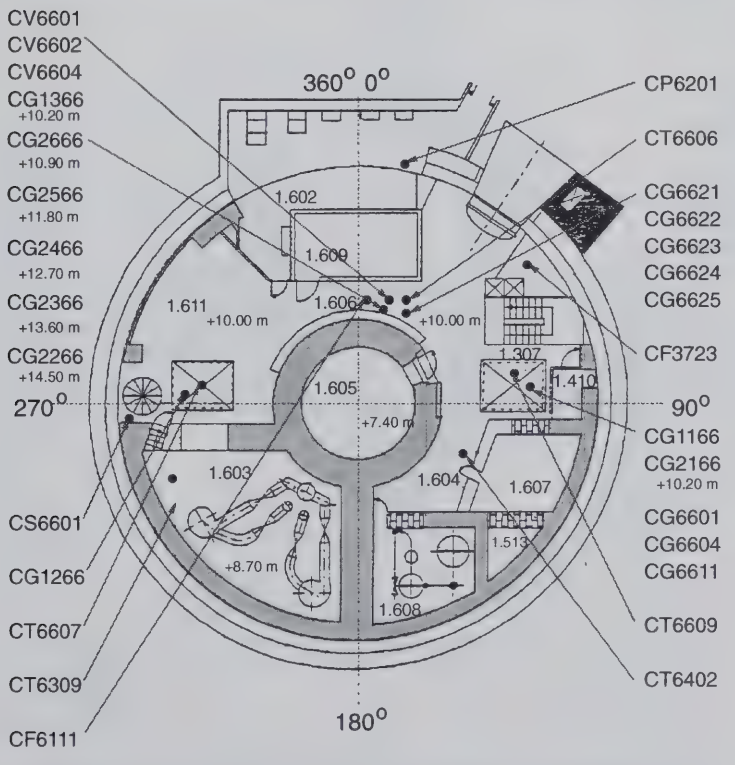

Figure 3.17: Level 1.600 at the +12.0 m Elevation

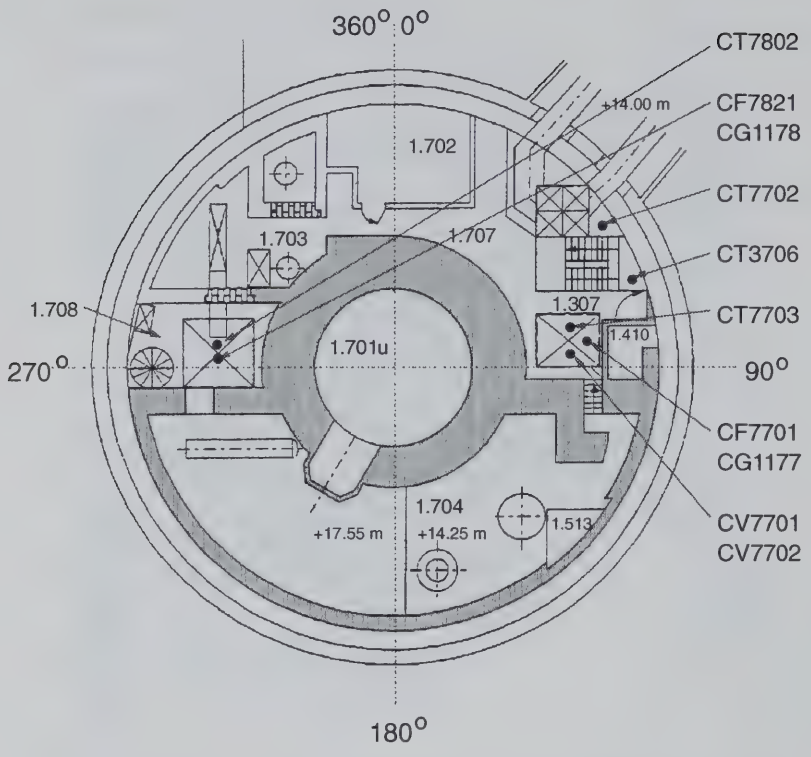

Figure 3.18: Level 1.700 at the +17.0 m Elevation

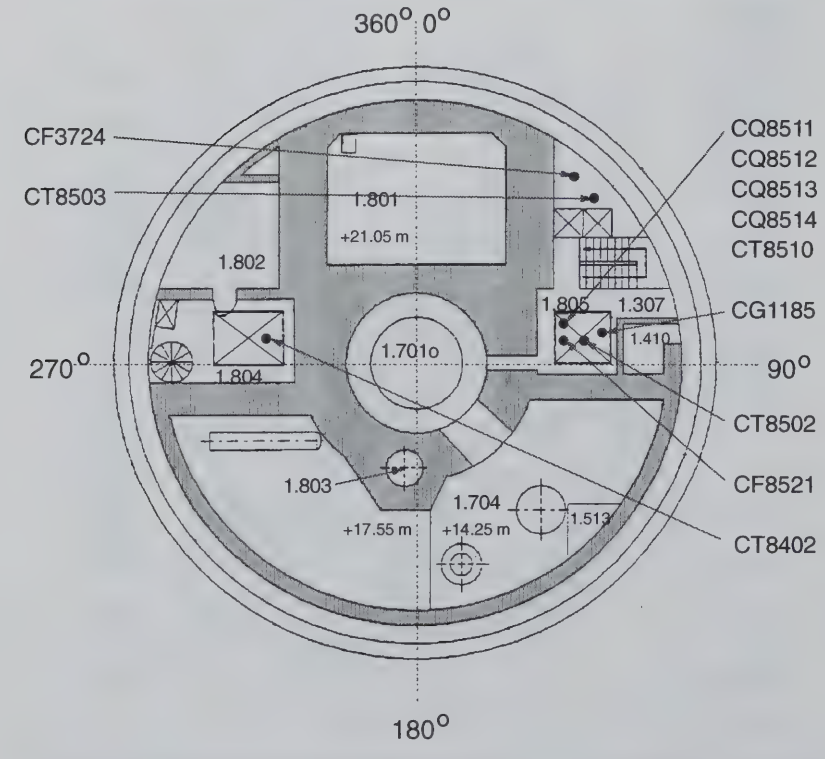

Figure 3.19: Level 1.800 at the +23.0 m Elevation

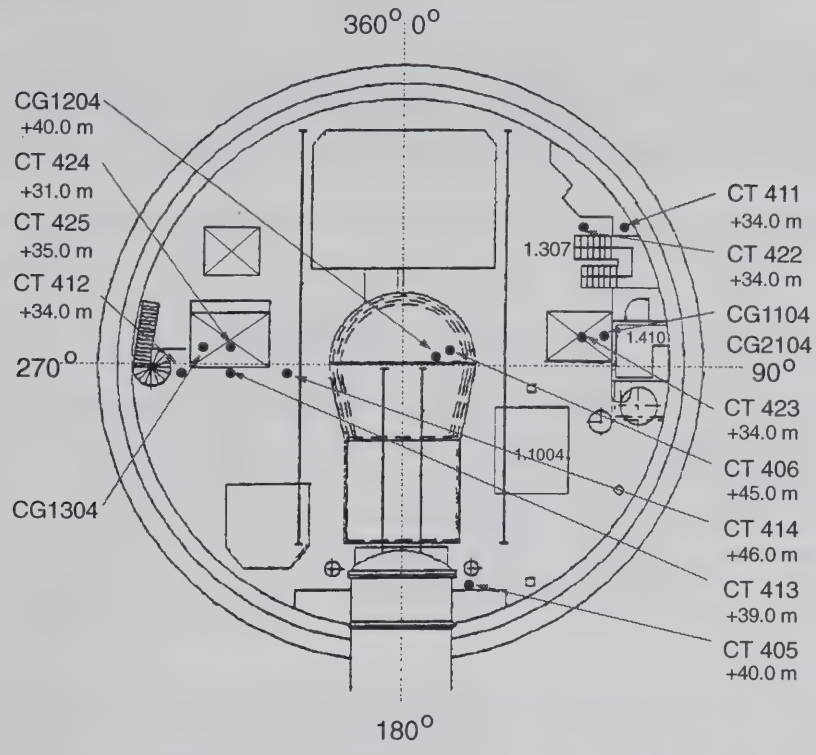

Figure 3.20: Dome Level at the +31.0 m Elevation

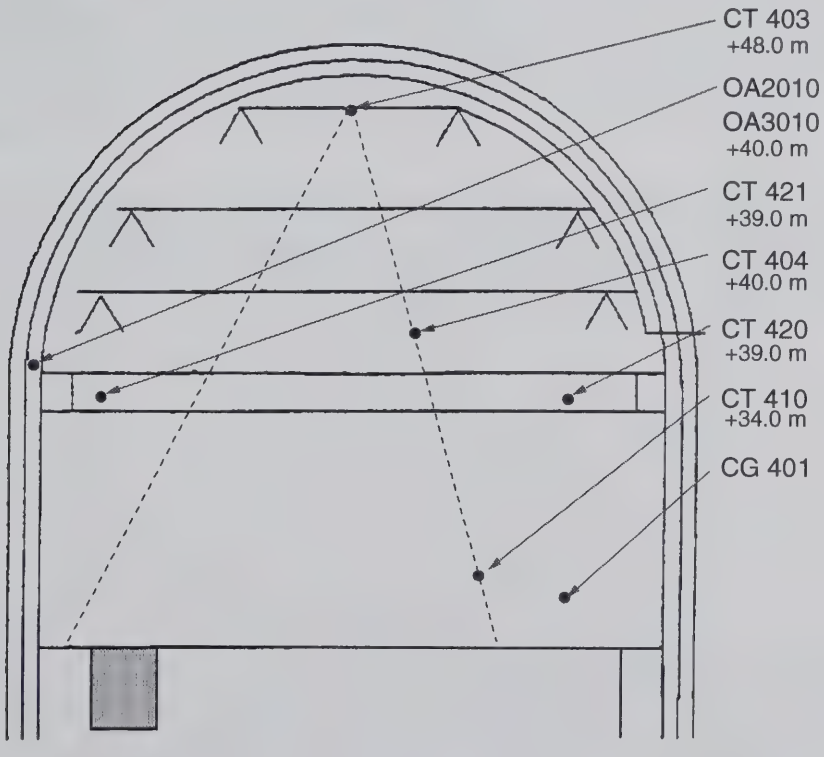

Figure 3.21: Dome Vertical Cross-Section

4 TEST EXECUTION

Test execution procedures for the wood crib tests were slightly more complex than for the gas fire tests. This extra complexity results mainly from pretest procedures for the handling of the wood. The procedures can be divided into pretest actions, test actions, and post test actions.

Before any given wood crib fire test was executed, the wood was pretreated to in order to obtain an initial 8% humidity.

The test execution procedure for the wood crib tests was as follows. Approximately one half hour before the start of each test the data acquisition system was activated. After verifying the operation of the data acquisition system the wood cribs were ignited. This was done by igniting a 300 ml of alcohol in a small canister located under crib number 2, see Figure 2.2. The ignition was done manually. The remainder of the wood cribs ignited from the radiative heat resulting from the ongoing fire. The wood crib fires lasted approximately 45 minutes. Data collected during each test was archived on reel-to-reel magnetic tape. During the archiving process the start of the fire was set to be zero minutes and ten minutes of data were stored from the prefire portion of the collected data .

Following the end of a wood crib test, the HDR containment building was ventilated to purge it of smoke and combustion product gasses. The ventilated gasses passed through filters, and data was collected on the filter loading. The levels of smoke and soot produced during the tests, especially during the T51.18 test, required the complete replacement of filters after each test in order to keep filter system pressure drops below regulatory requirements. After ventilation further sampling was performed on the containment building atmosphere. Levels of hazardous gasses were checked to determine if further ventilation was required before personnel could enter the building.

Following each test, cleaning was performed of the various sensors to remove any soot buildup that could interfere with their future performance. Test T51.18 with its high levels of soot production required a significant expenditure of manpower and materials to clean the facility and its sensors.

5 OVERVIEW OF EXPERIMENTAL RESULTS

This section contains selected results from the wood crib fire tests performed in the HDR facility. Data from selected instruments for the three tests are shown in the first subsection to give a general overview of the transient histories and their similarities and differences. These are followed by results representing zonal values from the test series plotted as a function of the number of wood cribs at 16 minutes from the start of the wood crib fires. Plot legends in the second section indicate the instrument names and elevations; their positions can be identified in Section 3 of this report.

5.1 Selected Results

Results from each wood crib test are shown in this section, tests T51.16 through T51.18. These tests involved the combustion of 5, 7 and 11 wood cribs respectively. The first figure, Figure 5.1, shows the pyrolysis rate for each of the three tests.

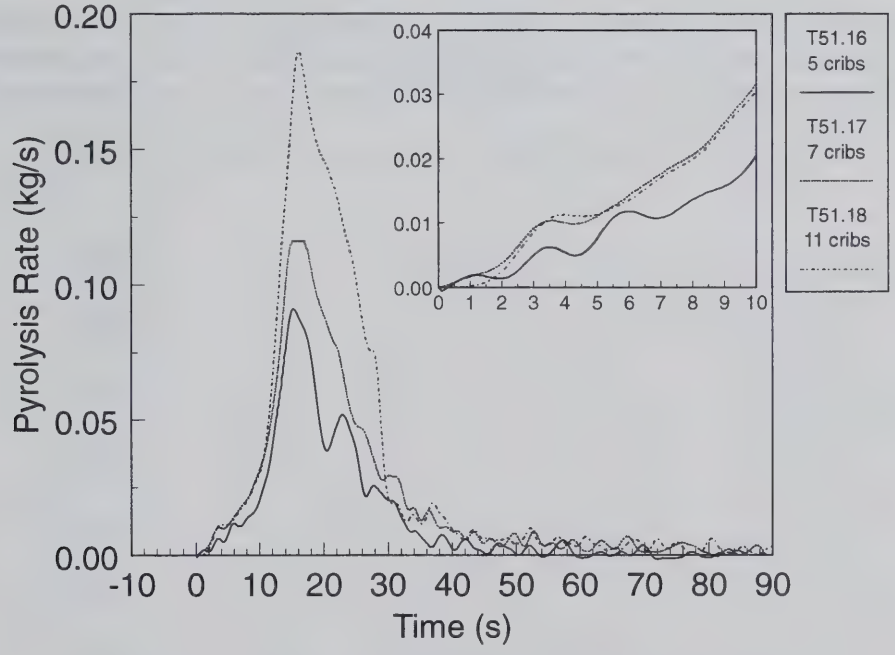

Figure 5.1: Wood Crib Pyrolysis Rate (CA4500)

The following observations hold:

- Each test has the same basic trends in pyrolysis rate of a slow initiation phase lasting for about 10 minutes which is followed by a steep increase. Two progressively smaller peaks follow after the maximum pyrolysis rate, which occurs at 16 minutes, although in tests T51.17 and T51.18 there is overlap between these secondary peaks.
- The duration of significant combustion activity is nearly equal for all three tests, approximately 35 minutes.
- There is an increase in the time to peak pyrolysis between tests T51.16 and T51.17, but not between tests T51.17 and T51.18, and all three achieve a maximum pyrolysis rate at 16 minutes.
- The increase in the number of wood cribs results in the increase of the maximum pyrolysis rate.
- Towards the end of the wood crib fire, the pyrolysis rate of each experiment shows sustained fluctuations.

The next two figures, Figures 5.2 and 5.3, show the upper and lower layer temperatures for the fire room. The figures display thermocouples CT4543 and CT4514 which are respectively located at the ceiling and floor of the fire room approximately two meters from the wood crib platform.

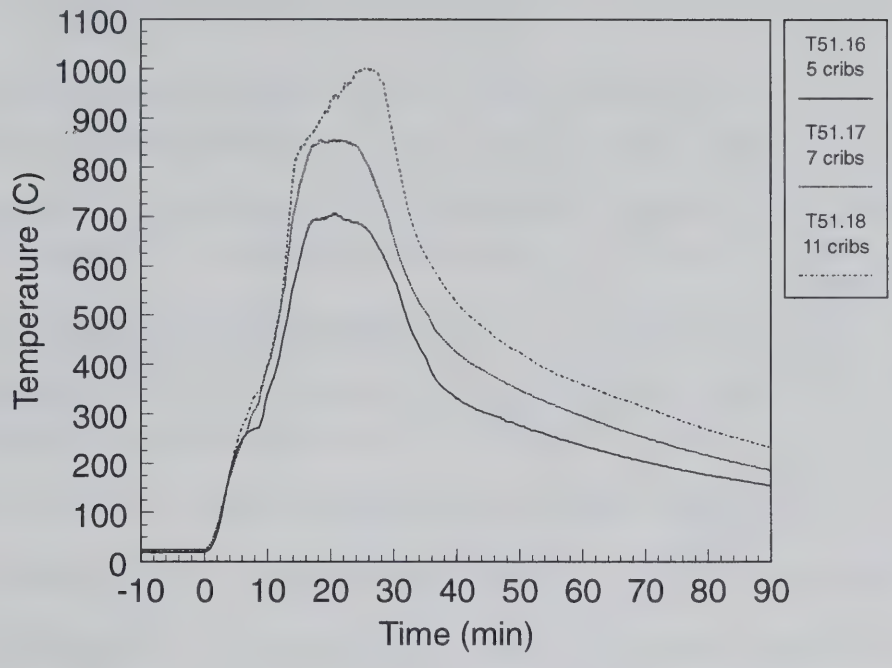

Figure 5.2: Fire Room Upper Layer Temperature (CT4543)

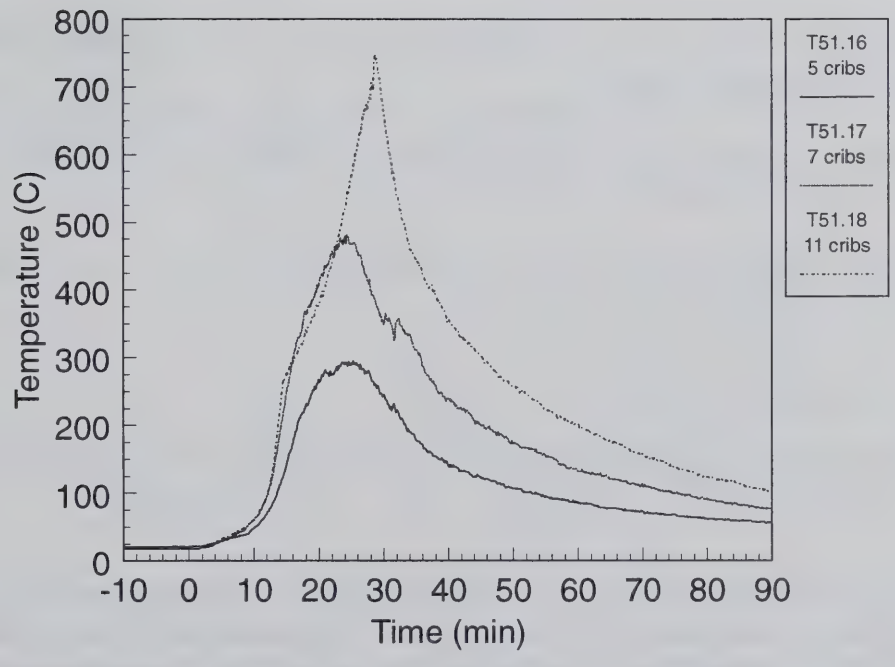

Figure 5.3: Fire Room Lower Layer Temperature (CT4514)

The following conclusions can be drawn for the upper layer temperature characteristics from Figure 5.2:

- All three tests depict an identical temperature behavior during the first six minutes after ignition. This most likely results from the fire at this stage being consisting solely of wood crib number 2 and the alcohol source used for ignition.
- While experiment T51.16 reaches a plateau at 300 °C, lasting for about 2 minutes, temperatures for T51.17 and T51.18 continuously increase with T51.18 showing slightly higher temperatures.
- At 10 min., all three tests undergo a very steep temperature gradient (flashover), with T51.16 depicting a slight time delay of 1 min. because of the preceding temperature plateau.
- At 15 min., test T51.18 has a large drop in the temperature gradient corresponding to the underventilation period shown in Figure 5.9. This new gradient lasts until the peak fire temperature is reached.
- Tests T51.16 and T51.17 both reach peak temperatures at 20 min. Test T51.18 reaches its peak temperature at 28 min.
- From 30 min. till the end of the tests, all the experiments show the same cooldown behavior.

From Figure 5.3, depicting the lower layer fire room temperatures for the three tests, the following observations hold:

- All three tests show identical temperature behavior, a benign and slow increase over the first 6 min.
- The same characteristics can be identified for the lower layer temperatures as for the upper layer temperatures beyond 6 min.
- Tests T51.17 and T51.18 show identical behavior; their temperature gradients in the lower layer are higher than in the upper layer, after flashover occurs, while the temperature gradient for T51.16 seemingly less than in the upper layer and obviously less than the other two tests.
- The maximum temperatures are reached at somewhat later time than for the upper layer.
- The following peak temperatures are reached:
  T51.16: 280 °C at 22 min.
  T51.17: 480 °C at 24 min.
  T51.18: 750 °C at 29 min.
- The temperature trace of CT4514 for test T51.16 and to some extent for test T51.17 indicates distinct fluctuations over the time period of 16 to 35 min which is indicative of a mixing layer.

The next two figures on the following page, Figures 5.4 and 5.5 depict temperatures in the hallway connecting the fire room to the curtained area. The sensors are located at the midpoint of the hallway both in terms of length and width. They are at elevations approximately 0.5 m below the ceiling and 0.5 m above the floor.

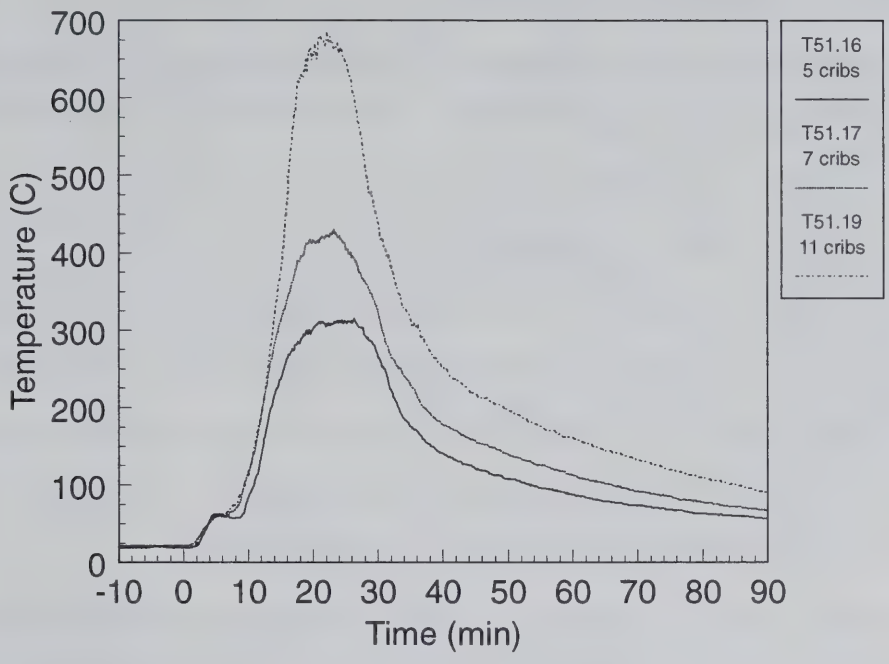

Figure 5.4: Hallway Upper Layer Temp. (CT4673)

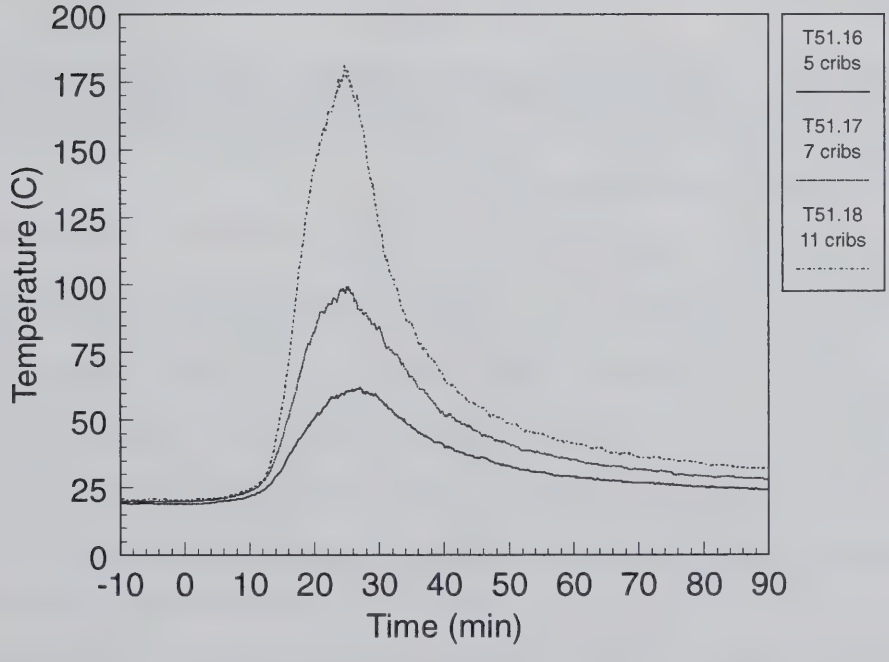

Figure 5.5: Hallway Lower Layer Temp. (CT4663)

The following items are observed in these figures:

- As in the fire room, the hallway temperatures in both the upper layer and the lower layer show a continuing increase with the number of wood cribs, but the maximum temperatures are even more distinctly separated.
- While T51.18 reaches a maximum of 680 °C at 23 minutes, experiment T51.17 reaches only 430 °C and T51.16 reaches 310 °C at the same time, e.g. times of peak temperatures of the upper gas layer in the hallway at that position coincide for all three tests.
- The percent change in temperatures between tests T51.16 and T51.17 was 60% for the lower layer and 40% for the upper layer. For tests T51.17 and T51.18 these values were 80% and 60% respectively. The change in percentage increase between T51.16/T51.17 and T51.17/T51/18 is the same for both layers, 20%.
- The hallway temperatures have nearly identical trends as a function of time with the exception of overall magnitude.
- The significantly cooler temperatures in the lower layer indicate the presence of a large flow of fresh air under the maintenance hatch curtain to the fire room.

The next three figures, Figures 5.6 through 5.8, show temperatures in the main staircase maintenance hatch on the 1.400 level and the 1.700 level and in the dome. Thermocouple CT4671 is located approximately 0.5 m below ceiling of the 1.400 level, CT7703 is located at the middle elevation of the 1.700 level, and CT0423 is located 3 m above the dome operating deck. The comparisons between these three figures as well as Figures 5.2 and 5.4 lead to the following observations:

- The upper gas layer temperatures for all three experiments drastically decrease along the flowpath from the fire room to the level 1.400 main staircase maintenance hatch (CT4671), such that for experiment T51.18, 11 cribs, the hot layer temperature drops from 1000 °C to 350 °C and similarly for the other two tests.
- The maximum temperatures are reached at the same time, 24 min, for all three experiments for the upper layer at the 1.400 level maintenance hatch.
- While a pronounced difference of 140 °C exists between the peak temperature between T51.17 and T51.18 much less of a difference, 50 °C, remains between the former and T51.16. In fact, both of these experiments indicate about the same cooldown behavior.
- The hot plume rising up the maintenance hatch cools quickly between the 1.400 level and the 1.700 level which indicates a large entrainment of air from the upper levels into the plume, by both entrainment via counter-current flow of cold air descending through the hatches and by entrainment from the surrounding compartments. As a result, the differences between the peak temperatures decrease and the overall appearances of the temperature traces become much more similar, Figure 5.7. Heat transfer to the structures also contributes toward cooldown.
- The temperature data for the plume shows oscillations of up to 20 °C at the entrance to the 1.500 level, Figure 5.6, demonstrating the turbulent nature of the plume.
- Between the 1.700 level and the dome the entrainment reduces due to limitation by the flow area restrictions in the maintenance hatch. Consequently, the cooldown of the plume is only minimal, a few °C, but the ranges of temperature increases are further broadened over time

while the overall shapes of the temperature curves become more similar with even further reduction of the original differences between T51.17 and T51.18, Figure 5.8.

- Although greatly dampened by entrainment and heat transfer, the plumes entering the dome are distinctly identifiable for all three tests despite the long complex flow path originating in the fire room , 30 m below.

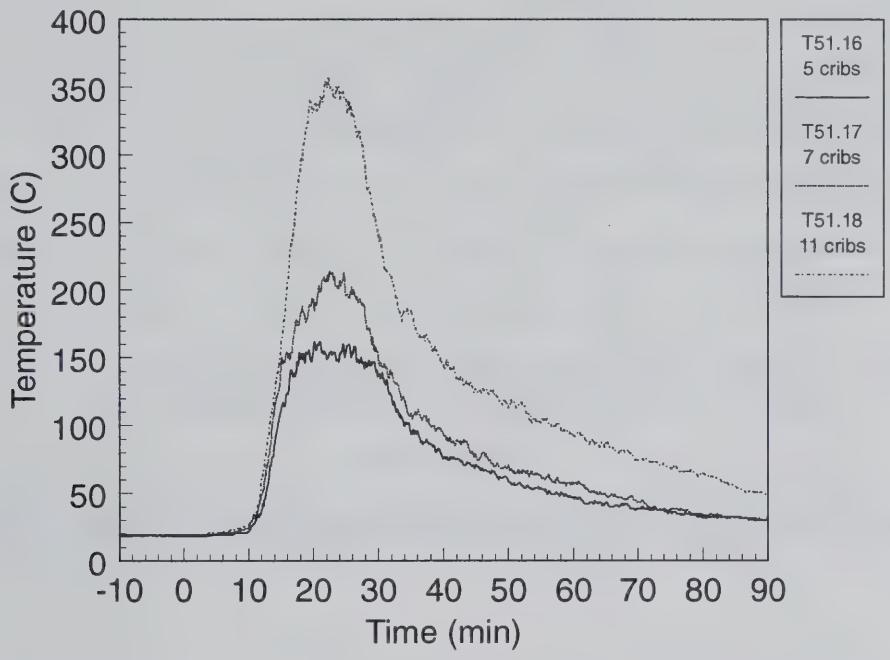

Figure 5.6: Level 1.400 Main Staircase Maintenance Hatch Temp. (CT4671)

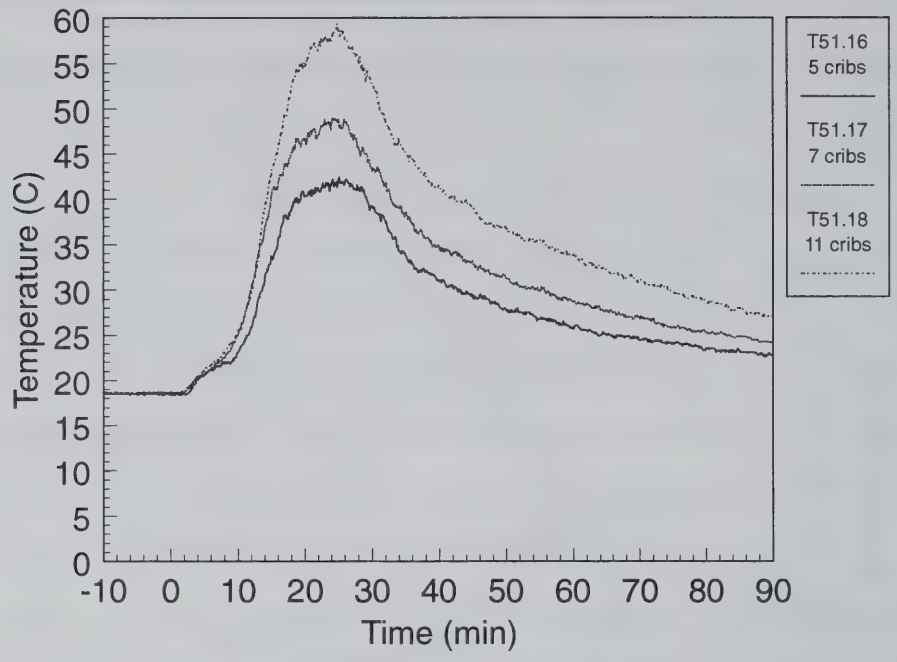

Figure 5.7: Level 1.700 Main Staircase Maintenance Hatch Temp. (CT7703)

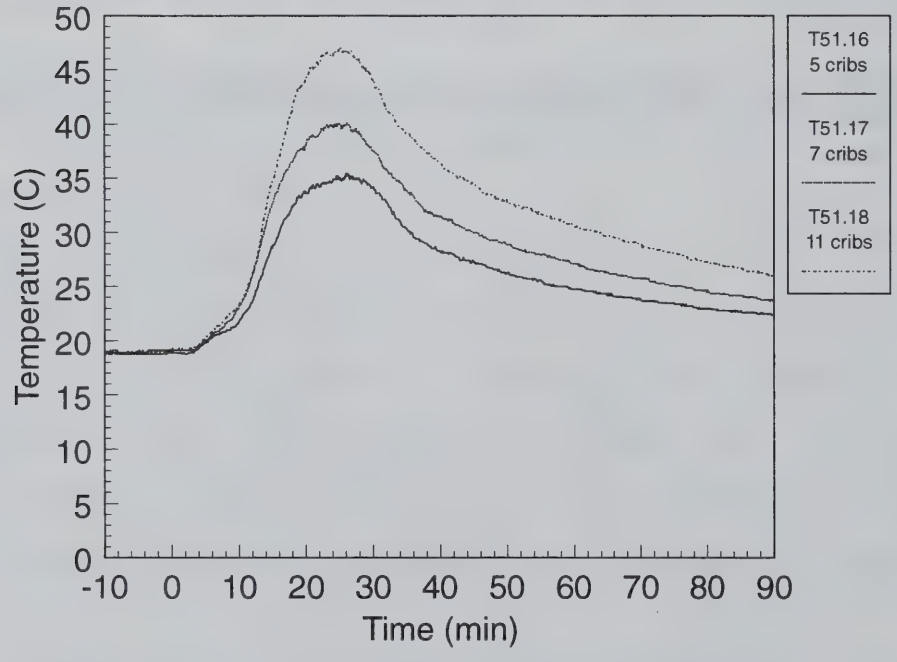

Figure 5.8: Dome Temp. (CT0423)

Figures 5.9 through 5.11 present the oxygen, carbon monoxide, and carbon dioxide concentrations in the upper layer of the fire room doorway. The following observations can be drawn:

- A steady drop in the minimum oxygen concentration is seen with an increase in the number of wood cribs.
- Test T51.18 reaches 0% oxygen concentration for a period of 15 minutes which indicates this fire is clearly underventilated.
- Tests T51.16 and T51.17 generate only minute amounts of CO while test T51.18 produces a significant amount of CO. This also indicates that T51.18 quickly became underventilated while the other two wood crib tests were able to maintain a sufficient airflow into the fire room from the hallway to completely combust the wood.
- CO_2 concentrations echo the reverse of the trends seen in the O_2 concentrations. A steady increase with the number of wood cribs and a plateau in the values for test T51.18 that corresponds to the period of complete oxygen depletion in the fire room.
- Many of the characteristic details seen in the temperature histories are reflected in the gas concentrations. Thus, they are confirmed independently by means of diverse measurement principles.
- CO concentrations in tests T51.16 and T51.17 peaked at 70 ppm and 100 ppm respectively, well below the minimum 30 minute exposure concentration for lethality which is 4000 ppm [35]. Test T51.18, however, reached a CO concentration of 30000 ppm or well above the minimum lethal concentrations.

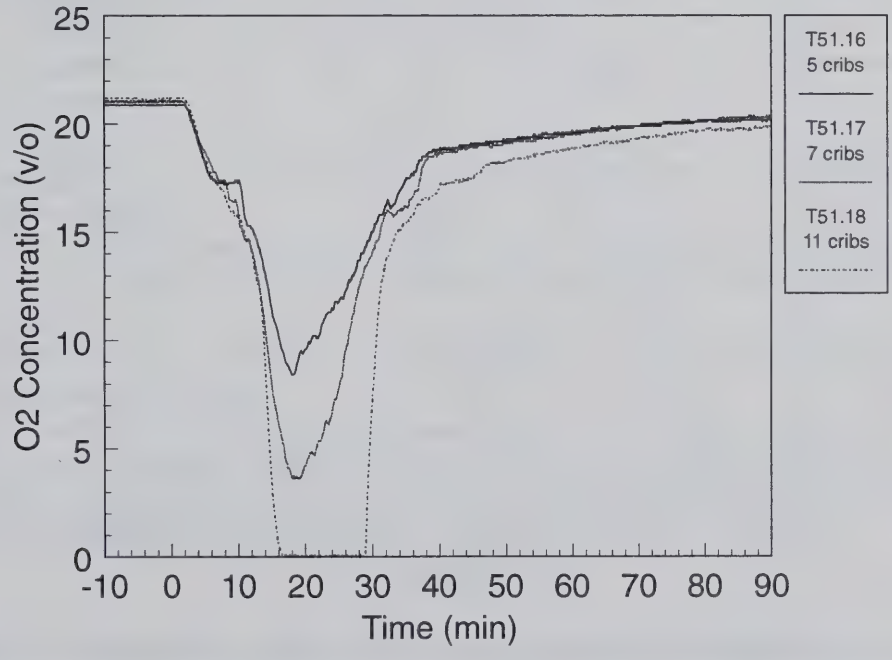

Figure 5.9: Fire Room Doorway Upper Layer O_2 Concentration (CG4642)

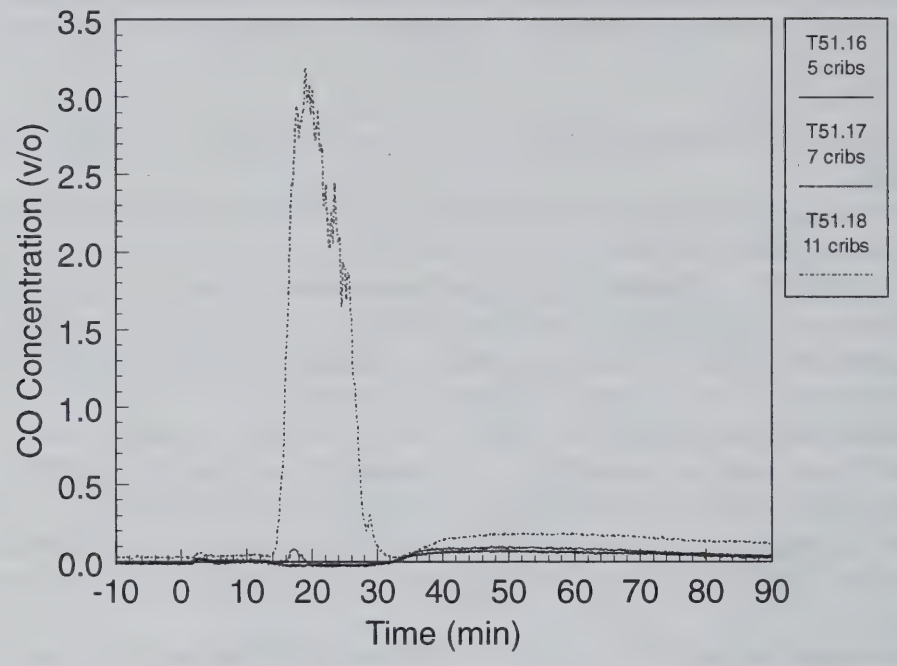

Figure 5.10 Fire Room Doorway Upper Layer CO Concentration (CG4641)

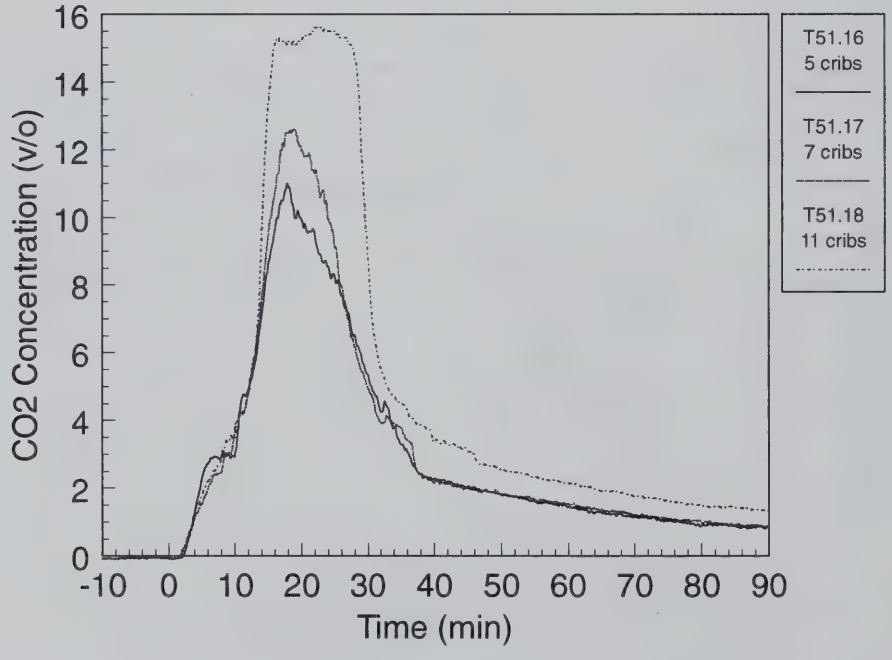

Figure 5.11: Fire Room Doorway Upper Layer CO_2 Concentration (CG4643)

The following two figures, Figures 5.12 through 5.14, show the measured velocities in the upper layer of the fire room doorway, the lower layer of the hallway near the curtained area, and in the main staircase maintenance hatch at the 1.700 level.

- All of the experiments reach a maximum velocity of about 6 m/s in the upper doorway region and maintaining that level over a time span of between 14 min. , T51.16, and 27 min., T51.18.
- Surprisingly, the highest measured velocity is for test T51.16, the lowest fire power of the wood cribs. This is probably due to the location of the peak of the velocity profile in the doorway. The velocity probe is located 0.17 m below the top of the doorway. For test T51.16, which had a smaller hot layer, the peak of the velocity profile was probably closer to the probe than during the other two tests.
- Measured velocities exiting the fire room are very similar for each of the tests.
- The change in the upper layer temperature gradient in the fire room during test T51.18 is also seen in the upper layer velocity for that test.
- Since the hallway sensor for test T51.16 failed, only tests T51.17 and T51.18 can be compared. The peak velocity in the hallway increased from 3.5 m/s to 5.1 m/s for these two tests, an increase of 44%. This compares well to the increase in the number of wood cribs from 7 cribs to 11 cribs which is an increase of 57%.
- A steady increase in the velocities measured in the maintenance hatch is seen for each increase in the number of wood cribs.
- The fire room and hallway velocities show some high frequency fluctuations which are indicative of turbulent flow. In the maintenance hatch, these high frequency fluctuations are superimposed on top of low frequency fluctuations. These low frequency fluctuations which can take minutes to occur suggest that the plume rotates its position about in the hatch. This behavior is considerably more complex than the simple static position plume models used in fire codes.
- All three experiments start with an initially existing velocity field in the containment with fire room and hallway velocities of about 0.5 m/s. T51.16 at the 1.700 level maintenance hatch depicts stagnation.
- The hallway lower velocities of 3.5 m/s and 5.1 m/s for experiments T51.17 and T51.18 indicate a strong counter-current flow of fresh air with nearly as high of velocities as seen in the upper layer.
- At the 1.700 level, peak velocities range between 3 m/s for T51.16 and 3.9 m/s for T51.18, e.g. a substantially high value.
- At 90 min., well after the end of combustion, velocities in the flow path range well above 1 m/s and 2.5 m/s depending on the proximity to the fire room, where they are higher.
- Also, details in the velocity traces independently confirm major characteristics observed in the temperature histories in the fire room.

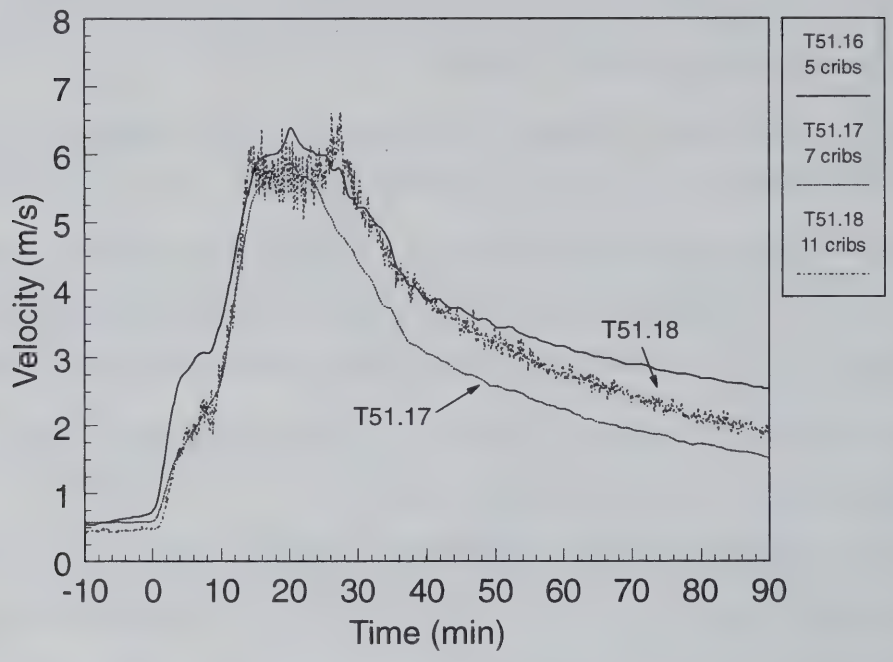

Figure 5.12: Fire Room Doorway Upper Layer Velocity (CV4640)

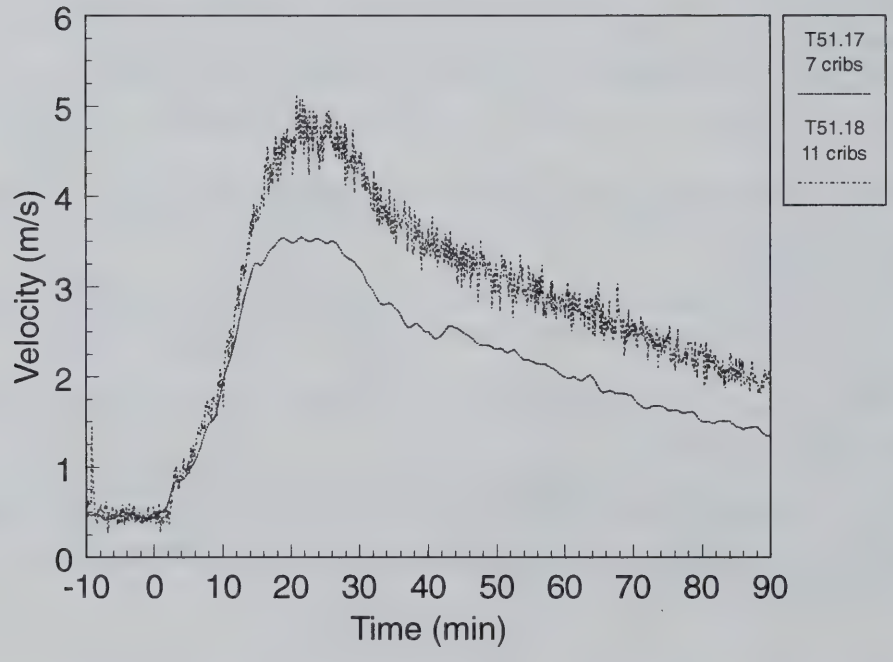

Figure 5.13: Hallway Lower Layer Velocity (CF4612)

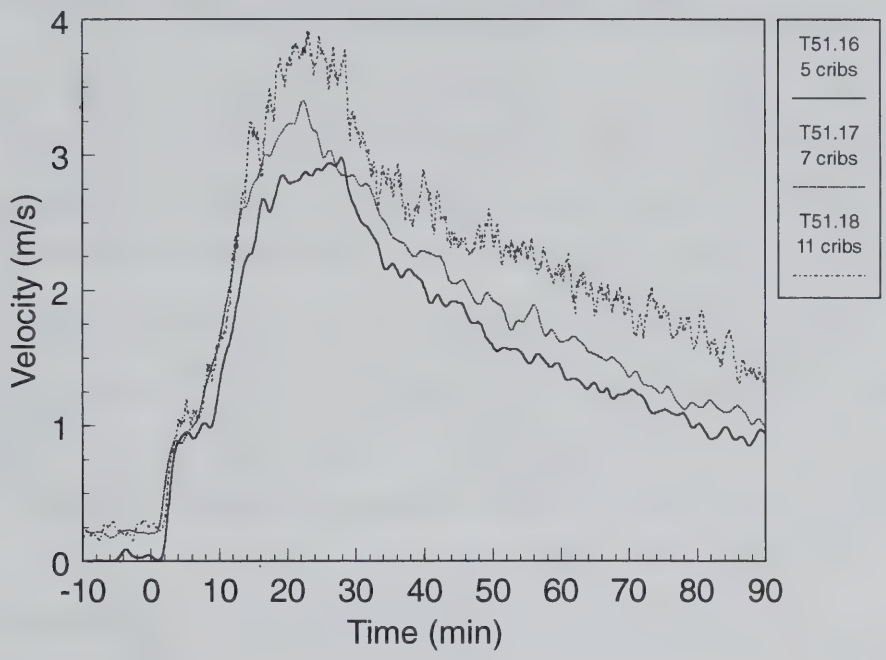

Figure 5.14: Level 1.700 Main Stairchase Maintenance Hatch Velocity (CF7701)

Figures 5.15 and 5.16 on the following page present the measured CO_2 concentrations in the main staircase maintenance hatch at the 1.600 level and in the dome.

- The CO_2 trends for both locations are similar in both magnitude and shape. The CO_2 concentration in the dome shows a spreading of the peak at 25 minutes compared to the hatch, but this is to be expected given the large free air volume present.
- The final, steady state concentrations at both locations are identical indicating that the flows induced in the containment lead to a total mixing of the containment atmosphere, homogenizing the CO_2 concentrations.
- The percent increase in the steady state CO_2 concentration from test T51.16 to test T51.17 was 35%. This matches closely the increase in the amount of fuel, 5 cribs to 7 cribs or 40%. Given that both of these tests were well ventilated, this serves to qualitatively confirm the sensor readings. The percent increase between test T51.17 and test T51.18 is slightly lower than the increase in the number of wood cribs, a 42% CO_2 increase compared to a 57% fuel increase; however, this also acts to confirm the sensor readings and the general underventilated nature of test T51.18.

The final two figures of this subsection, Figures 5.17 and 5.18, show the extinction coefficients in the main staircase maintenance hatch on the 1.700 level and in the dome.

- There is a fairly small increase in the extinction coefficients between test T51.16 and T51.17, since both of these tests were rather well ventilated. Contrary, test T51.18 shows a very large increase that clearly demonstrates the tremendous amounts of smoke produced during this test.
- Smoke density drops by nearly a factor of two from its maximum value as the containment atmosphere continues to mix, cooldown, and particulate matter settles out onto the building surfaces.
- Assuming a visibility limit of 0.5 for trained rescue personnel familiar with the facility [8], test T51.18 very quickly reached a point where rescue operations within the facility would have become impossible.
- For untrained personnel, assuming a visibility limit of 0.15 [8], it would have been impossible to successfully evacuate for the entire T51.17 and the T51.18 tests and during the peak combustion portion of the T51.16 test.

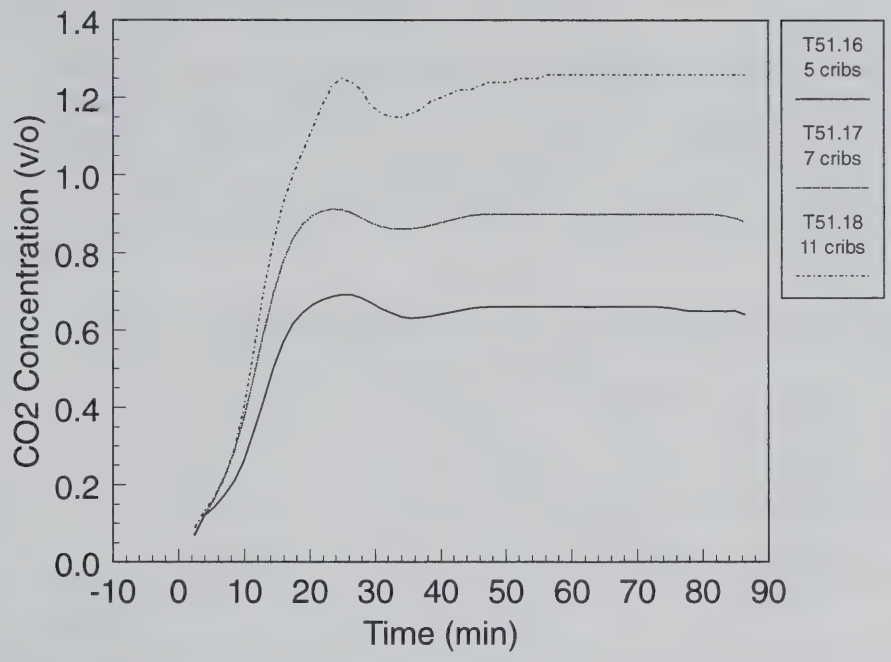

Figure 5.15: Level 1.600 Main Staircase Maintenance Hatch CO_2 Conc. (CG1166)

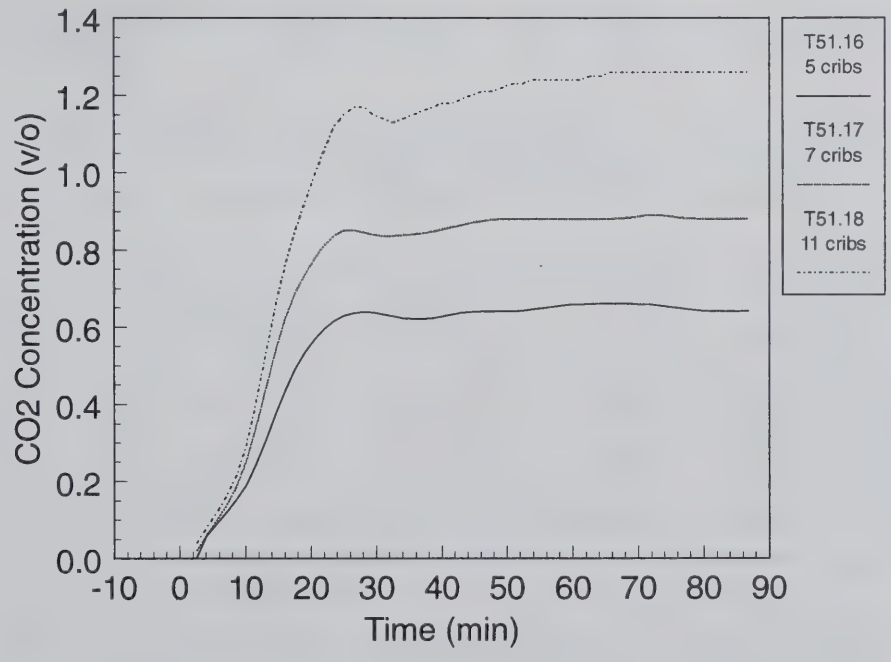

Figure 5.16: Dome CO_2 Concentration (CG1104)

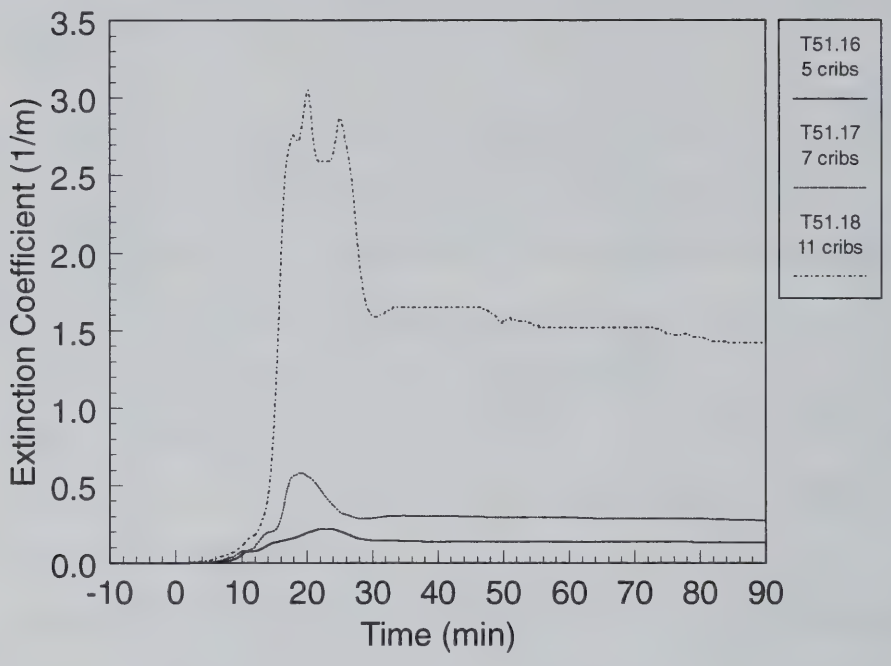

Figure 5.17: Level 1.600 Main Staircase Maint. Hatch Extinction Coeff. (CG2166)

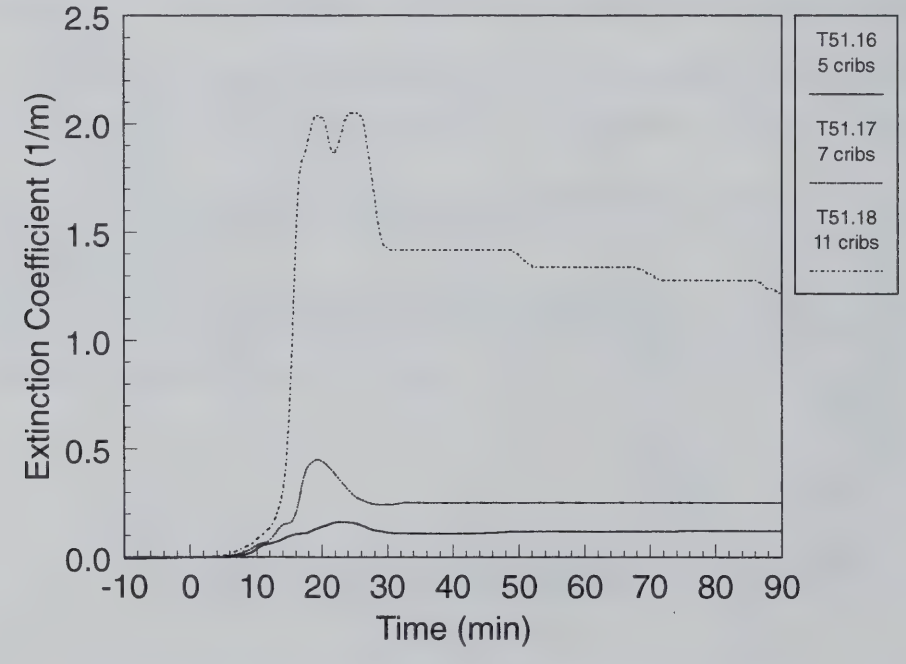

Figure 5.18: Dome Extinction Coefficient (CG2104)

5.2 Representative Experimental Results

This subsection gives the value of various parameters for each of the wood crib tests at 16 minutes after the start of the fire. This time represents the peak pyrolysis rate for all three tests. The figures are plotted as parameter vs. number of wood cribs combusted. This allows for an easy comparison of the parameters on the basis of available fuel. Figures 5.19 and 5.20 show the upper and lower layer temperatures in the fire room. The following observations are made from these figures:

- Upper layer temperatures increase between tests T51.16 and T51.17. Little change in layer temperatures is seen between tests T51.17 and T51.18.
- Lower layer temperatures increase between test T51.16 and T51.17. During test T51.18 the lower layer temperatures do not increase further.
- Both layers have a non-uniform temperature distribution clearly showing the effects of the doorway, the location of the fire, and a cold region along the wall furthest from the wood cribs.
- Actually, CT4512 reaches the highest temperatures recorded for T51.16 with five wood cribs in the lower layer.
- The maximum temperature difference between the upper and lower layers for all three tests is identical, 700 °C. Since this difference remains constant, rather then increasing, with the number of would cribs it indicates that the tests become increasingly ventilation controlled as the number of wood cribs increases.
- Given the large overlap of temperatures between the two layers, and the temperature distribution itself, the concept of layers seems to be questionable at this point in the tests.

Figures 5.21 and 5.22 compare temperatures along the upper and lower layers of the hallway leading from the fire room to the maintenance hatch. Most of the observations made above for the fire room also apply to the hallway. In addition the following conclusions can be drawn:

- Both layers show nearly linear increases in temperatures with the number of wood cribs.
- The upper layer plume cools significantly as it moves down the hallway; however, during test T51.18 the cooling of the plume does not begin until a point halfway down the hallway as seen by the nearly identical temperatures for CT4674 and CT4673. Due to the underventilated nature of T51.18 burning may have occurred in the hallway beyond the fire room doorway. This would prevent the cooling of the plume in the hallway.
- The air entering the hallway's lower layer is just above the ambient temperature. This cold air is coming underneath the curtain surrounding the maintenance hatch. Its near ambient temperature indicates that the hot plume from the fire room does not mix with the cold returning air in the curtained area.
- The air exiting the hallway's lower layer into the fire room is significantly above the ambient temperature indicating a large degree of thermal mixing between the hot and cold gas streams occurs in the hallway.

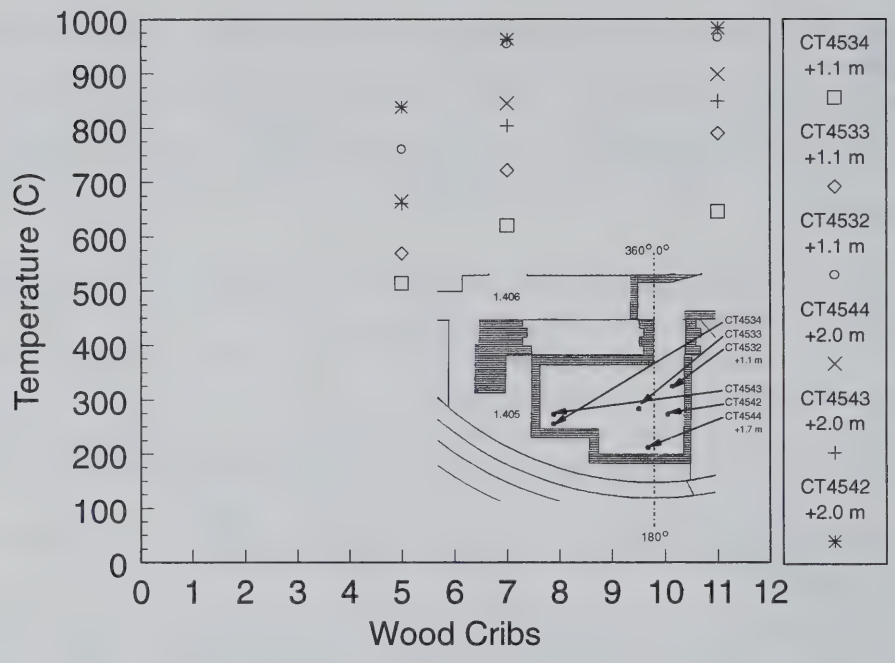

Figure 5.19: Fire Room Upper Layer Temperatures at 16 Minutes

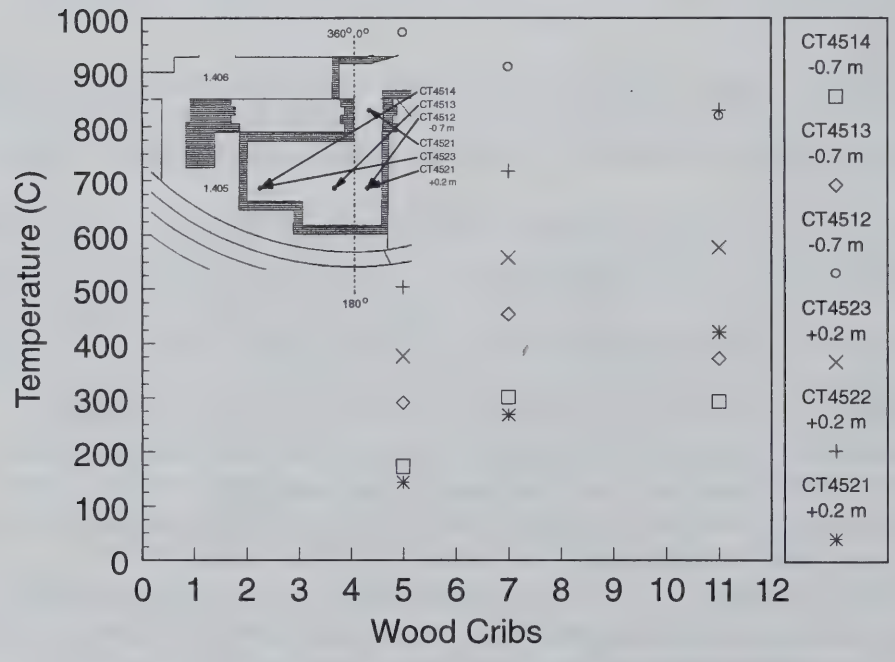

Figure 5.20: Fire Room Lower Layer Temperatures at 16 Minutes

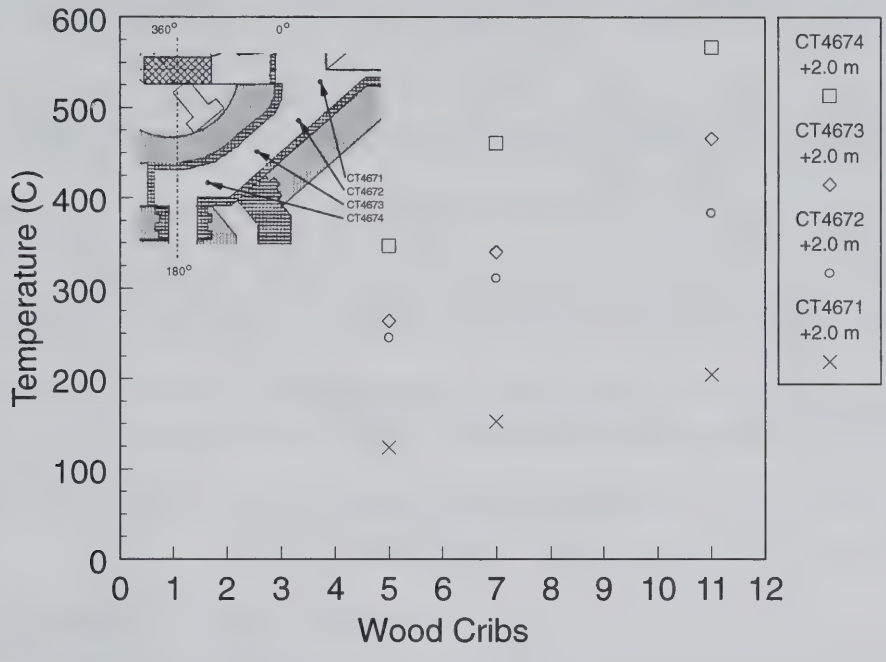

Figure 5.21: Hallway Upper Layer Temperatures at 16 Minutes

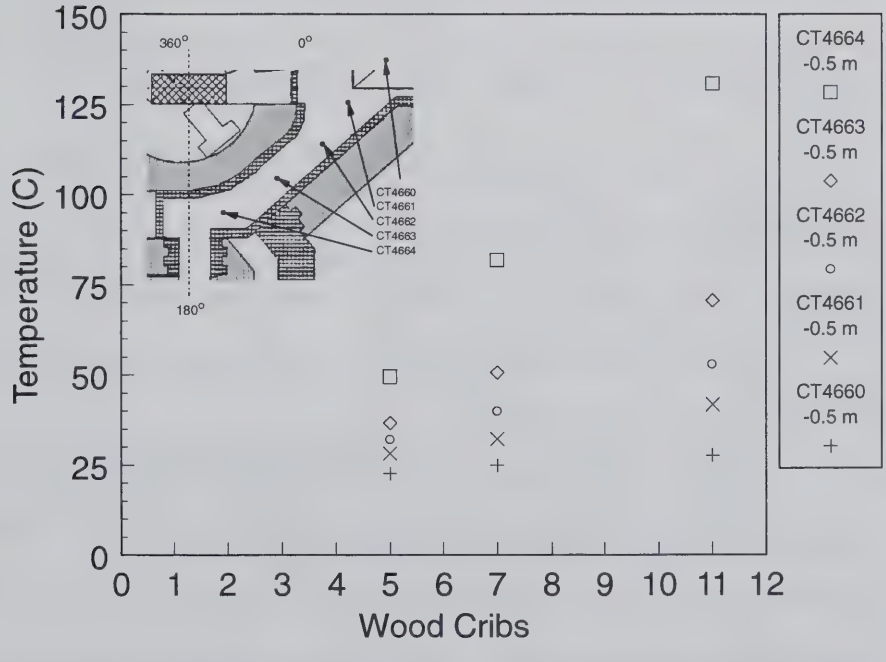

Figure 5.22: Hallway Lower Layer Temperatures at 16 Minutes

The next two figures, Figures 5.23 and 5.24, show temperatures in the main staircase maintenance hatch and in the dome. The following observations are made:

- CT5303 which lies in the open area of the maintenance hatch on the 1.500 level is seemingly located on the edge of the plume because its temperatures are lower than the thermocouple above it, CT6609 for all three tests.
- The plume entrains significantly and cools between the 1.500 level and the 1.600 level; however, it cools only slightly between the 1.600 level and the 1.700 level. At some point on the 1.600 level the plume becomes constrained due to the flow restrictions created by the walls and the limited opening of the maintenance hatches, it can partly spread over to the staircase.
- Within the dome the plume cools to ambient temperatures as it reaches the spiral staircase. The large free air volume in the dome allows for significant entrainment into the remaining buoyant plume.
- All the temperatures show an increase with the number of wood cribs; however, this increase is not linear due to the underventilated nature of test T51.18.

Figures 5.25 and 5.26 display the O_2 and CO_2 concentrations measured in the upper layer of the fire room doorway. As expected, the data indicate that as fire power increases the hot gasses leaving the fire room become increasingly depleted in O_2 and increasingly enriched in CO_2 at the same time. The underventilated nature of test T51.18 is clearly indicated by both the 0% O_2 concentration and by the nonlinear increase in CO_2 concentrations as the number of wood cribs increases.

The final figures in this section, Figures 5.27 and 5.28, show CO_2 concentrations at various axial levels in main and spiral staircase maintenance hatches. The following is noted:

- CG1146 in the main staircase is located in the lower layer of the curtained area. It shows nonzero CO_2 levels in the airflow beneath the curtain. This results from the global circulation of combustion products throughout the HDR facility as a result of the vertical shafts formed by the staircases and maintenance hatches. At 16 min. combustion products have been transported up to the dome via the main staircase flowpaths and back down to the lower levels by the spiral staircase flowpaths.
- CG1153 does not appear to be within the plume as it shows much lower CO_2 levels than other instruments in the main staircase region.
- As already seen in the main staircase temperatures, Figure 5.22, also confirms that the CO_2 levels decrease insignificantly in the upper levels of the facility just below the dome. This further supports the conclusion that the plume has become limited by flow restrictions and bounding walls and that the entrainment is small little air in that region.
- A continuous drop in the CO_2 concentration is achieved as the plume circulates through the HDR facility.
- Dilution of the CO_2 concentration between 10.2 m and 31.0 m along the plume is 0.14 vol % to 0.17 vol %.
- CO_2 concentration decreases by a factor of two to three between the main and the spiral staircases due to mixing and entrainment in the dome.

- CO_2 concentration increases in the spiral staircase in the direction of lower axial positions, e.g. toward the fire room.

Figure 5.23: Main Staircase Hatch Temperatures at 16 Minutes

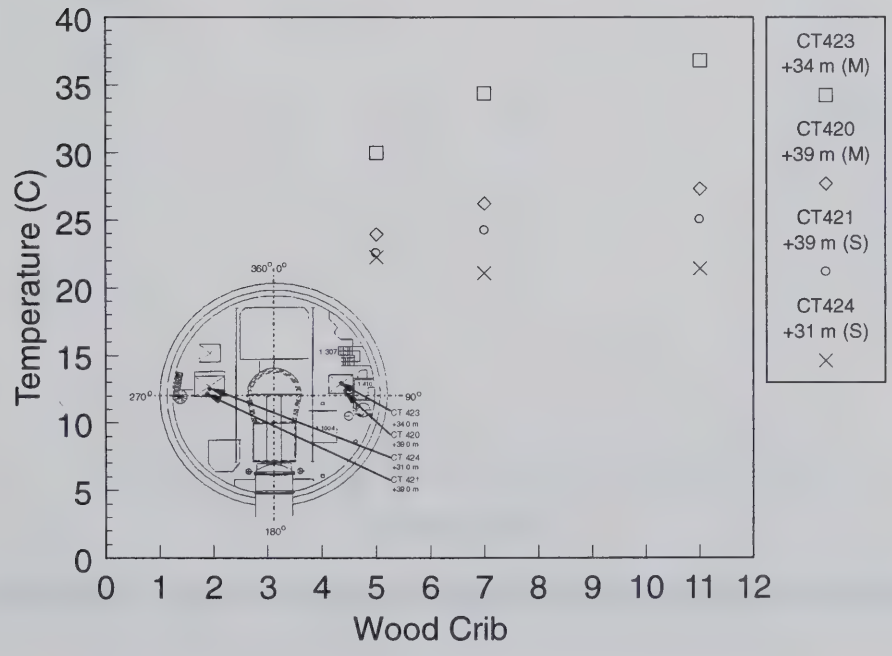

Figure 5.24: Dome Temperatures at 16 Minutes

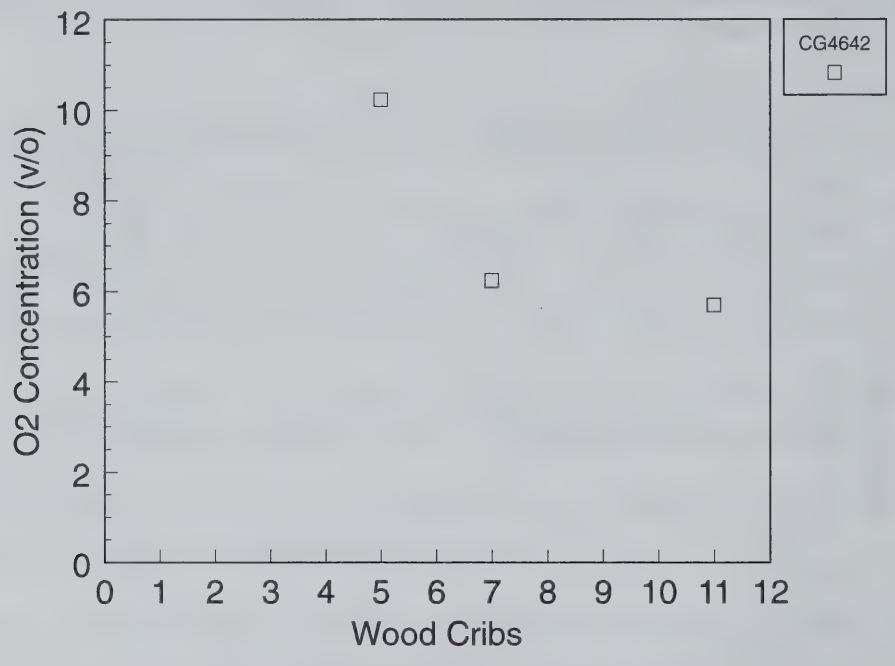

Figure 5.25: Doorway Upper Layer O_2 Concentration at 16 Minutes

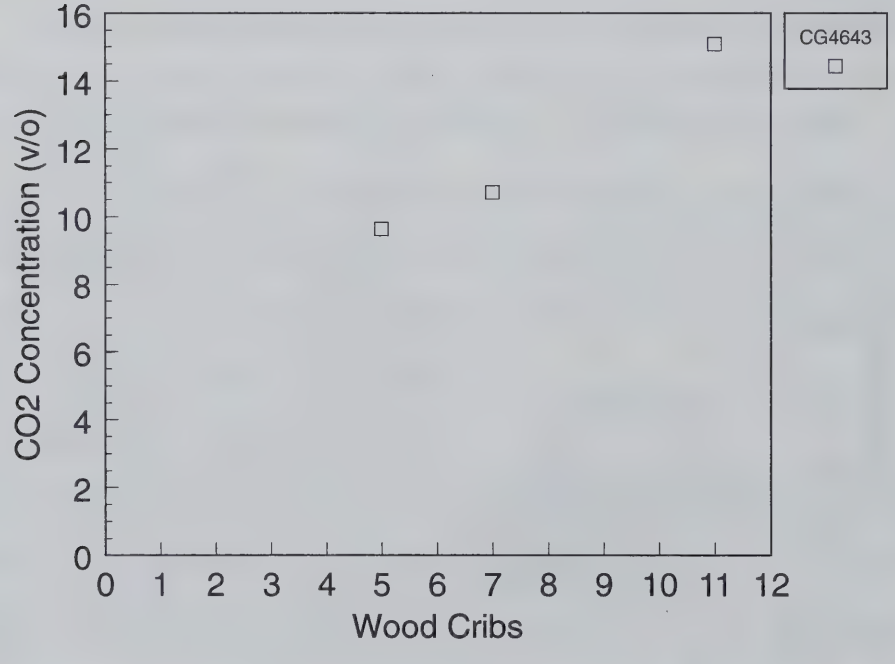

Figure 5.26: Doorway Upper Layer CO_2 Concentration at 16 Minutes

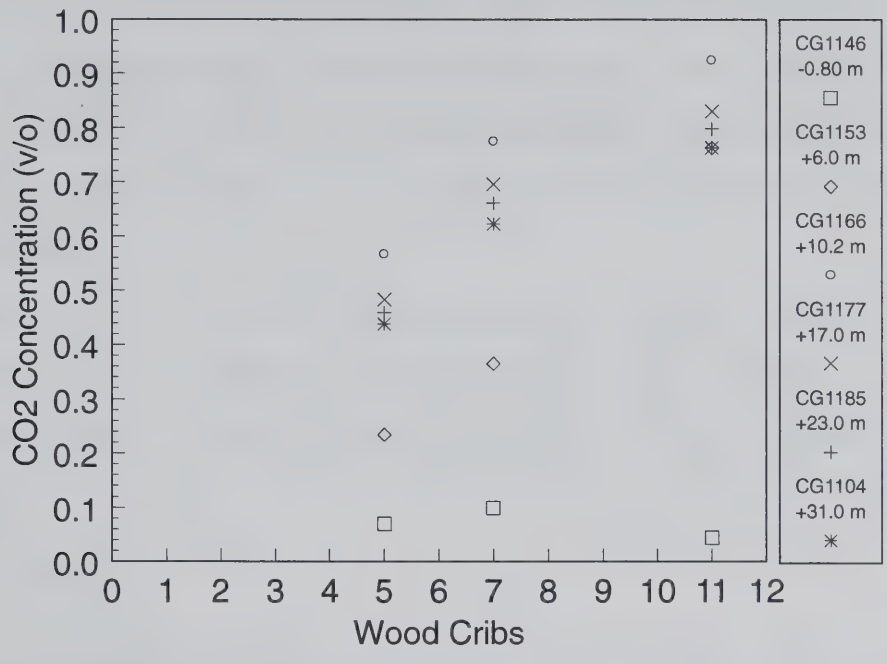

Figure 5.27: Main Staircase Maint . Hatch CO_2 Concentrations at 16 Minutes

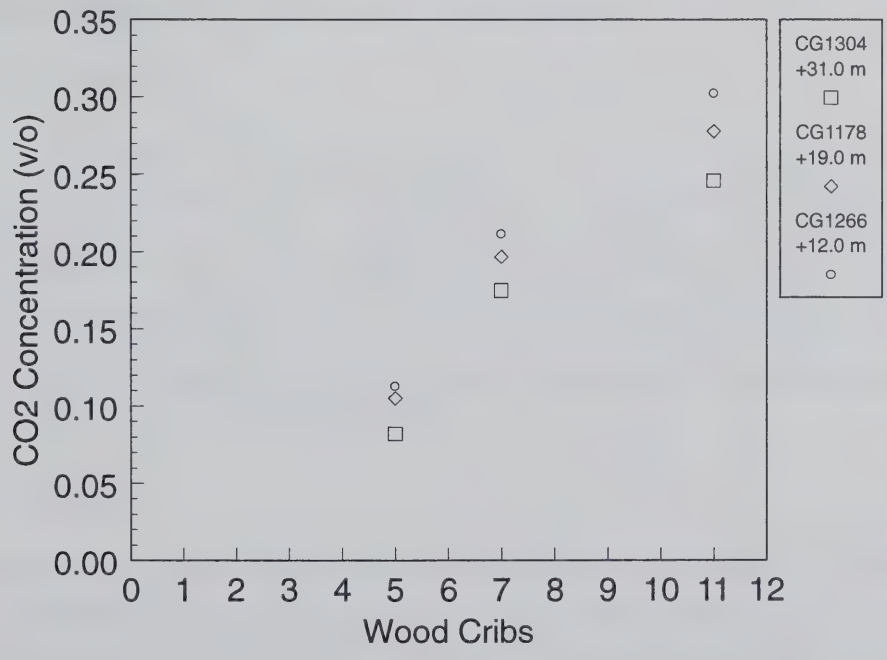

Figure 5.28: Spiral Staircase Maint. Hatch CO_2 Concentrations at 16 Minutes

6 POTENTIAL OF EXPERIMENTAL DATA FOR CODE VALIDATION

One of the primary purposes of the HDR fire experiments was to create a database of experimental data for use in code validation and model development. This section will discuss aspects of the T51 wood crib fire tests and the related data that can be used for code validation. The tests will be discussed in terms of zone models, containment system codes and field models.

6.1 Zone Models

Zone model fire codes, such as CFAST [29,30] and MRFC, operate by assuming that in a fire situation every room in a building can be represented by two layers: a hot layer containing the combustion products from the fire and a cold layer which is oxygen rich. A number of elements of the instrumentation plan for the T51 wood crib tests were established for the purpose of collecting data for the evaluation of zone model codes. Some of these elements are discussed in this subsection.

6.1.1 Layer Height

The key parameter calculated by a zone model code is the layer height. The instrumentation plan for the wood crib tests was such that layer heights are only obtainable in the fire room and the fire room doorway. The fire room was instrumented with an array of thermocouples that had four axial levels and the doorway with a rake of thermocouples having five axial levels. The remainder of the facility lacked vertical rakes of thermocouples.

6.1.2 Layer Temperatures

For the three wood crib fires sufficient thermocouples are available to evaluate the layer temperatures in the fire room, the fire room doorway, and the hallway. The fire room thermocouples were discussed above. In the hallway instrumentation consisted of three sets of thermocouples along its length. Two of these were triplets of thermocouples with one near the floor of the hallway, one near the hallway's middle elevation, and one near the hallway's ceiling. The third set was a pair of thermocouples with one at the floor and the other in the middle of the hallway. Thus, the temperature for each layer in the hallway can be obtained an average of the temperatures for the entire length of the hallway.

6.1.3 Mass Flow Rate

In those locations were layer height and velocity information exist or where a velocity sensor is located in a maintenance hatch, mass flow rates between compartments or between levels can be determined. In the case of horizontal flow the doorway dimensions and layer height information is used to determine the flow area of the layer. This along with the ideal gas law and layer temperature then yields the mass flow rate. For vertical flow, assuming that the plume occupies the whole hatch can also yield a rough estimate of the mass flow estimate.

During the wood crib fire tests T51.1 experiments only two velocity sensors yield horizontal mass flow data. These were located in the upper layer of the fire room doorway and in the lower layer of the hallway.

A number of sensors were positioned in the hatches for the wood crib fire tests. Mass flow data is therefore available for the main staircase on three levels: the 1.500 level, the 1.700 level, and the 1.800 level. Data are also available for flow down the spiral staircase hatch on the 1.700 level.

6.1.4 Optical Smoke Densities (Extinction Coefficients)

The wood crib fire tests produced varying quantities of smoke which were transported throughout the HDR facility. Test T51.18 produced large quantities of smoke which heavily coated the surfaces in the facility. A number of sensors were placed in the facility to measure the optical smoke density. The sensors were in three locations: a vertical rake in the hall connecting the spiral and main staircases on the 1.600 level, in the main staircase hatch on the 1.600 level, and in the main staircase hatch in the dome.

6.2 Containment System Codes

Containment system codes, such as GOTHIC [31] and RALOC, owe there origin to the nuclear power industry. The need to evaluate the effects of loss-of-coolant accident scenarios in a containment building requires thermal hydraulic codes that accurately model the two-phase, thermal-hydraulic response of a large building to a source of energy, mass, and momentum, e.g. a break in a reactor coolant pipe. Containment system codes commonly use the lumped parameter method, that is a compartment is considered to be a single point whose properties represent the volume-averaged properties of the compartments. By modifying the source to be combustion gases and radiant heat rather than steam and water, containment system codes can be applied to computing the effects of fires on large structures. These codes usually model all vents between compartments, heat transfer to structures, sprays, ventilation systems, etc. In the case of GOTHIC, the discretization options also include a combination of lumped and distributed parameter nodalizations (1-D, 2-D, and 3-D).

For the purpose of fire modeling some adjustments to the typical lumped parameter approach must be made. In order to appropriately generate the buoyant driving force for fire drive flow, the fire compartment and any immediately adjoining rooms cannot be modeled as lumped volumes. Rather each room must be subdivided into a network of lumped volumes to allow for thermal stratification in these compartments.

6.2.1 Compartment Temperatures

As many regions outside the fire compartments and adjoining compartments are modeled as lumped volumes, this results in more useable temperature information in the T51 data set than for the zone models. For all of the T51 tests, temperatures can be obtained for the fire room, the doorway, the hallway, the curtained area, the 1.400 level outside the curtain, at each level for both the ascending and descending flow through the maintenance hatches, the dome, and the connecting hallway between the spiral and main staircases. These regions represent the entire circulation loop induced by the wood crib fires.

6.2.2 Compartment Mass Flows

For the most part, system codes rely on single or multiple openings to connect compartments. Therefore, the wood crib tests are not very useful for system codes for comparing mass flows due to the lack of velocity sensors. The vertical flows up the hatches are suitable for comparison with system codes.

6.2.3 Wall Heat Conduction

The wood crib tests featured heat transfer blocks. The data from these sensors have been used to determine the time-dependent heat transfer into the HDR surfaces. As the storage and release of energy into structures is very important in nuclear accident analysis, system codes tend to contain robust algorithms for heat conduction into layered structures, e.g the coated and painted wall surfaces. The measurement blocks used in the HDR were designed for the purpose of evaluating these algorithms as well as obtaining the steady-state and the transient behavior of the heat transfer coefficient to compare with common correlations.

6.2.4 Combustion Models

The nuclear containment codes were originally designed for the purpose of calculating a containment building's response to a loss of coolant accident in a nuclear power plant. Therefore, the energy, mass, and momentum sources that were originally coded were steam-water mixtures and hydrogen from metal-water reactions. For these codes to be used to model the effects of fires in containment buildings, additional models relating to the calculation of combustion physics were added. Unlike the models relating to energy and mass inputs from pipe breaks, these new combustion models have not been thoroughly tested. Therefore the pyrolysis and combustion product measurements made during these tests are invaluable to evaluating the effectiveness of these models.

6.3 Field Models

Field models, such as FLUENT [36], FLOW-3D, and NIST-LES [37], operate by solving a discretized form of the three-dimensional equations for mass, momentum, and energy conservation. For most real structures, accurate resolution of the velocity, temperature, and species field for a fire require a large number of computational nodes. Therefore, use of field models is typically restricted to smaller subsets of a larger structure to reduce the computational resource requirements.

The wood crib fire tests were sparsely instrumented for the needs of a field model; however, the fire room instrumentation is sufficient for some field model testing. Since the wood cribs were located in front of the fire room doorway, the region of the fire room without the wood crib was a cooler region of the fire room. A field model code should be able to reproduce that local phenomena. Also, the field model should be able to reproduce the temperature distribution seen as a result of the fire itself and due to the inrush of cooler air from the hallway. This information along with velocity and gas sensors in the doorway can be used to qualitatively and for some aspects quantitatively verify a field model of the fire room. The adequacy of this approach may depend on the accuracy of the boundary conditions to be applied to the model based on rather coarse instrumentation.

7 T51 WOOD CRIB CFAST MODEL

The T51 wood crib fire tests were modeled using a modified version of the C model used for the T51 gas fire tests [34]. This section will discuss the runtime and environmental parameters, the combustion properties for the fire, the room surface properties, and the geometric model developed for the CFAST computations [29,30]. A full description of the development path for this CFAST model can be found in Volume 2 of the report [34]. It is noteworthy to mention that the most significant change to the gas fire model, other than the fuel, is that the upgraded version of CFAST used for this report, v3.1.1, was capable of modeling the HDR as an enclosed facility unlike the gas fire model which unrealistically required a vent open to the outside for the duration of the run.

7.1 Environment and Runtime Control

The T51 wood crib tests had a fire duration of approximately 45 minutes. Data collection during the tests began 10 minutes prior to the fire's start and continued for a period of 40 to 60 minutes after the end of the fire. No preconditioning of the containment building was performed before the start of any tests, i.e. the containment was at ambient conditions at the start of each test in the series. The CFAST model reproduced these conditions with a 100 s pretest period with no fire to generate a baseline followed by the appropriate fire conditions for a duration of 90 minutes from the ignition of the wood cribs. Table 7.1 below shows the CFAST input cards for environment and runtime control.

Table 7.1: Environment and Runtime Control Input Cards for CFAST

Card	Variable	Value	Reason
TIMES	Simulation Time (s)	5500	100 s pre-fire + 90 min post-fire
	Print Interval (s)	100	
	History Interval (s)	50	
	Display Interval (s)	0	No graphics
	Copy Count	0	No graphics to copy
STPMAX	Maximum Time Step (s)	1	Advice of code developers
TAMB/ EAMB	Ambient Temperature (K)	288	15° C
	Ambient Pressure (Pa)	101300	1 atm.
	Station Elevation (m)	0	Set hallway floor as 0 elevation

7.2 Combustion Model

Each of the tests in the T51 wood crib series used a different number of identically constructed wood cribs set on a platform in the fire room, see Figure 2.2 on page 2-5. This platform was placed on top of three digital scales from which the pyrolysis rate was determined. These measurements form the basis for the combustion parameters used for the CFAST models.

Wood has an approximate empirical chemical formula of $C_{0.95} H_{2.4} O$. The heat of combustion of the TYPE OF WOOD used in the T51 wood crib tests is estimated to be 12600 kJ/kg. This estimate is based on the maximum fire powers developed during the wood crib tests as reported

in [10]. However, this empirical formula cannot be directly used in CFAST v3.1.1. Specifying oxygen as part of a fuel description in CFAST results in the formation of unrealistic combustion products. This is discussed in Appendix B. Therefore, the oxygen in the wood was ignored and the pyrolysis rate and heat of combustion adjusted as follows to conserve species mass and energy input for the models:

- Wood is 38.3% C, 21.1% H, and 53.6% O. Therefore, when the oxygen is considered absent 53.6% of the experimentally pyrolyzed mass must be removed in order to keep constant the mass of carbon and hydrogen available for combustion. The experimentally measured pyrolysis rates were reduced by 53.6% before being input into CFAST.
- If the mass of fuel is reduced by 53.6%, the heat release rate will also be reduced if the heat of combustion is not adjusted. To preserve total energy release, the heat of combustion was increased by 116% to 27200 kJ/kg.

Testing on these changes was performed using a single room model to verify that the appropriate total heat release and CO_2 was achieved.

The final parameters required for specifying the fuel was to provide the CO and soot production values. In reality these parameters are quite complex for a wood fire, and given the available data for the HDR, they were not known. Therefore, the CFAST preprocessor was used to define a single compartment fire using plywood as a fuel. The preprocessor determined values were assumed to be reasonably representative of wood crib fires and thus subsequently used for input into CFAST.

With the combustion product information and the basic fuel information, the CFAST input cards relating to combustion were completed. The applicable cards and their values are shown in Table 7.2 for test T51.16 which was a test with 5 wood cribs. For the other tests modeled, modified cards include FAREA (changed to reflect the number of wood cribs used), FMASS (to reflect the measured pyrolysis rate for each test), and FQDOT (to reflect the current test's fire power). These fire power related changes are documented in the input decks presented in Appendix A. The remaining combustion parameters were not changed between the tests modeled.

Table 7.2: Combustion Related Input Cards for CFAST

Card	Variable	Value	Reason
LFBO	Fire Origin	1	Fire is in compartment 1
LFBT	Fire Type	2	Constrained fire
CHEMI	Molar Weight (GMW) Relative Humidity (%) Lower Oxygen Limit (%) Heat of Combustion (J/kg) Initial Fuel Temp. (K) Gas Ignition Temp. (K) Radiative Fraction (%)	13.8 20 0 2.721E+07 293. 493. 0.20	Molar weight of empirical wood with no O_2. Default value. Experimental data shows very low O_2 levels. Adjusted heat of combustion of wood. Room temperature. 200 K over initial temperature. Default value.
CJET	Ceiling Jet	Off	No reason to use the additional model.
FAREA	Fuel Area (m^2)	0.0 0.0 0.709 0.709 0.709 0.709 0.709 0.709 0.709 0.709 0.0	Floor area of 5 wood cribs.
FHIGH	Fuel Height (m)	0.0 0.0 0.281 0.281 0.281 0.281 0.281 0.281 0.281 0.281 0.0	Platform is 0.281 m high.
FMASS	Mass Loss Rate (kg/s)	0.0 0.0 0.00926 0.0426 0.03705 0.01806 0.02454 0.01158 0.00232 0.00116 0.0	Taken from experimental data.
FPOS	Depth (m) Breadth (m) Height (m)	1.475 1.825 0.000	Locate fire in center of compartment.
FQDOT	Heat Release Rate (W)	0.0 0.0 252000 1159200 1008000 491400 667800 315000 63000 31500 0.0	Calculated from FMASS and heat of combustion.
FTIME	Time Points (s)	100. 700. 1000. 1126. 1306. 1480. 1720. 2260. 3100. 4900.	Taken from experimental data.
HCR	H to C Mass Ratio for Fuel	0.0 0.0 0.2105 0.2105 0.2105 0.2105 0.2105 0.2105 0.2105 0.2105 0.0	$\frac{2.4\times1}{12\times0.95} = 0.2105$
OD	C to CO_2 Ratio for Combustion Products	0.0 0.0 0.03 0.03 0.03 0.03 0.03 0.03 0.03 0.03 0.0	Taken from predefined plywood wardrobe fire.
CO	CO to CO_2 Ratio for Combustion Products	0.0 0.0 0.03 0.03 0.03 0.03 0.03 0.03 0.03 0.03 0.0	Taken from predefined plywood wardrobe fire.

7.3 Surface Properties

To model the HDR with CFAST requires generating material properties for the HDR's construction materials. For the T51 wood crib tests there are three materials which must be defined which are the HDR structural concrete, Ytong fire brick, and Alsiflex fireproof, glass fiber matting. A CFAST material library was created for these materials and the surfaces which were constructed from them. Table 7.3 gives the thermophysical material properties which were obtained from [20].

Table 7.3: Thermophysical Properties for HDR Construction Materials

Material	Density (kg/m^3)	Conductivity (W/m·K)	Heat Capacity J/(kg·K)	Emissivity
Concrete	2,225	2.10	879	0.8[1]
Ytong Firebrick	340	0.24	950	0.8[1]
Alsiflex Mats	130	0.17	1,000	0.9[2]

[1] Taken as firebrick from default CFAST material library
[2] Taken from Alsiflex properties in [35]

The above thermophysical properties were used to create a seven material library for use with CFAST. The seven materials included five, single layer materials and two, two layer materials. The materials in the order listed below are 3 cm thick Alsiflex matting, 100 cm of concrete, 50 cm of concrete, 10 cm of Ytong firebrick, 25 cm of Ytong firebrick, the Alsiflex matting and Ytong firebrick ceiling for the fire room, and the Ytong firebrick and concrete floor of the fire room. The material library is shown below. For single layer materials the format is material name, conductivity, density, heat capacity, thickness, emissivity, and seven parameters for HCl production. For multiple layer materials the format is the same with a '/' denoting values for each layer.

```
ALSIFLEX  0.17 1000 130 0.03 0.9 0 0 0 0 0 0 0
CONCR100  2.1 879 2225 1 0.8 0 0 0 0 0 0 0
CONCR050  2.1 879 2225 0.5 0.8 0 0 0 0 0 0 0
YTONG100  0.24 950 340 0.1 0.8 0 0 0 0 0 0 0  0
YTONG250  0.24 950 340 0.25 0.8 0 0 0 0 0 0 0  0
FIRECEIL  0.17/0.24 1000/950 130/340 0.03/0.25 0.9 0 0 0 0 0 0 0
FIRE_FLR  0.24/2.1 950/879 340/2225 0.25/1 0.8 0 0 0 0 0 0 0
```

7.4 Compartments and Compartment Interconnections

The final portion of the CFAST model is the compartment definitions and the compartment interconnections. As the HDR facility contains 9 levels and over 60 compartments with complex interconnections, it is not feasible to model it explicitly with CFAST. Therefore, simplifications were made to model the HDR facility with CFAST. These simplifications reduced the HDR to a three level structure composed of the fire compartments on the 1.400 level, the 1.600 level, and a lumped level consisting of all building elevations above the 1.600 level. The development of the

CFAST model benefited greatly from the experience gained simulating the gas fire tests [34] plus some progress made in version 3.1.1 relating to completely enclosed fires.

Figure 7.1 shows the 1.400 level. From this figure it is obvious that the important compartments were the fire room and its doorway, the hallway, and the curtained area as these compartments defined the location of the fire and the flowpath taken by the combustion products. The curtained area had a 0.5 m gap at the floor for the return of cold air. This air could come from either room 1.402 or the main staircase, which in itself was connected to room 1.402. Room 1.402 had a fairly narrow connection to the rest of the containment building, so this restriction should be accounted for to create a flowpath resistance for returning cold air. Therefore, the 1.400 level of the model consisted of five compartments which were the fire room and its doorway, the hallway, the curtained area, the main staircase, and room 1.402.

From the dimensions given in Figure 7.2, the volume of the fire room and doorway was calculated to be 29.6 m^3 with the doorway having 3 m^3 of that volume. Since the doorway was such a small volume in comparison to the fire room and the hallway, it was assumed to be part of the fire room. Therefore, as the fire room was 2.75 m in height, the floor area of the fire room is 10.77 m^2. If the linear distance from the fire room's back wall to the doorway opening into the hallway was preserved, as this is represents the room dimension about the wood crib platform, the floor dimensions of the fire room became 3.65 m x 2.95 m. The surfaces of the fire room consisted of a ceiling lined with 0.25 m of Ytong firebrick covered by 0.03 m of Alsiflex mats, the walls of the fire room lined with 0.25 m of Ytong firebrick, and the fire room floor which was 0.25 m of Ytong firebrick on top of a 1 m thick concrete floor. The fire room was connected to the hallway by a 1.01 m x 1.975 m doorway.

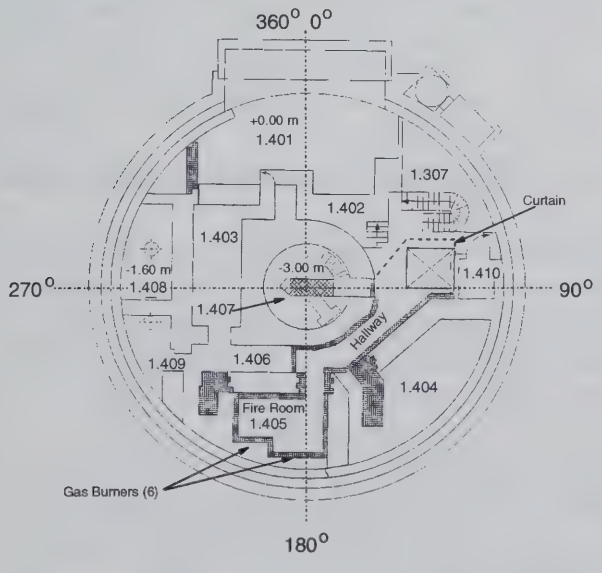

Figure 7.1: Level 1.400

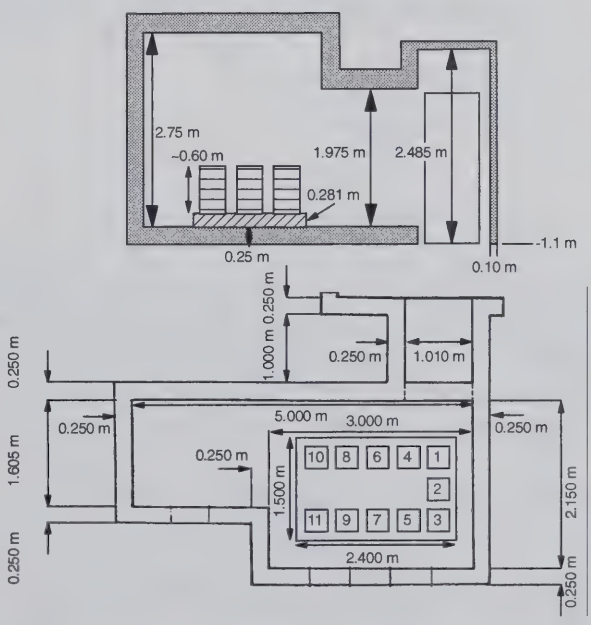

Figure 7.2: Fire Room and Doorway

Figure 7.3 shows the hallway that connected the fire room to the maintenance hatch. Reference [9] gives the volume of the hallway as 22.15 m^3 with a ceiling height of 2.485 m. The hallway had a variable width and a curved length which did not readily translate into a rectangular parallelepiped for modeling purposes with CFAST. The dimensions of significance for the hallway were the height and the width of the hallway where it connected to the maintenance hatch; this was also the widest cross section of the hallway. This resulted in the hallway having floor dimensions of 1.8 m x 4.95 m. The hallway surfaces were 0.10 m of Ytong firebrick for the walls and ceiling and 0.50 m of concrete for the floor. The hallway was connected to the curtained area by a 1.8 m x 2.75 m opening.

Figure 7.4 shows the curtained area beneath the maintenance hatch. The hatch itself was a rectangular opening 4.54 m^2 in area. Using the hatch dimensions shown in the figure and assuming the figure was to scale, the curtained area floor dimensions were found to be 4.30 m x 2.75 m. The height of this region was 4.60 m. All surfaces were assumed to be 0.50 m thick concrete. The hatch was connected to the outside by a 4.54 m^2 rectangular opening. From Figure 7.4, the flow path underneath the curtain to room 1.402 and the main staircase was estimated to be 2.0 m x 0.5 m and 4.3 m x 0.5 m, respectively.

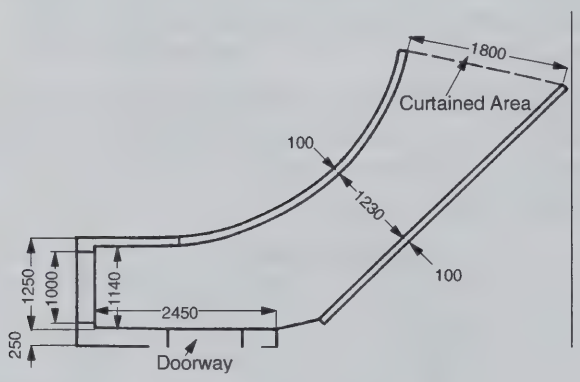

Figure 7.3: Hallway

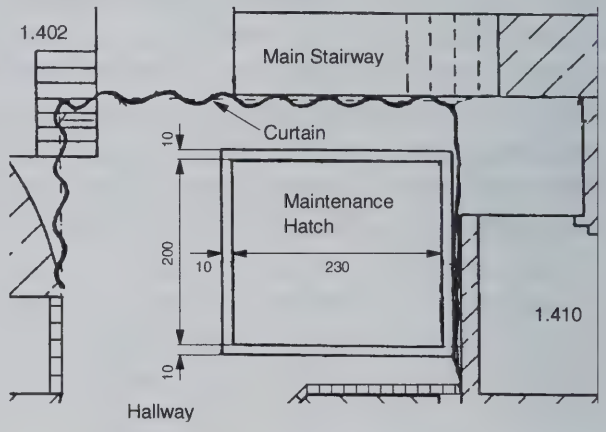

Figure 7.4: Maintenance Hatch and Curtain

The main staircase had the same floor and ceiling elevations as the hatch area, 4.60 m in height. The floor area of the main staircase was estimated to be 11.78 m^2, 4.33 m x 2.72 m, by using Figure 7.1 and the HDR steel shell diameter of 20 m. All surfaces were again assumed to be 0.50 m thick concrete. The vertical flow path up the main staircase was 5.75 m^2. The connection to room 1.402 was estimated from Figure 7.1 to be 2.7 m x 3.1 m.

Since experimental data from the T51 test series indicated that the 1.500 level was not involved in the global flows during the tests it was not modeled in CFAST. Therefore, the 1.400 level vertical connections from the hatch and staircase had their ceiling heights extended to connect them directly to the 1.600 level. This resulted in the compartment height for these two compartments to be implemented as 11.10 m rather than 4.60 m.

Room 1.402 also had its floor area dimensions estimated from Figure 7.1. The floor dimensions were estimated to be 1.80 m x 6.50 m with a height of 3.50 m. All surfaces were 0.50 m thick concrete. The connection from room 1.402 to the outside is given in [1] as 0.8 m x 1.5 m.

On the 1.600 level, there were three significant regions, as shown in Figure 7.5. The vertical flow paths created by the 1.400 level main staircase and maintenance hatch must be continued. The portion of the 1.600 level connecting the two staircase regions needed to be included. Finally, the spiral staircase and its maintenance hatch also needed to be included. Since room 1.603 is an isolated compartment that is connected solely to the spiral staircase it can be considered part of the staircase region. Therefore, the 1.600 level portion of the model contained four compartments: the curtained area on the 1.600 level, the main staircase on the 1.600 level , the spiral staircase and room 1.603, and the remainder of the 1.600 level.

The main staircase and hatch compartments were given the same floor dimensions on the 1.600 level as they were on the 1.400 level. The height of these compartments was set to 5.05 m which places the ceiling of these compartments at the elevation of the 1.700 level's floor. All surfaces were set to 0.50 m thick concrete. The maintenance hatch area leading to the outside remained unchanged from the A model, but the main staircase vent was set to a 6.97 m^2 rectangle.

The volume of the room 1.603 and spiral staircase compartment was set to equal the sum of the compartment volumes for 1.603 and 1.611 which is 472 m^3. A height of 5.05 m was also used for this compartment. The dimensions of the floor were set to a square as there was no dominant linear dimension of interest for this compartment. The floor area was therefore set to 9.67 m x 9.67 m and all room surfaces were 0.50 m thick concrete. The hatch and spiral staircase vent to the outside was set to a 5.28 m^2 rectangle.

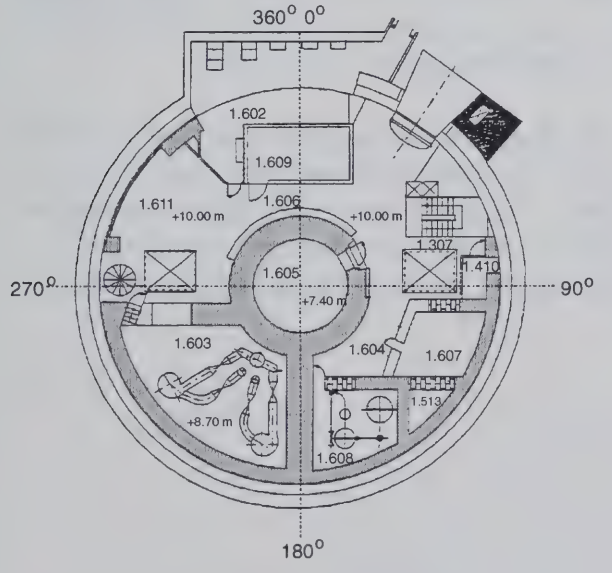

Figure 7.5: Level 1.600

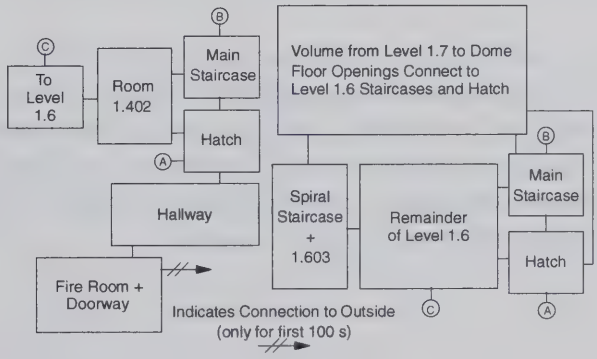

Figure 7.6: CFAST Model Block Diagram

The remainder of the 1.600 level included all of this level except for rooms 1.602 and 1.609 which were closed off. This resulted in a compartment volume of 288 m^3. The resulting compartment dimensions using a square floor were 7.92 m x 7.92 m x 4.60 m. All room surfaces were set to 0.50 m thick concrete. Vent connections were established between this compartment and the other three compartments on the level as well as between the main staircase and hatch.

The portion of the HDR facility above the 1.600 level was modeled as a single compartment. The volume of this compartment was obtained by summing up the volume of all compartments above the 1.600 level excluding rooms 1.702 and 1.706. This yielded a total volume of 7215 m^3 and preserving the full HDR height resulted in a compartment with dimensions of 14.37 m x 14.37 m x 39.95 m. All wall surfaces for this compartment were set to 0.5 m thick concrete which is not a true representation for the steel shell dome. The level 1.600 hatch and staircase openings to the were connected to this compartment.

There was one final compartment that was incorporated into the model. This compartment was added to allow flow to return from the dome, down the spiral staircase, and then down to the 1.400 level at room 1.402. Even though the spiral staircase hatch to the 1.500 level was closed, there did exist numerous floor penetration in the form of pipe channels, cable trays, and other conduits that connected the 1.600 level to the 1.500 level and the 1.400 level and these need to be included to properly model the HDR facility. The room connection list [1] was consulted and the area of available connections from the 1.400 level to the 1.600 level (excluding hatches and staircases) was totaled. This yielded a flow area of 9 m^2. Since CFAST would not initialize successfully with a completely enclosed geometry, a vent to the outside was created in this compartment which was closed after the 100 s null transient portion of the model. The resultant compartment started at an elevation of 0.3 m and extended vertically for 13.2 m, 2.4 m above the floor of the 1.600 level. The 1.600 level compartment connected with a 3.0 m x 2.4 m doorway, room 1.402 connected with a 1.8 m x 3.2 m doorway, and the vent to the outside was 0.05 m wide that extended from the ceiling of room 1.402 to the floor of the 1.600 level.

A block diagram of the wood crib model is shown in Figure 7.6 on page 7-7. The final CFAST model contained eleven compartments on three levels, the 1.400 level and part of the 1.500 level, the 1.600 level, and levels above the 1.600 level. These compartments were connected by a total of eighteen vents of which five were vertical flow vents. There was one vent to the outside which was closed before the start of the fire. Shown on the next page below are the CFAST input cards for this model.

```
HI/F   0.250  0.000  0.000  0.000  0.000 11.100 11.100 11.100 11.100 16.150  0.300
WIDTH  2.950  4.950  4.300  4.330  1.800  7.920  4.300  4.330  9.670 14.370  3.000
DEPTH  3.650  1.800  2.750  2.720  6.350  7.920  2.750  2.720  9.670 14.370  3.000
HEIGH  2.750  2.485 11.100 11.100  3.500  4.600  5.050  5.050  5.050 34.950 13.200
CEILI FIRECEIL YTONG100 CONCR050 CONCR050 CONCR050 CONCR050 CONCR050 CONCR050 CONCR050 CONCR050 CONCR050
WALLS YTONG250 YTONG100 CONCR050 CONCR050 CONCR050 CONCR050 CONCR050 CONCR050 CONCR050 CONCR050 CONCR050
FLOOR FIRE_FLR CONCR100 CONCR050 CONCR050 CONCR050 CONCR050 CONCR050 CONCR050 CONCR050 CONCR050 CONCR050
HVENT  1  2  1  1.010  1.975  0.000
CVENT  1  2  1  1.000  1.000  1.000  1.000  1.000  1.000  1.000  1.000  1.000  1.000  1.000
HVENT  2  3  1  1.800  2.485  0.000
CVENT  2  3  1  1.000  1.000  1.000  1.000  1.000  1.000  1.000  1.000  1.000  1.000  1.000
HVENT  3  4  1  4.300  0.500  0.000
CVENT  3  4  1  1.000  1.000  1.000  1.000  1.000  1.000  1.000  1.000  1.000  1.000  1.000
HVENT  3  5  1  2.000  0.500  0.000
CVENT  3  5  1  1.000  1.000  1.000  1.000  1.000  1.000  1.000  1.000  1.000  1.000  1.000
HVENT  4  5  1  2.700  3.100  1.100
CVENT  4  5  1  1.000  1.000  1.000  1.000  1.000  1.000  1.000  1.000  1.000  1.000  1.000
HVENT  5 11  1  1.800  3.500  0.300
CVENT  5 11  1  1.000  1.000  1.000  1.000  1.000  1.000  1.000  1.000  1.000  1.000  1.000
HVENT  6  7  1  3.000  4.250  0.000
CVENT  6  7  1  1.000  1.000  1.000  1.000  1.000  1.000  1.000  1.000  1.000  1.000  1.000
HVENT  6  8  1  3.000  4.250  0.000
CVENT  6  8  1  1.000  1.000  1.000  1.000  1.000  1.000  1.000  1.000  1.000  1.000  1.000
HVENT  6  9  1  3.000  4.250  0.000
CVENT  6  9  1  1.000  1.000  1.000  1.000  1.000  1.000  1.000  1.000  1.000  1.000  1.000
HVENT  7  8  1  3.000  4.250  0.000
CVENT  7  8  1  1.000  1.000  1.000  1.000  1.000  1.000  1.000  1.000  1.000  1.000  1.000
HVENT 11 12  1  0.030  9.800  3.300
CVENT 11 12  1  1.000  0.000  0.000  0.000  0.000  0.000  0.000  0.000  0.000  0.000  0.000
HVENT  6 11  1  3.000  2.400  0.000
CVENT  6 11  1  1.000  1.000  1.000  1.000  1.000  1.000  1.000  1.000  1.000  1.000  1.000
VVENT  7  3  4.54000  2
VVENT  8  4  5.75000  2
VVENT 10  7  4.54000  2
VVENT 10  8  6.97000  2
VVENT 10  9  5.28000  2
```

8 CFAST RESULTS AND COMPARISONS WITH HDR DATA

This section compares the CFAST predictions using the model described in Section 7 with measured data from the actual tests for each of the three wood crib tests. Instrument descriptions and locations can be found in Section 3 of this report. The text and figures that follow will compare predictions made for the three wood crib tests with CFAST predictions to examine the effects of fire power and fuel availability on CFAST's predictive capabilities. In each of the figures that follow, the HDR sensor is identified by its instrument number and its axial position in terms of the HDR coordinate.

As this section discusses model comparisons with data, it is important to define what the authors consider a good versus a poor comparison. CFAST is designed to be a quickly executed engineering tool with a relatively small learning curve. Therefore, CFAST cannot be expected to make exact or near exact predictions to the data especially given the complexity of the HDR facility. However, it can be expected that CFAST should reproduce the same regional and transient trends as seen in the data, predict with reasonable accuracy the significant phenomena of the experiments, and not introduce significant non-existing phenomena.

The first set of figures, Figures 8.1 through 8.3, shows the pyrolysis rates used as inputs to CFAST vs. the pyrolysis rates as measured by the digital scales. It is clear from these figures that the pyrolysis rate utilized by CFAST closely matches the data, both in terms of maximal values and net mass input into the fire room. For the three tests the deviation from net mass input is 3.5%, 1.0%, and 0.4% respectively.

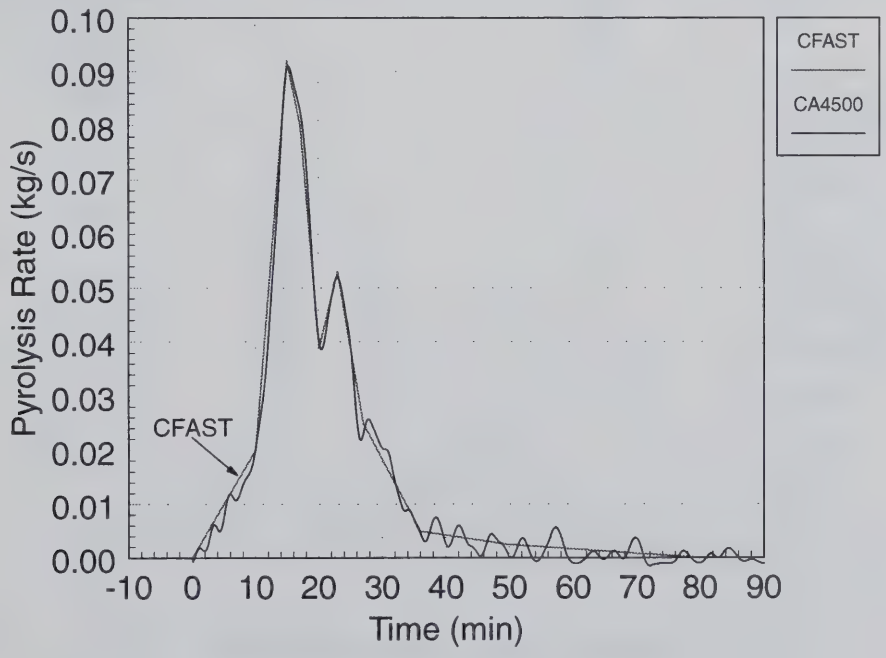

Figure 8.1: T51.16 Pyrolysis Rate

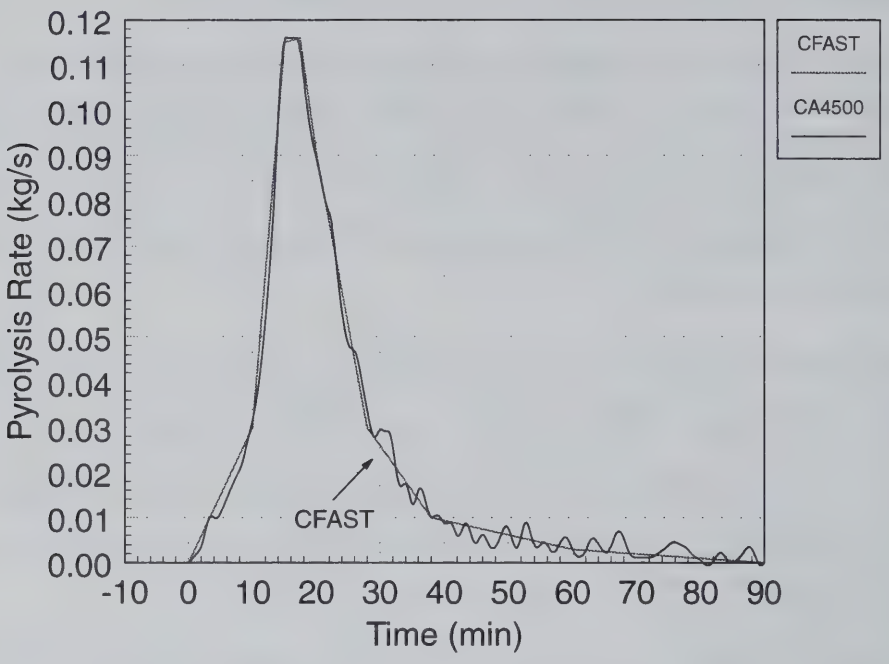

Figure 8.2: T51.17 Pyrolysis Rate

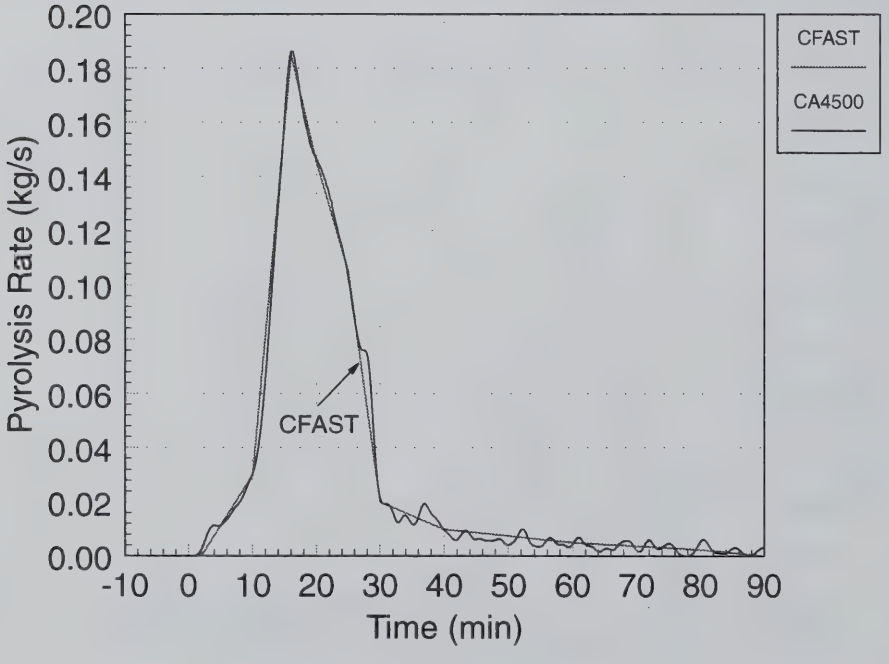

Figure 8.3: T51.18 Pyrolysis Rate

The next three figures, Figures 8.4 through 8.6, show the upper layer temperature in the fire room. The peak temperature predictions for all three tests are high with the maximum increasing with the number of wood cribs. The CFAST predictions agree surprisingly well during the heatup phase and match the transient temperature gradients of the fire room upper layer extremely well. However, the predicted cooldown is much to fast and thus leads to substantial non-conservative underpredictions. In other words, for the conditions examined, CFAST appears to be transferring energy appropriately to the fire rooms surfaces during the heatup phase, but is not releasing that energy correctly during the cooldown phase. CFAST results for test T51.18 show a puzzling behavior of the temperature increasing 80 ° C above the cooldown temperatures well after the fire was over As the only difference between the cases was the fuel availability, this indicates a possible problem within CFAST's algorithms..

The three figures following Figures 8.4 through 8.6 show the lower layer temperatures in the fire room, Figures 8.7 through 8.9. As with the upper layer, CFAST overpredicts the lower layer temperature with the prediction worsening as fuel availability increases. Unlike the upper layer, CFAST continues to overpredict the temperature during the cooldown period after the fire. Lastly, during tests T51.17 and T51.18 there are plateaus and secondary peaks in the measured data which are not predicted by CFAST. This last observation most likely results partially from artifacts caused by the approximated smoothly varying pyrolysis rate given to CFAST as input and mostly from the inability of a zone model code to calculate local temperature behaviors resulting from detailed geometric aspects of a compartment. It is quite obvious from the comparison between data and CFAST predictions for all three wood crib tests that the agreement both with respect to transient characteristics as well as quantitative values of the temperature in the lower layer leaves much to be desired. On the other hand, the predicted temperatures are seemingly conservative.

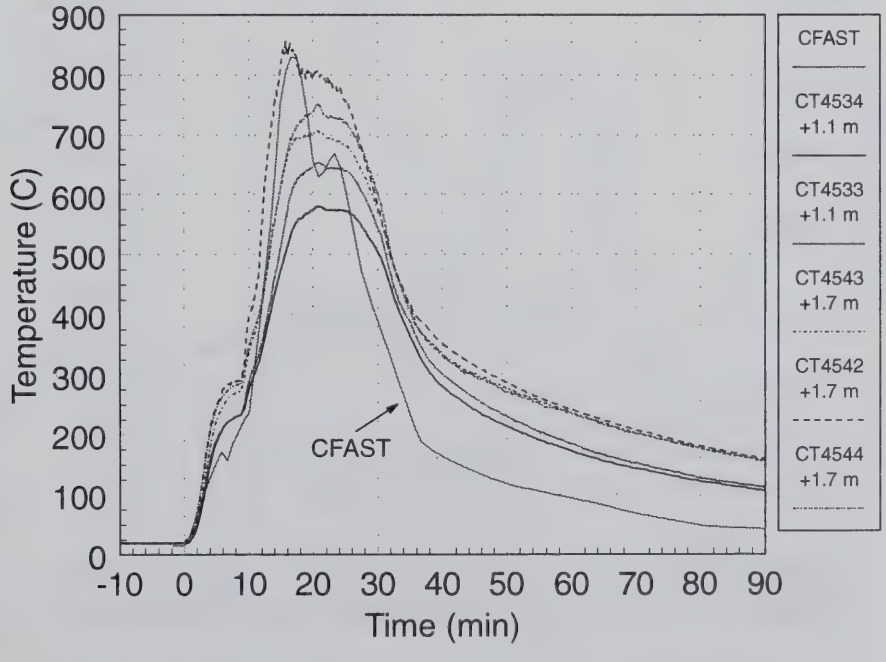

Figure 8.4: T51.16 Fire Room Upper Layer Temperature

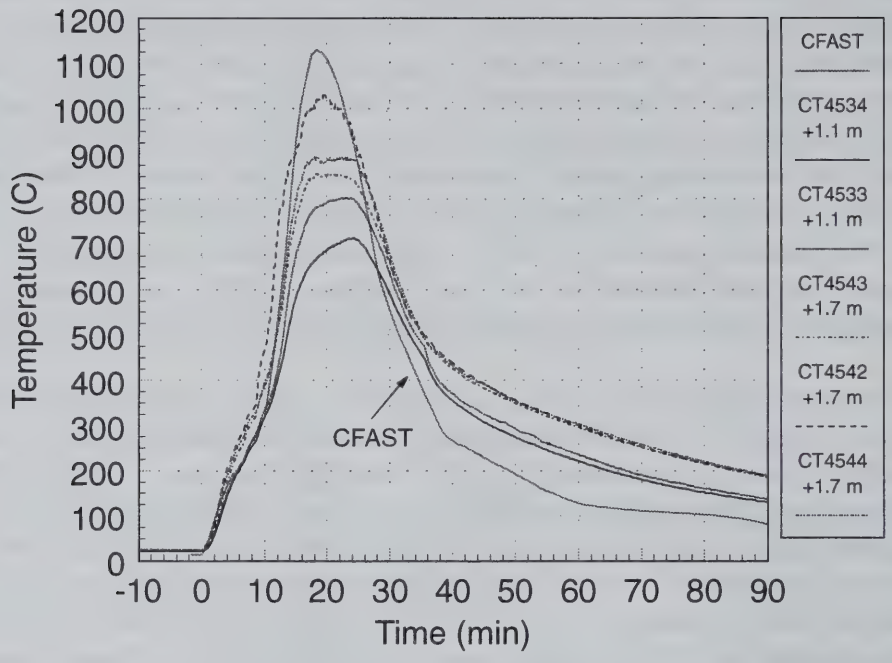

Figure 8.5: T51.17 Fire Room Upper Layer Temperature

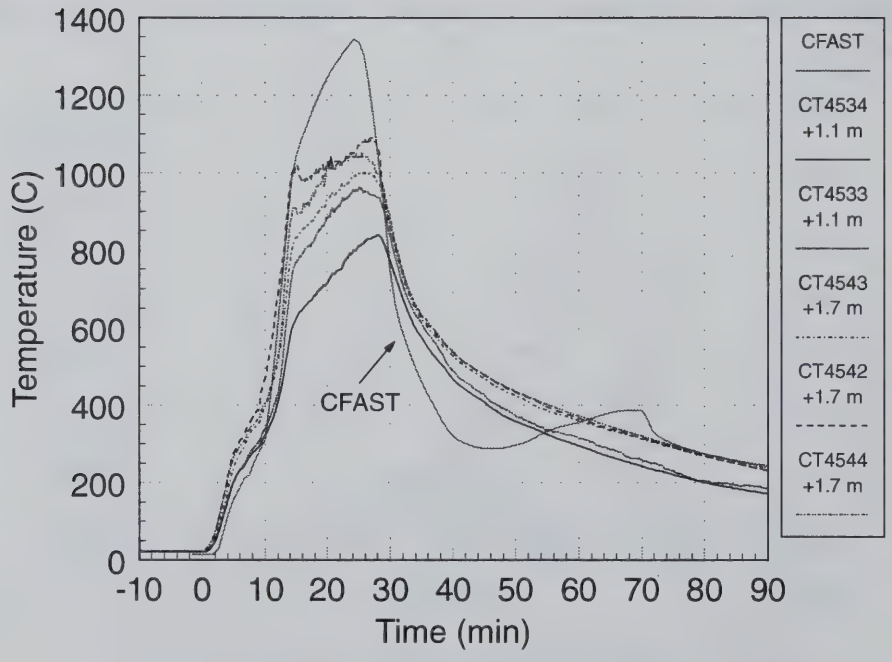

Figure 8.6: T51.18 Fire Room Upper Layer Temperature

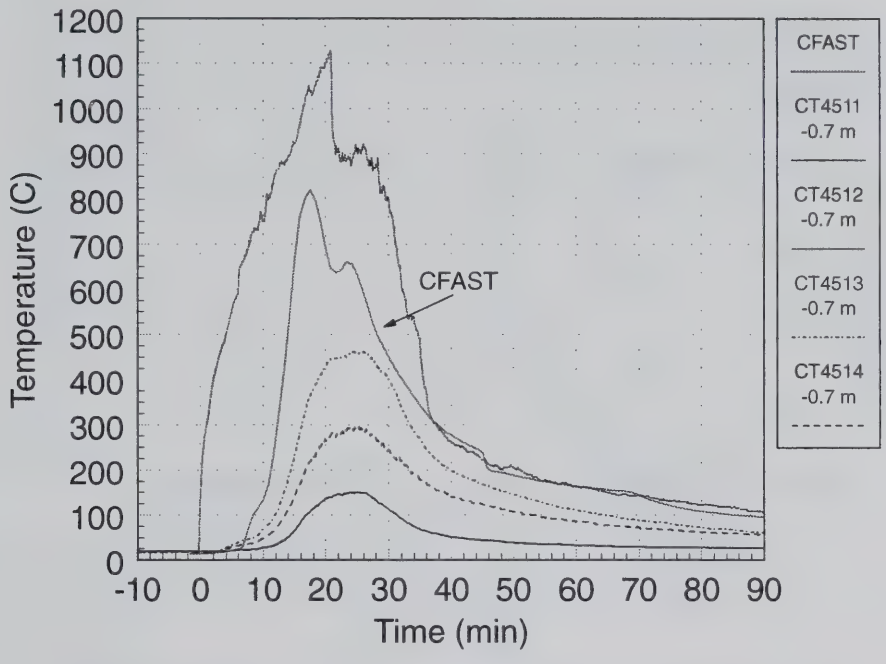

Figure 8.7: T51.16 Fire Room Lower Layer Temperature

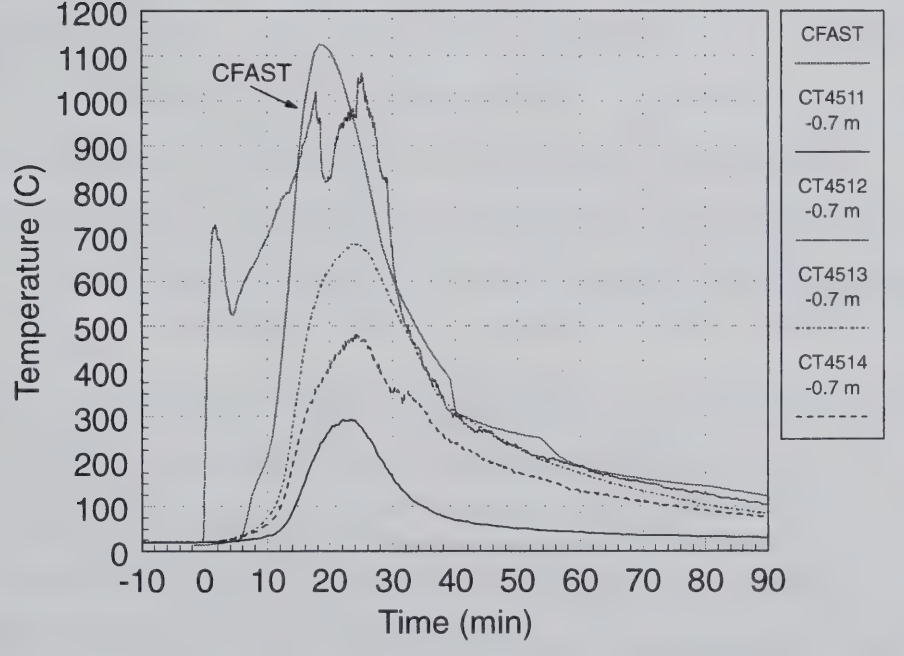

Figure 8.8: T51.17 Fire Room Lower Layer Temperature

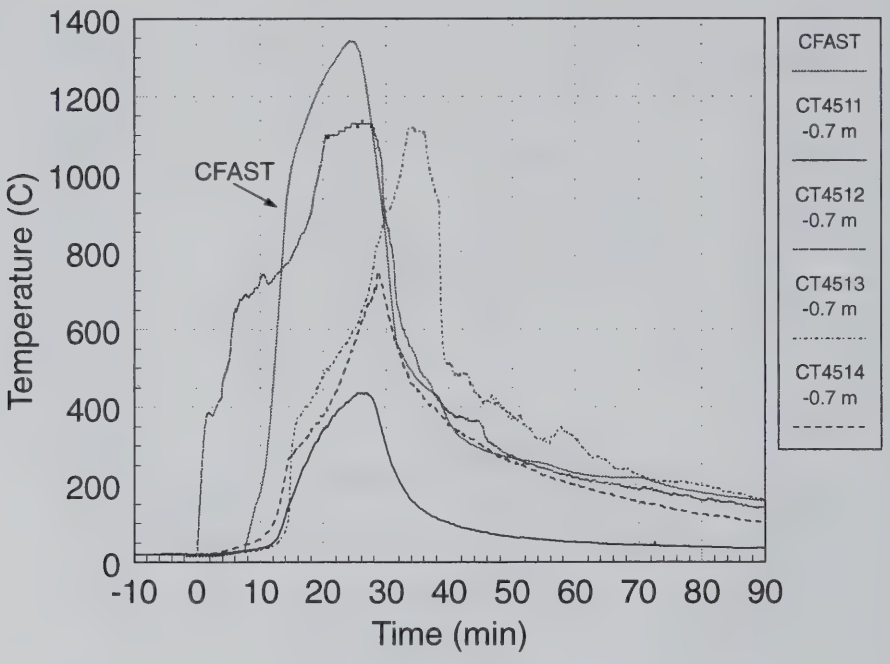

Figure 8.9: T51.18 Fire Room Lower Layer Temperature

The two figures the next page, Figures 8.10 and 8.11, display the CFAST predicted fire room layer height for test T51.16 and the measured temperatures from the thermocouple rake located in the fire room doorway. The thermocouple temperatures indicate that the layer height in the fire room lies somewhere between the -0.1 m elevation and the +0.5 m elevation. CFAST predicts the layer height to be just above the floor of the fire room near -0.7 m. This is a significant underprediction of the layer height. Although it does explain the elevated temperatures predicted in the previous lower layer figures, as the almost nonexistent layer will experience a larger temperature rise from radiative heat. It does not, however, explain the upper layer temperature results. A significantly larger upper layer should tend towards underprediction due to the larger mass present in the layer. Results for the other two tests are equivalent.

The next three figures, Figures 8.12 through 8.15, show the upper layer velocity of the hot gasses exiting the fire room. Note that the measured velocities are not zero at the beginning of the tests. This is due to naturally existing circulation patterns with the HDR facility. For each of the three wood crib tests, CFAST underpredicts the velocity by a factor of six. Accounting for the overprediction in the upper layer size by close to a factor of two, CFAST is still underpredicting the velocity by a factor of three. Also CFAST starts to predict the velocities reasonably well for the first five minutes of the fire, but then the predicted velocity drops suddenly to near zero before recovering slightly. This drop and recovery may indicative a possible instability within the code's predictive capabilities. Lastly, at the end of test T51.18, CFAST predicts a slow rise in velocity, followed by a sharp oscillation. Though this echoes the hot layer temperature results, since the pyrolysis rate has been nearly zero for thirty minutes, it is completely nonphysical.

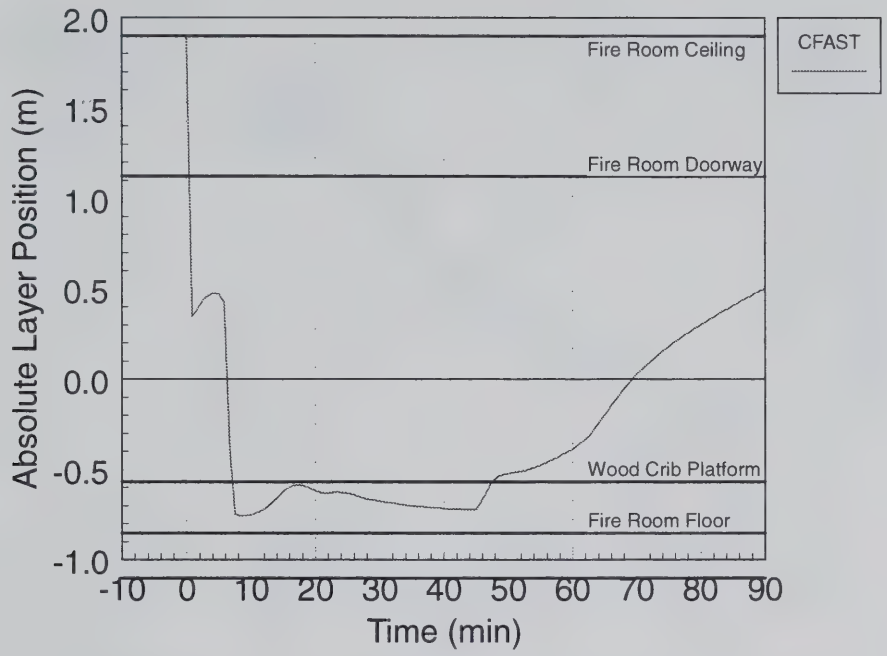

Figure 8.10: T51.16 CFAST Fire Room Layer Height

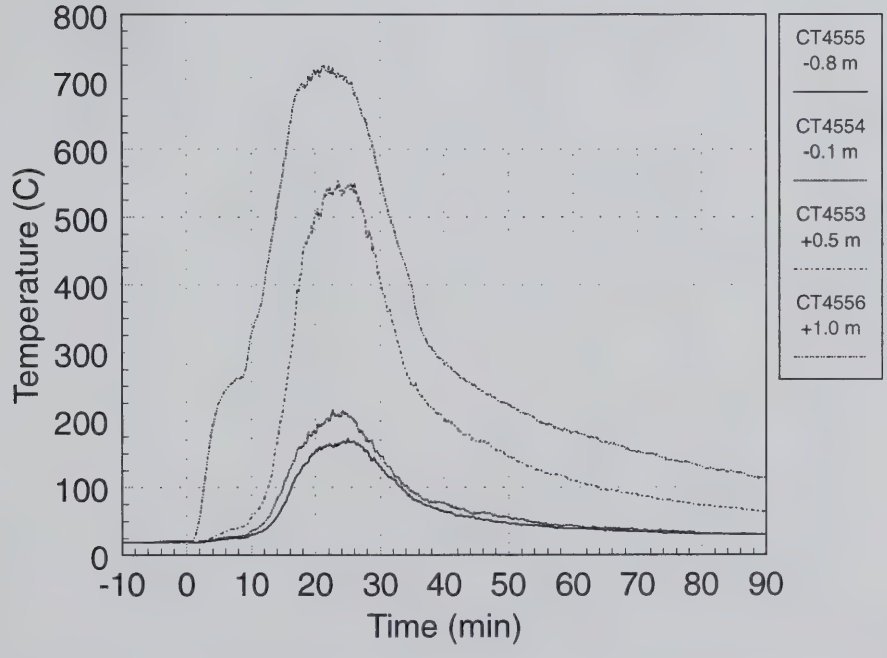

Figure 8.11: T51.16 Measured Fire Room Layer Height

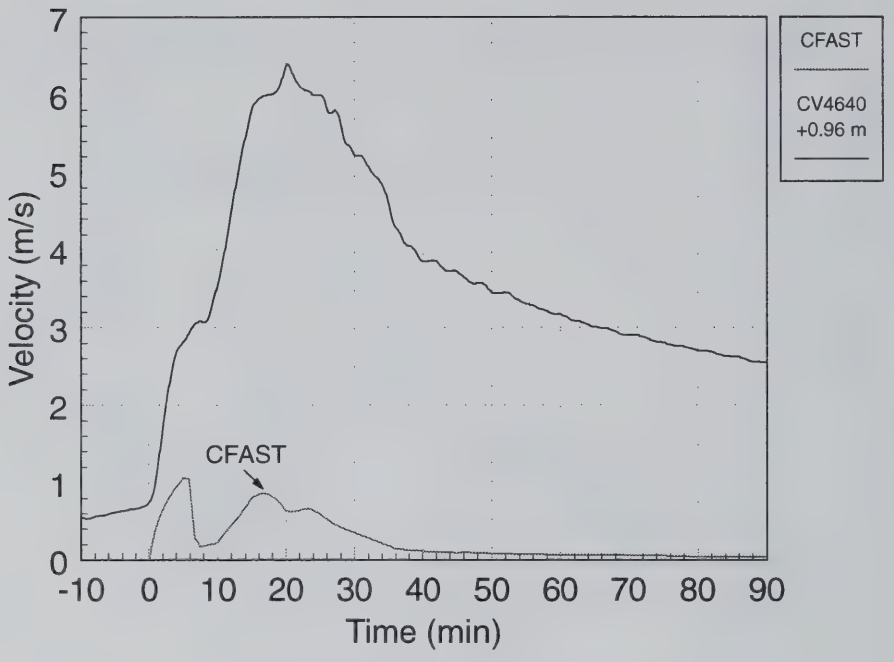

Figure 8.12: T51.16 Fire Room Upper Layer Velocity

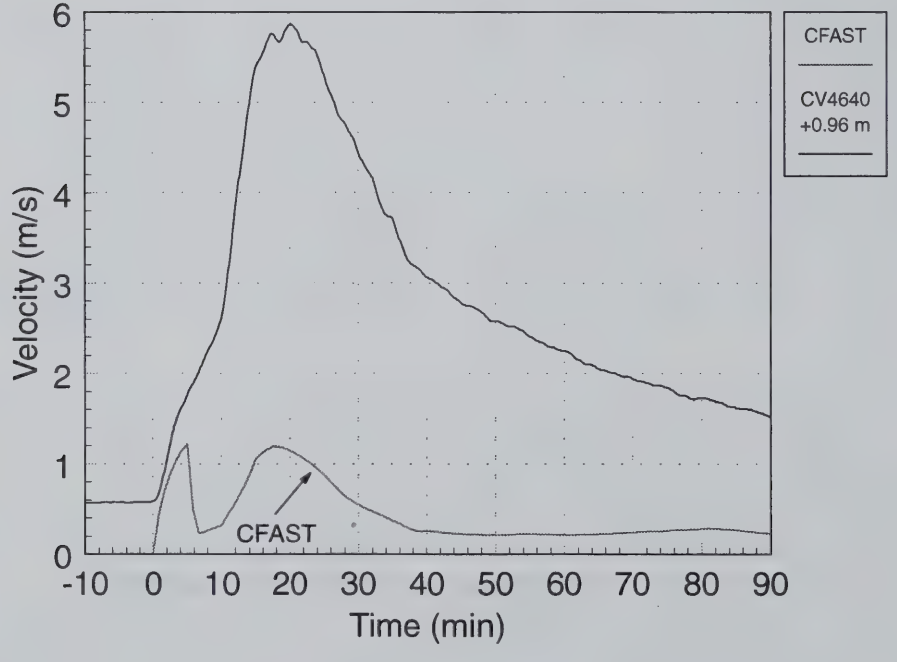

Figure 8.13: T51.17 Fire Room Upper Layer Velocity

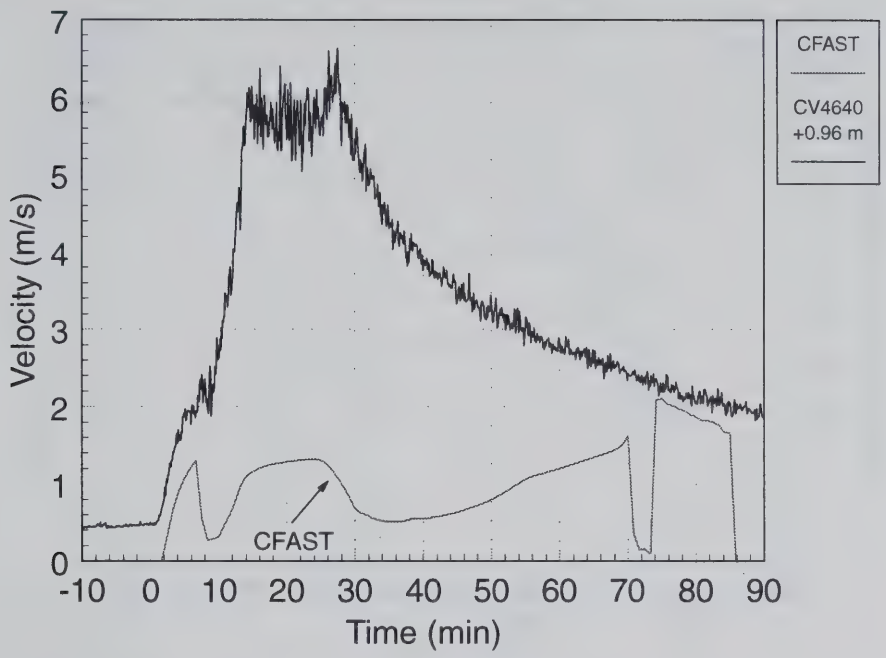

Figure 8.14: T51.18 Fire Room Upper Layer Velocity

CFAST predicted oxygen concentrations are shown with the corresponding measured data for the fire room hot layer in Figures 8.15 through 8.17. During the fire for tests T51.17 and T51.18, CFAST predicts very well the O_2 concentrations measured in the upper layer of the fire room. However, the CFAST prediction of the O_2 concentration for test T51.16 fails to match the data. This failure most likely results from the poor agreement of the layer prediction. A higher layer position during the end of the fire would have the effect of lowering the predicted O_2 concentration and improving the prediction. At the end of test T51.18, a nonphysical result shows up in the prediction. With almost all the fuel consumed by combustion, the O_2 concentration drops unexpectedly to zero for the last 20 minutes of the cooldown period.

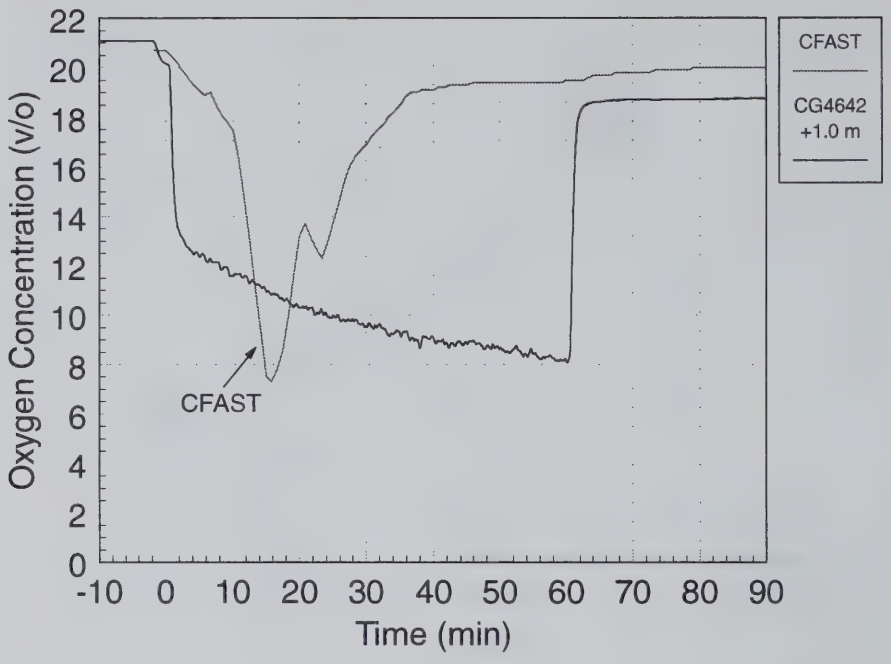

Figure 8.15: T51.16 Fire Room Upper Layer O_2 Concentration

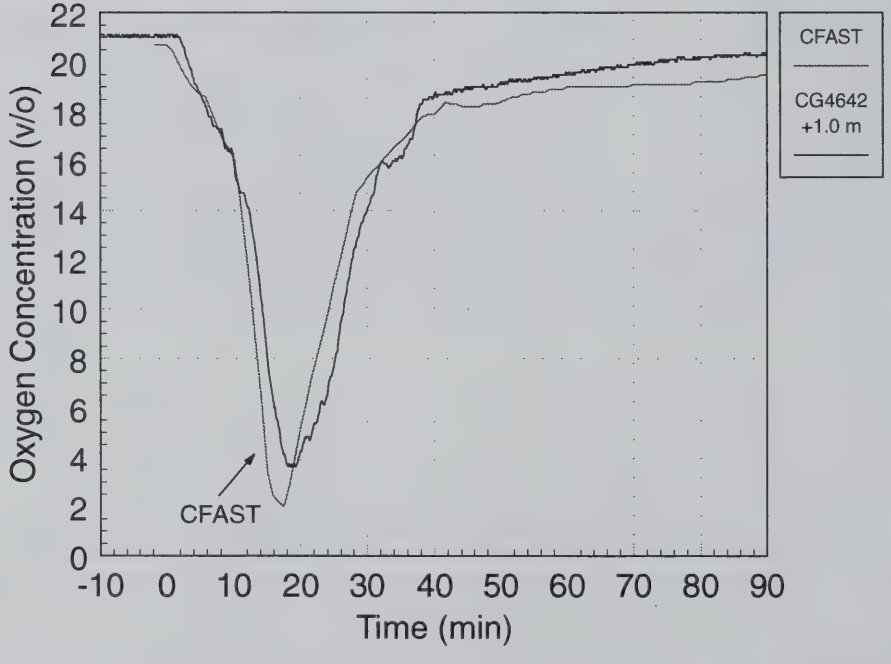

Figure 8.16: T51.17 Fire Room Upper Layer O_2 Concentration

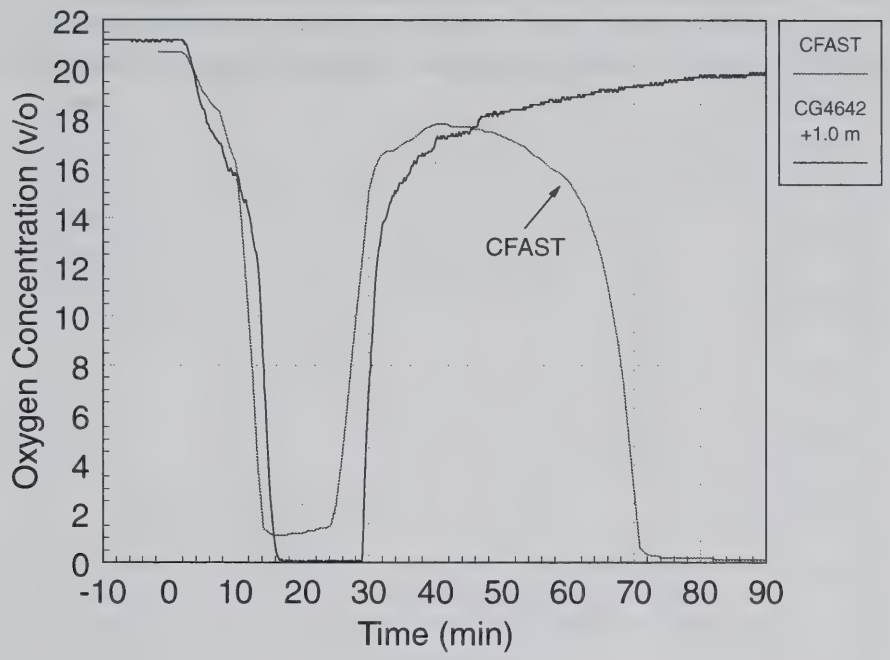

Figure 8.17: T51.18 Fire Room Upper Layer O_2 Concentration

The next set of figures, Figures 8.18 to 8.20, shows the CO_2, CO, and unburned hydrocarbon concentrations in the fire room upper layer for test T51.18. CFAST CO_2 predictions for T51.16 and T51.17 are equivalent to the predictive capability shown for T51.18, and for test T51.17 and T51.17 CO and unburned hydrocarbons are not a significant parameter due to the well ventilated nature of the fires. The CO_2 prediction by CFAST in Figure 3.18 is a factor of two lower than the measured concentration. However, since the layer height is underpredicted by CFAST, this low CO_2 prediction is to be expected. CO predictions during the fire in Figure 3.19 are also underpredicted, but by a much larger factor. Therefore, the layer height error cannot explain all of the CO deviation. Since CO production in CFAST relies mainly on the user input for the CO to CO_2 production ratio during ventilated burning, a large portion of the CO discrepancy probably results from a poorly chosen input value for the CO card. As is the value is chosen by the preprocessor when a wooden object fire was created, it suggests that better values might be required for that object definition as well. The unburned hydrocarbon concentration during the fire is slightly overpredicted by CFAST. This overprediction probably results from the underpredicted velocities in the fire room doorway. This would result in CFAST predicting the fire to be more oxygen starved than it was during the actual experiment and thus boosting the unburned hydrocarbon production.

Each of the combustion product predictions in the fire room show a large concentration increase at the end of the fire by. The CO and CO_2 concentrations increase by a factor of four from their minimum post-fire values. The unburned hydrocarbon concentration increases by a factor of almost one thousand, to nearly 35% from almost 0%. This cannot be attributed to the hot layer collapsing back to the ceiling after the fire as the layer reduces by a factor of three whereas the unburned hydrocarbon concentration increases by nearly three orders of magnitude. It would

appear that CFAST is creating a source of fuel from nothing that is combusted as an underventilated fire. This hypothesis would explain the exotic behavior of the O_2 concentration behavior displayed in Figure 8.17, the temperature anomaly in Figure 8.6, and the velocity oscillations in Figure 8.14.

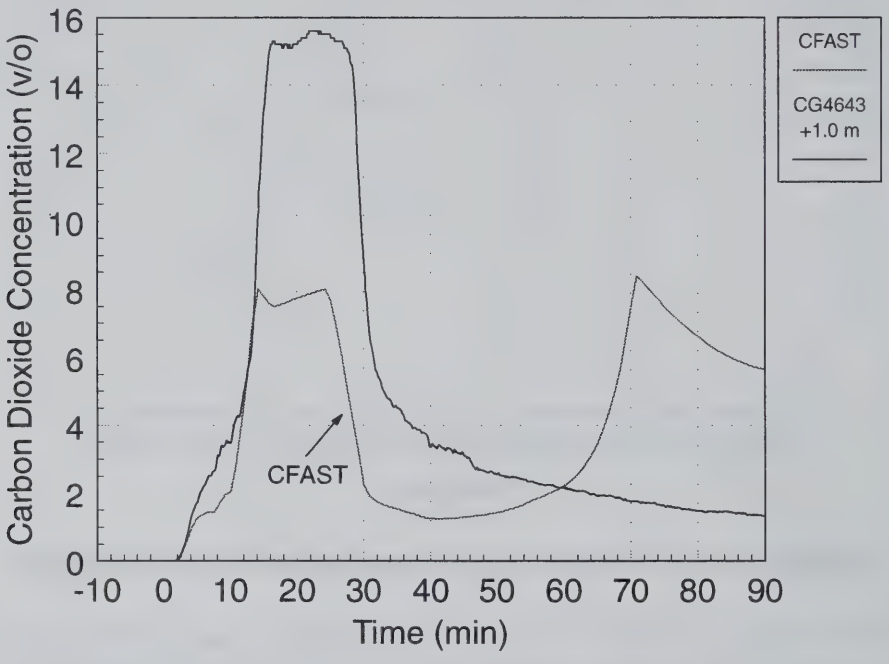

Figure 8.18: T51.18 Fire Room Upper Layer CO_2 Concentration

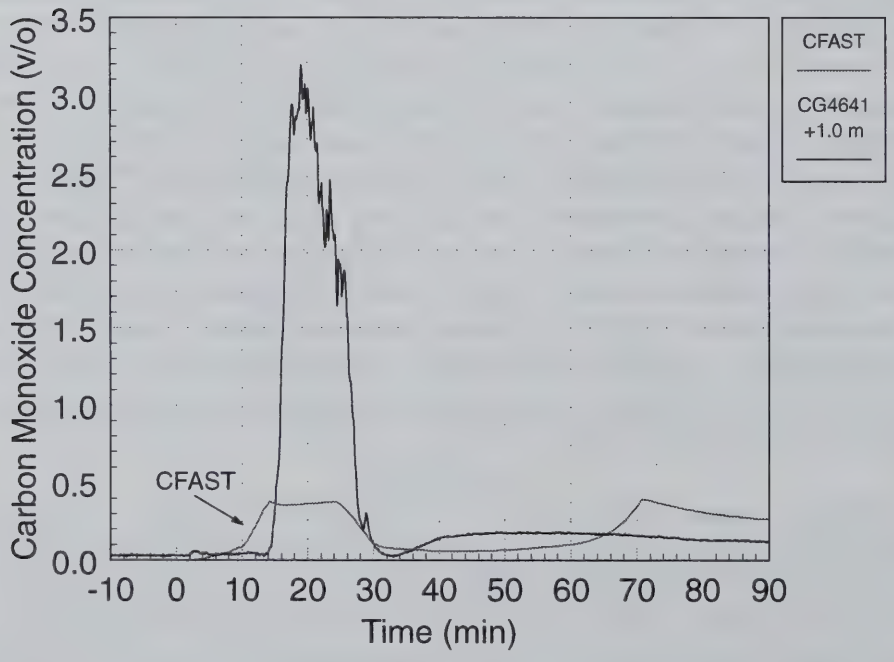

Figure 8.19: T51.18 Fire Room Upper Layer CO Concentration

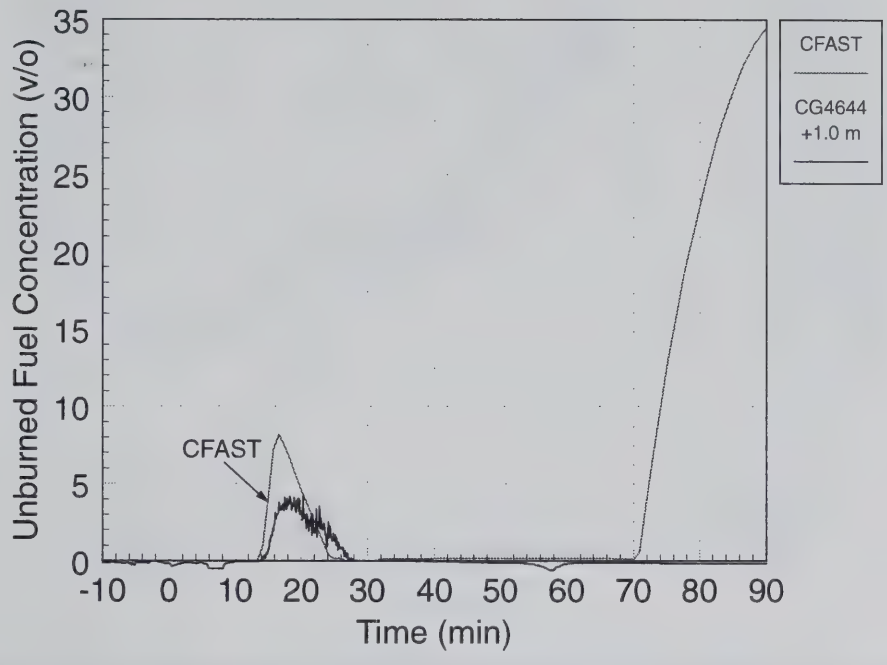

Figure 8.20: T51.18 Fire Room Upper Layer Unburned Hydrocarbon Concentration

Figures 8.21 and 8.22 on the following page display the predicted vs. measured velocities for test T51.17 in the main staircase and spiral staircase maintenance hatches at the 1.700 level. Results for tests T51.16 and T51.17 have a similar predictive quality. The CFAST predictions for the main staircase are below the measured values by a factor of three. This is similar to the predictive capability seen in the fire room velocities after taking into account the error in the layer height. This discrepancy is consistent with other velocity predictions. Surprisingly, the velocity prediction in the spiral staircase predictions agrees nearly exactly with the data. The prediction is somewhat below the data; however, since the measured value was located in the center of the hatch and CFAST's prediction is for the average flow, one would expect the CFAST velocity to be slightly underpredicted.

The final two figures, Figures 8.23 and 8.24, show the CO_2 concentrations and the extinction coefficients respectively in the dome for test T51.18. Again CFAST predictive abilities were equivalent for the other wood crib tests for these quantities. The CO_2 concentration in the dome is underpredicted by a factor of two by the end of the cooldown period. This is the opposite of what was expected. Since the HDR as modeled in CFAST contains less free air volume than the actual facility, one would expect CFAST to overpredict the CO_2 concentration no underpredict it. The extinction coefficient prediction during the cooldown period is quite accurate; however, the prediction during the heatup phase of the fire is not. CFAST fails to predict the sharp peak in the extinction coefficient associated with the highly underventilated portion and does not calculate any decrease in the optical density at the end of the fire. The latter results from CFAST not accounting for the aerosol behavior of smoke, i.e. settling, agglomeration, etc.

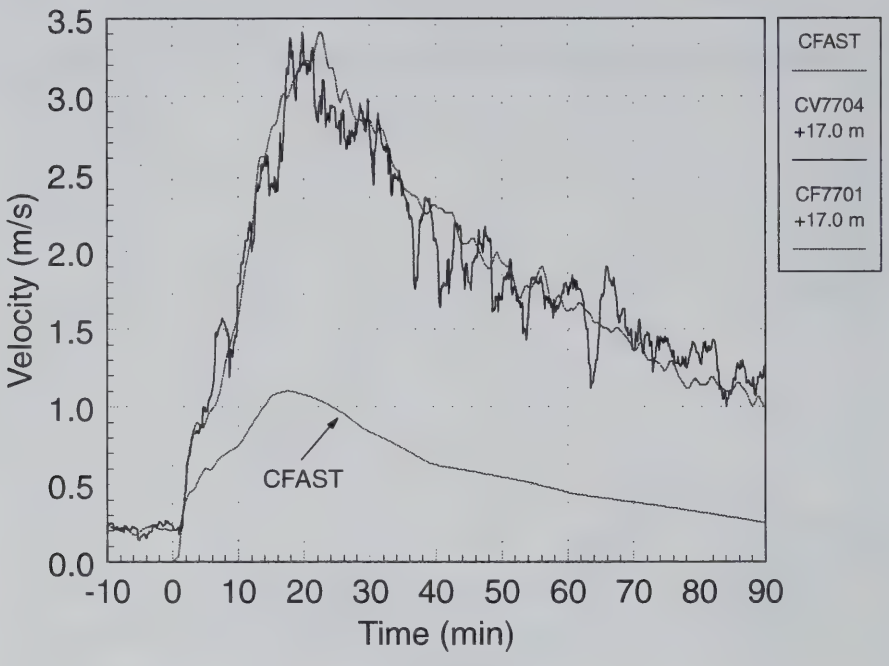

Figure 8.21: T51.17 Level 1.700 Main Staircase Maintenance Hatch Velocity

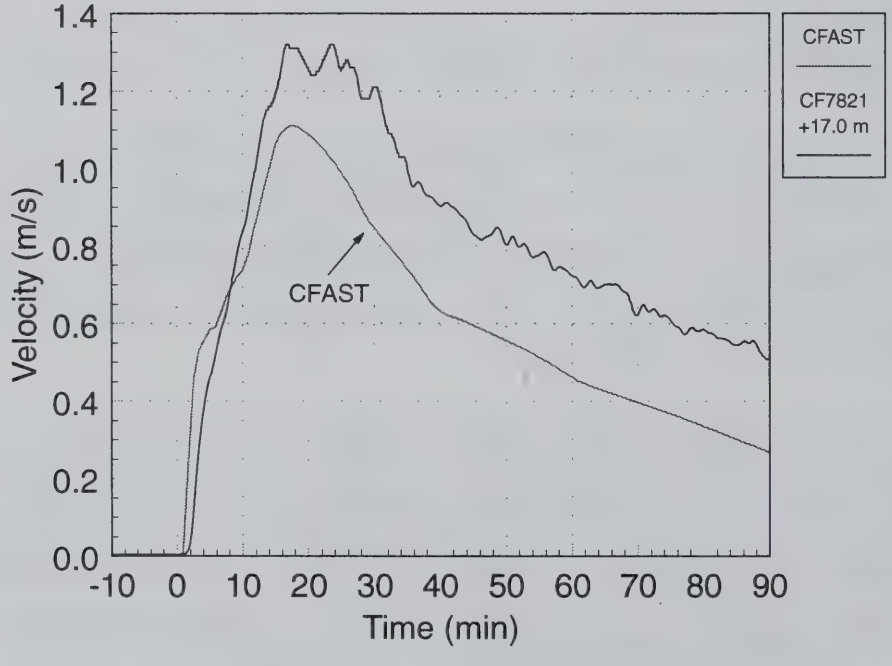

Figure 8.22: T51.17 Level 1.700 Spiral Staircase Maintenance Hatch Velocity

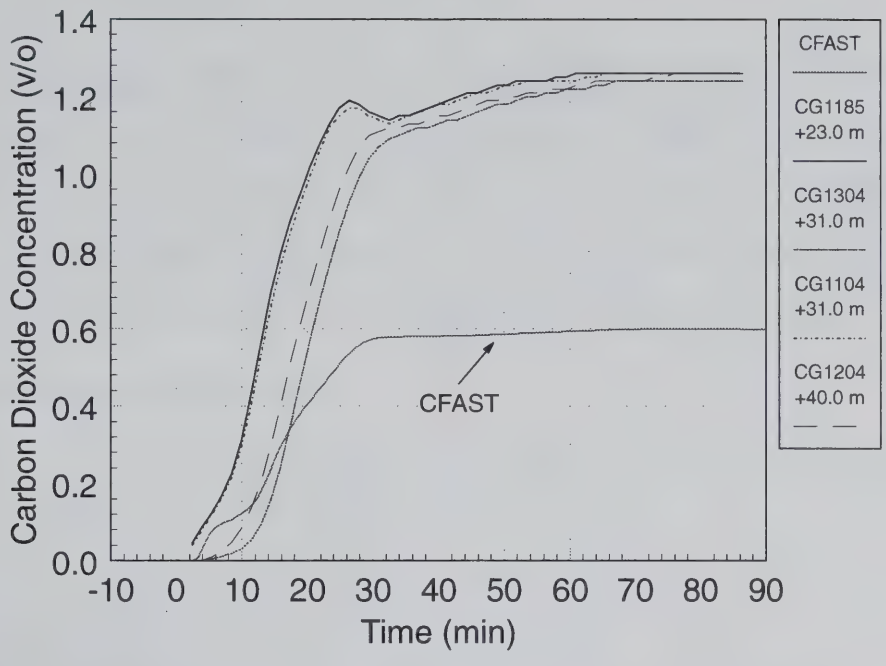

Figure 8.23: T51.18 Dome CO_2 Concentration

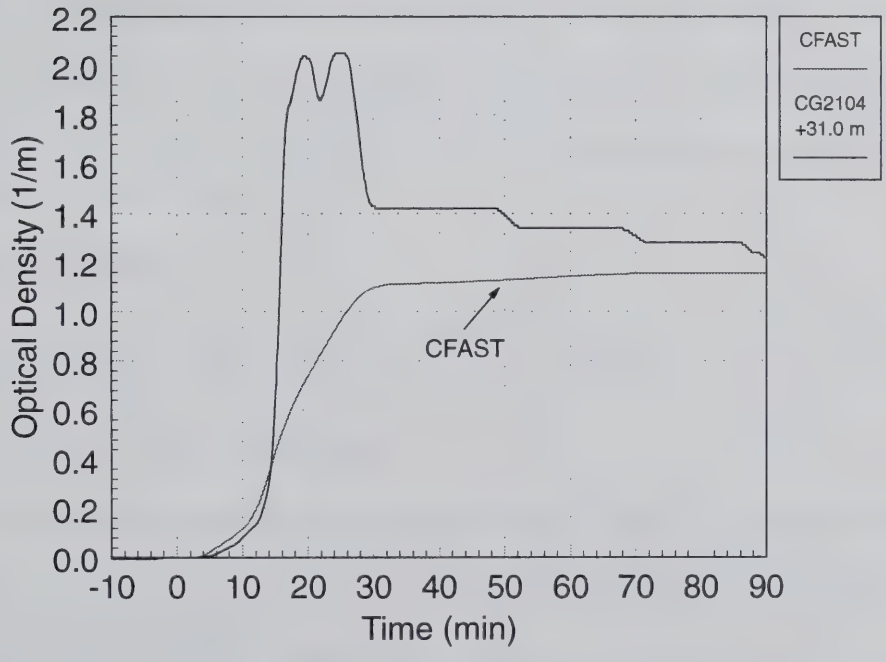

Figure 8.24: T51.18 Dome Extinction Coefficient

9 CFAST OBSERVATIONS AND COMMENTS

This section documents the general usability impressions the authors had while using CFAST for simulating the HDR T51 wood crib fire experiments. The first part addresses the accomplishments by and with CFAST over the spectrum of experiments covered during this validation effort. The second part covers differences and deviations in comparison with the data, behavior during code execution, performance of the implemented models, comments about the documentation, and comments about the capabilities and limitations of pre- and post-processors. The comments are made with respect to performance based trends as they impose requirements in terms of quality. The chapter closes with suggestions for continued validation.

9.1 Accomplishments with CFAST

The following accomplishments were achieved with CFAST during the validation efforts using the wood crib fire tests T51.16, T51.17, and T51.18:

- CFAST v3.1.1 was capable of modeling the HDR facility as a completely enclosed volume after a brief prefire period with an opening to the outside.
- CFAST predicted upper layer temperatures in the fire room agree very well during the heatup phase with the data for all three experiments. The maximum temperature predicted by CFAST tends to be conservative with increasing fire power.
- Oxygen concentration in the fire room during the fire is well predicted.
- CO_2 concentration in the fire room is reasonably well predicted once layer height errors are accounted for.
- Unlike the predictions for the gas fire tests, CFAST computed O_2 concentration in the fire room returned to ambient levels after the fire ended.
- During the underventilated portion of test T51.18, CFAST performed well in calculating the percentage of unburned hydrocarbons.

9.2 User Observations

This subsection documents various aspects of code usage, applications, and executions that were observed by the authors during this project.

9.2.1 Observations During Code Execution

These are some observations made regarding the version of CFAST used for this report:

- The added runtime feature of alerting the code user when time steps become very small for extended periods is a useful one.
- The new postprocessing utility, REPORTSS, which allows for the output of CFAST results in a spreadsheet compatible format is also very useful.

9.2.2 Physical Models

The following are some observed deficiencies in the CFAST physical models:

- The O2 card is not implemented properly within the code as is shown in Appendix B. Furthermore, the code documentation makes no mention that the O2 card has implementation difficulties even though this has been the case for many years.
- The CFAST model for the wood crib fires calculated essentially no flow in or out of the fire room when in fact substantial flows existed.
- CFAST predicts the lower layer height much too low, which leads to a substantial overprediction of the upper layer thickness.
- CFAST does not appear to compute any settling of particulate matter which acts to reduce the optical density and improve visibility in the far field from a fire and in the long term cooldown after a fire.
- CO_2 levels in the facility were predicted to be much lower than indicated by the data.
- During the underventilated portion of test T51.18, CO production did not substantially increase as it should during an underventilated fire.
- At the end of test T51.18, CFAST calculates a significant amount of combustion products, in particular unburned hydrocarbons, even though no more fuel is available in the fire room.

9.3 CFAST Status

Based on all of the experiences with the CFAST code at UMCP in comparison with the HDR data, code performance, utilization and applicability have advanced over the last years. In fact as documented by many contributions at national and international conferences, the CFAST code has left the realm of exploratory research and entered into the competitive, highly demanding industrial market and regulatory decision making.

For many aspects the CFAST predictions satisfy the stringent requirements. For others, however, it dramatically fails in a rather erratic manner and one has to wonder how the favorable agreements with data may change once the major remaining discrepancies have been resolved.

The current efforts of UMCP, Department of Materials and Nuclear Engineering, were not designed to solve these broader aspects of balanced code behavior. They rather contribute towards the identification of remaining issues.

However, it seems appropriate to point out that additional efforts are needed to maintain CFAST's current position and impact. This especially in view of the fast evolution of performance based methodologies.

9.4 Suggestions for Further Validation

One fact that is clear from the work performed for this report is that further work is needed in resolving the exact nature of the O2 card failure. Further test of this card along with a detailed examination of its use within the source code may resolve this problem.

Only one of the wood crib tests became completely underventilated. CFAST results for this test were mixed. While CFAST did predict well the O_2 and unburned hydrocarbon levels, it did not do as well predicting other combustion products or the optical density. Further validation efforts with underventilated fires are needed especially considering that it is the high smoke and CO production by such fires that pose some of the greatest risks to human life and intervention efforts.

It is suggested that the CFAST code developer group consistently evaluate some of the observed deficiencies. The UMCP input models will be made available electronically. Lastly, it is clear that the default values for CO and soot/smoke production used in the predefined object descriptions do not function well in modeling real fires. More effort is needed in validating and developing reliable values for use in modeling real fires.

10 REFERENCES

1. Schall, M. and Valencia, L. *Data Compilation of the HDR Containment for Input Data Processing for Pre-Test Calculations* (English Translation of PHDR Working Report 3.143/79). Project HDR Nuclear Center. Karlsruhe, Germany. PHDR Working Report 3.279/82. Jan. 1982.

2. Müller, K. and Dobbernack, R. *Evaluation of Fire Behavior in Compartment Networks in a Closed Containment, Design Report, Test Group BRA-E, Exploratory Experiments T51.1* (In German). Project HDR Nuclear Center. Karsruhe, Germany. PHDR Working Report 5.025/84. Dec. 1984.

3. Tenhumberg. *Evaluation of Fire Behavior in Compartment Networks inc a Closed Containment, Data Report, Test Group BRA-E, Experiments T51.11-T51.15, Test Period 01/24 - 02/01/1985* (In German). Project HDR Nuclear Center. Karlsruhe, Germany. PHDR Working Report 5.43/85. Feb. 1985.

4. *Supplemental Data Report, Test Group BRA-E, Experiments T51.11-T51.15* (In German). Project HDR Nuclear Center. Karlsruhe, Germany. PHDR Working Report 5.038/85. April 1985.

5. Tenhumberg. *Evaluation of Fire Behavior in Compartment Networks in a Closed Containment, Data Report, Test Group BRA-E, Experiments T51.16-T51.19, Test Period 06/25 - 07/01/85* (In German). Project HDR Nuclear Center. Karlsruhe, Germany. PHDR Working Report 5.055/85. July 1985.

6. Müller, K., Wegener, H. and Dobbernack, R. *Evaluation of Fire Behavior in a Compartment Network in a Closed Containment, Supplemental Design Report, Test Group BRA, Experiments T51.2.* Project HDR Nuclear Center. Karlsruhe, Germany. PHDR Working Report 5.069/86. June 1986.

7. Grimm, R. *Evaluation of Fire Behavior in a Compartment Network in a Closed Containment, Supplemental Design Report, Test Group BRA, Test Group T51.21-T51.24* (In German). Project HDR Nuclear Center. Karlsruhe, Germany. PHDR Working Report 5.078/86. May 1986.

8. *Evaluation of Fire Behavior in a Compartment Network in a Closed Containment, Quick Look Report, Test Group BRA, Experiments T51.11-T51.19* (In German). Project HDR Nuclear Center. Karlsruhe, Germany. PHDR Working Report 61-85. June 1986.

9. Rautenberg, J., Dobbernack, R., Müller, K., and Volk, R. *Evaluation of Fire Behavior in a Compartment Network in a Closed Containment, Final Evaluation Report, Test Group BRA, Experiments T51.1; T51.2* (In German). Project HDR Nuclear Center. Karlsruhe, Germany. PHDR Working Report 82-91. March 1991.

10. Nowlen, S.P. *A Summary of the Fire Testing Program at the German HDR Test Facility.* Sandia National Laboratories. NUREG/CR-6173. Nov. 1995.

11. Müller, K. and Valencia, L. *Experiments with Hydrocarbon Fire in the Dome Region of the HDR Under Natural Ventilation Conditions, Design Report, Test Group BRA, Experiments T52.1/T52.2* (In German). Project HDR Nuclear Center. Karlsruhe, Germany. PHDR Working Report 5.075/86. Feb. 1987.

12. Bader and Jansen. *Experiments with Hydrocarbon Fire in the Dome Region of the HDR Under Natural Ventilation Conditions, Supplemental Data Report, Test Group BRA, Experiments T52.1-4* (In German). Project HDR Nuclear Center. Karlsruhe, Germany. PHDR Working Report 5.115/87. June 1987.

13. Rautenberg, J., Müller, K., Volk, R., Max, U., and Dobbernack, R. *Experiments with Hydrocarbon Fire in the Dome Region of the HDR Under Natural Ventilation Conditions, Final Evaluation Report, Test Group BRA, Experiments T52.1-14* (In German). Project HDR Nuclear Center. Karlsruhe, Germany. PHDR Working Report 89-90. March 1991.

14. Müller, K., et al. *Evaluation of the Behavior of Compartment Networks During a Large Hydrocarbon Fire in a Closed Containment, Design Report, Test Group: Large Hydro-carbon Fire, Experiments E41.1-5* (In German). Project HDR Nuclear Center. Karlsruhe, Germany. PHDR Working Report 40.002/88. Oct. 1988.

15. Wenzel, H., Grimm, L. and Löhr, L. *Evaluation of the Behavior of Compartment Networks During a Large Hydrocarbon Fire in a Closed Containment, Data Report, Experiments E41.1-4* (In German). Project HDR Nuclear Center. Karlsruhe, Germany. PHDR Working Report 40.008/89. Dec. 1989.

16. Jansen and Bader. *Evaluation of the Behavior of Compartment Networks During a Large Hydrocarbon Fire in a Closed Containment, Supplemental Data Report, Experiments E41.1-4* (In German). Project HDR Nuclear Center. Karlsruhe, Germany. PHDR Working Report 40.002/88. Feb. 1989.

17. Rautenberg, J., Dobbernack, R., Müller, K., and Volk, R. *Evaluation of the Behavior of Compartment Networks During a Large Hydrocarbon Fire in a Closed Containment, Final Evaluation Report, Experiments E41.1-4* (In German). Project HDR Nuclear Center. Karlsruhe, Germany. PHDR Technical Report 103-92. Dec.. 1992.

18. Müller, K. and Volk, R. *Behavior of Oil Fires in a Closed Subsystem With Ventilation Connected and Variable Door Opening, Design Report, Experiments E41.5-10* (In German). Project HDR Nuclear Center. Karlsruhe, Germany. PHDR Working Report 40.024/90. Aug. 1990.

19. Wenzel, H., Grimm, L. and Löhr, L. *Behavior of Oil Fires in a Closed Subsystem With Ventilation Connected and Variable Door Opening, Data Report, Experiments E41.5-10* (In German). Project HDR Nuclear Center. Karlsruhe, Germany. PHDR Working Report 40.026/90. Vol. 1 and 2.

20. Max, U., Müller, K., et al. *Behavior of Oil Fires in a Closed Subsystem With Ventilation Connected and Variable Door Opening, Quick Look Report, Experiments E41.5-10* (In German). Project HDR Nuclear Center. Karlsruhe, Germany. PHDR Technical Report 122-93. 1993.

21. Müller, K., Wegener H., and Löhr, L. *Cable Fire in an Enclosed Multi-Compartment Arrangement in the Containment, Design Report, Experiments E42* (In German). Project HDR Nuclear Center. Karlsruhe, Germany. PHDR Working Report 40.03/91. Feb. 1992.

22. Wenzel, H. and Löhr, L. *Cable Fire in an Enclosed Multi-Compartment Arrangement in the Containment, Data Report, Experiments E42, Time Period 01/21-02/18/92* (In German). Project HDR Nuclear Center. Karlsruhe, Germany. PHDR Working Report 40.042/91. Aug. 1992.

23. Rautenberg, J., Max U., Müller, K., and Hans, J. *Cable Fire in an Enclosed Multi-Compartment Arrangement in the Containment, Final Evaluation Report, Experiments E42* (In German). Project HDR Nuclear Center. Karlsruhe, Germany. PHDR Technical Report 123-94. April 1994.

24. Karwat, H., Müller, K., and Max, U. *CEC Standard Problem: Prediction of Effects Caused by a Cable Fire Experiment Within the HDR Containment, Task Specification.* Feb. 1992. (Revision July 1992.)

25. Karwat, H., Müller, K., and Max, U. *CEC Standard Problem: Prediction of Effects Caused by a Cable Fire Experiment Within the HDR Containment, Final Comparison Report.* EUR 15648 EN. Aug. 1993.

26. Green, J. Notebook for Development of E11.4 CONTAIN Model for the HDR Hydrogen Mixing Test. Dept. of Materials and Nuclear Engineering. University of Maryland. College Park, MD. 1992.

27. Holzbauer, H. *Blind Post-Test Predictions of HDR-H_2-Distribution Experiements E11.2 and E11.4 Using FATHOMS* (In German).Batelle Institute e.v. Frankfurt/Main, FRG. Final Report BIEV R67238-1. Dec. 1990.

28. Holzbauer, H. *Parametric Open Post-Test Predictions and Analysis of the HDR-H_2-Distribution Experiment E11.2 and E11.4 with the Computer Code GOTHIC* (In German). Batelle Institute e.v. Frankfurt/Main, FRG. Final Report BIEV R67706-1. August 1990.

29. Portier, R., Reneke, P., Jones, W., and Peacock, R. *User's Guide for CFAST Version 1.6.* Building and Fire Research Laboratory, NIST. Gaithersburg, MD. NISTIR 4985. Dec. 1992.

30. Peacock, R., et al. *CFAST, the Consolidated Model of Fire Growth and Smoke Transport.* Building and Fire Research Laboratory, NIST. Gaithersburg, Maryland. NIST Technical Note 1299. Feb. 1993.

31. George, T. et. al. *GOTHIC Containment Analysis Package Technical Manual, Version 3.4.* Numerical Applications Inc. for EPRI. RP3408-1. July, 1991. .

32. McGrattan, K., Baum, H., and Rehm, R. *Buoyant Convection of a Thermally Expandable Fluid in a 3D Enclosure.* Building and Fire Research Laboratory, NIST. Gaithersburg, MD. June, 1997.

33. Floyd, J. and Wolf. , L. *Evaluation of the HDR Fire Test Data and Accompanying Computational Activities with Conclusions from Present Code Capabilities, **Volume 1**: Test Series Description Report for T51 Gas Fire Test Series.* Dept. Materials and Nuclear Engineering, University of Maryland. College Park, Maryland. Report NUMAFIRE:04-97. 1997.

34. Floyd, J. and Wolf. , L. *Evaluation of the HDR Fire Test Data and Accompanying Computational Activities with Conclusions from Present Code Capabilities, **Volume 2**: CFAST Validation Report for T51 Gas Fire Test Series.* Dept. Materials and Nuclear Engineering, University of Maryland. College Park, Maryland. Report NUMAFIRE:04-97. 1997.

35. Rockett, J. *HDR Reactor Containment Fire Modeling with BR12.* Fire Technology Laboratory. Technical Research Centre of Finland (VTT). VTT Publication 113. 1992.

36. *FLUENT User's Guide, Release 4.4.* Fluent Incorporated. Lebanon, NH. 1996.

37. McGrattan, K., Baum, H., and Rehm, R. *Buoyant Convection of a Thermally Expandable Fluid in a 3D Enclosure.* Building and Fire Research Laboratory, NIST. Gaithersburg, MD. June, 1997.

APPENDIX A: INPUT FILES

This appendix gives the complete CFAST input files for all computations documented in this report. The filename nomenclature isT51XX-C.INP where XX indicates the test number in the wood crib test series.

T5116-C.INP:CFAST input file for Test T51.16 (5 cribs)

```
VERSN    3T51-16: 9 Room+Dome+Level 1.4 Connect
TIMES   5500    100     50      0      0
DUMPR T5116-C.HIS
STPMAX  1.00000
TAMB  288.000  101300. 0.000000
EAMB  288.000  101300. 0.000000
HI/F   0.250  0.000  0.000  0.000  0.000 11.100 11.100 11.100 11.100 16.150  0.300
WIDTH  2.950  4.950  4.300  4.330  1.800  7.920  4.300  4.330  9.670 14.370  3.000
DEPTH  3.650  1.800  2.750  2.720  6.350  7.920  2.750  2.720  9.670 14.370  3.000
HEIGH  2.750  2.485 11.100 11.100  3.500  4.600  5.050  5.050  5.050 34.950 13.200
CEILI FIRECEIL YTONG100 CONCR050 CONCR050 CONCR050 CONCR050 CONCR050 CONCR050 CONCR050 CONCR050 CONCR050
WALLS YTONG250 YTONG100 CONCR050 CONCR050 CONCR050 CONCR050 CONCR050 CONCR050 CONCR050 CONCR050 CONCR050
FLOOR FIRE_FLR CONCR100 CONCR050 CONCR050 CONCR050 CONCR050 CONCR050 CONCR050 CONCR050 CONCR050 CONCR050
HVENT  1  2  1  1.010  1.975  0.000
CVENT  1  2  1  1.000  1.000  1.000  1.000  1.000  1.000  1.000  1.000  1.000  1.000  1.000
HVENT  2  3  1  1.800  2.485  0.000
CVENT  2  3  1  1.000  1.000  1.000  1.000  1.000  1.000  1.000  1.000  1.000  1.000  1.000
HVENT  3  4  1  4.300  0.500  0.000
CVENT  3  4  1  1.000  1.000  1.000  1.000  1.000  1.000  1.000  1.000  1.000  1.000  1.000
HVENT  3  5  1  2.000  0.500  0.000
CVENT  3  5  1  1.000  1.000  1.000  1.000  1.000  1.000  1.000  1.000  1.000  1.000  1.000
HVENT  4  5  1  2.700  3.100  1.100
CVENT  4  5  1  1.000  1.000  1.000  1.000  1.000  1.000  1.000  1.000  1.000  1.000  1.000
HVENT  5 11  1  1.800  3.500  0.300
CVENT  5 11  1  1.000  1.000  1.000  1.000  1.000  1.000  1.000  1.000  1.000  1.000  1.000
HVENT  6  7  1  3.000  4.250  0.000
CVENT  6  7  1  1.000  1.000  1.000  1.000  1.000  1.000  1.000  1.000  1.000  1.000  1.000
HVENT  6  8  1  3.000  4.250  0.000
CVENT  6  8  1  1.000  1.000  1.000  1.000  1.000  1.000  1.000  1.000  1.000  1.000  1.000
HVENT  6  9  1  3.000  4.250  0.000
CVENT  6  9  1  1.000  1.000  1.000  1.000  1.000  1.000  1.000  1.000  1.000  1.000  1.000
HVENT  7  8  1  3.000  4.250  0.000
CVENT  7  8  1  1.000  1.000  1.000  1.000  1.000  1.000  1.000  1.000  1.000  1.000  1.000
HVENT 11 12  1  0.030  9.800  3.300
CVENT 11 12  1  1.000  0.000  0.000  0.000  0.000  0.000  0.000  0.000  0.000  0.000  0.000
HVENT  6 11  1  3.000  2.400  0.000
CVENT  6 11  1  1.000  1.000  1.000  1.000  1.000  1.000  1.000  1.000  1.000  1.000  1.000
VVENT  7  3  4.54000  2
VVENT  8  4  5.75000  2
VVENT 10  7  4.54000  2
VVENT 10  8  6.97000  2
VVENT 10  9  5.28000  2
CHEMI  13.800 20.000  0.000  2.721E+007  293.000  493.000 0.200
LFBO 1
LFBT 2
CJET OFF
FPOS   1.475  1.825  0.000
FTIME   100.00    700.00   1000.00   1126.00   1306.00   1480.00   1720.00   2260.00   3100.00   4900.00
FHIGH  0.00000   0.00000   0.28100   0.28100   0.28100   0.28100   0.28100   0.28100   0.28100   0.28100   0.00000
FAREA  0.00000   0.00000   0.70900   0.70900   0.70900   0.70900   0.70900   0.70900   0.70900   0.70900   0.00000
FMASS  0.00000   0.00000   0.00926   0.04260   0.03705   0.01806   0.02454   0.01158   0.00232   0.00116   0.00000
FQDOT  0.00000   0.00000   252000.  1159200.  1008000.   491400.   667800.   315000.   63000.0   31500.0   0.00000
HCR    0.00000   0.00000   0.21050   0.21050   0.21050   0.21050   0.21050   0.21050   0.21050   0.21050   0.00000
OD     0.00000   0.00000   0.03000   0.03000   0.03000   0.03000   0.03000   0.03000   0.03000   0.03000   0.03000
CO     0.00000   0.00000   0.03000   0.03000   0.03000   0.03000   0.03000   0.03000   0.03000   0.03000   0.03000
#GRAPHICS ON
DEVICE 1
WINDOW    0.    0.    0. 1279. 1023. 4095.
```

T5117-C.INP:CFAST input file for Test T51.17 (7 cribs)

```
VERSN    3T51-17: 9 Room+Dome+Level 1.4 Connect
TIMES   5500    100     50      0      0
DUMPR T5117-C.HIS
STPMAX  1.00000
TAMB  288.000  101300. 0.000000
EAMB  288.000  101300. 0.000000
HI/F   0.250  0.000  0.000  0.000  0.000 11.100 11.100 11.100 11.100 16.150  0.300
WIDTH  2.950  4.950  4.300  4.330  1.800  7.920  4.300  4.330  9.670 14.370  3.000
DEPTH  3.650  1.800  2.750  2.720  6.350  7.920  2.750  2.720  9.670 14.370  3.000
HEIGH  2.750  2.485 11.100 11.100  3.500  4.600  5.050  5.050  5.050 34.950 13.200
CEILI FIRECEIL YTONG100 CONCR050 CONCR050 CONCR050 CONCR050 CONCR050 CONCR050 CONCR050 CONCR050 CONCR050 CONCR050
WALLS YTONG250 YTONG100 CONCR050 CONCR050 CONCR050 CONCR050 CONCR050 CONCR050 CONCR050 CONCR050 CONCR050
FLOOR FIRE_FLR CONCR100 CONCR050 CONCR050 CONCR050 CONCR050 CONCR050 CONCR050 CONCR050 CONCR050 CONCR050
HVENT  1  2  1  1.010  1.975  0.000
CVENT  1  2  1  1.000  1.000  1.000  1.000  1.000  1.000  1.000  1.000  1.000  1.000  1.000
HVENT  2  3  1  1.800  2.485  0.000
CVENT  2  3  1  1.000  1.000  1.000  1.000  1.000  1.000  1.000  1.000  1.000  1.000  1.000
HVENT  3  4  1  4.300  0.500  0.000
CVENT  3  4  1  1.000  1.000  1.000  1.000  1.000  1.000  1.000  1.000  1.000  1.000  1.000
HVENT  3  5  1  2.000  0.500  0.000
CVENT  3  5  1  1.000  1.000  1.000  1.000  1.000  1.000  1.000  1.000  1.000  1.000  1.000
HVENT  4  5  1  2.700  3.100  1.100
CVENT  4  5  1  1.000  1.000  1.000  1.000  1.000  1.000  1.000  1.000  1.000  1.000  1.000
HVENT  5 11  1  1.800  3.500  0.300
CVENT  5 11  1  1.000  1.000  1.000  1.000  1.000  1.000  1.000  1.000  1.000  1.000  1.000
HVENT  6  7  1  3.000  4.250  0.000
CVENT  6  7  1  1.000  1.000  1.000  1.000  1.000  1.000  1.000  1.000  1.000  1.000  1.000
HVENT  6  8  1  3.000  4.250  0.000
CVENT  6  8  1  1.000  1.000  1.000  1.000  1.000  1.000  1.000  1.000  1.000  1.000  1.000
HVENT  6  9  1  3.000  4.250  0.000
CVENT  6  9  1  1.000  1.000  1.000  1.000  1.000  1.000  1.000  1.000  1.000  1.000  1.000
HVENT  7  8  1  3.000  4.250  0.000
CVENT  7  8  1  1.000  1.000  1.000  1.000  1.000  1.000  1.000  1.000  1.000  1.000  1.000
HVENT 11 12  1  0.030  9.800  3.300
CVENT 11 12  1  1.000  0.000  0.000  0.000  0.000  0.000  0.000  0.000  0.000  0.000  0.000
HVENT  6 11  1  3.000  2.400  0.000
CVENT  6 11  1  1.000  1.000  1.000  1.000  1.000  1.000  1.000  1.000  1.000  1.000  1.000
VVENT  7  3  4.54000  2
VVENT  8  4  5.75000  2
VVENT 10  7  4.54000  2
VVENT 10  8  6.97000  2
VVENT 10  9  5.28000  2
CHEMI  13.800 20.000  0.000  2.721E+007  293.000  493.000 0.200
LFBO 1
LFBT 2
CJET OFF
FPOS   1.475  1.825  0.000
FTIME   100.00    700.00   1000.00   1144.00   1300.00   1780.00   2380.00   3700.00   5500.00
FHIGH  0.00000   0.00000   0.28100   0.28100   0.28100   0.28100   0.28100   0.28100   0.28100   0.00000
FAREA  0.00000   0.00000   1.10300   1.10300   1.10300   1.10300   1.10300   1.10300   1.10300   0.00000
FMASS  0.00000   0.00000   0.01389   0.05326   0.05372   0.04168   0.01389   0.00463   0.00139   0.00000
FQDOT  0.00000   0.00000   378000.  1449000.  1461600.  1134000.   378000.   126000.   37800.0   0.00000
HCR    0.00000   0.00000   0.21050   0.21050   0.21050   0.21050   0.21050   0.21050   0.21050   0.00000
OD     0.00000   0.00000   0.03000   0.03000   0.03000   0.03000   0.03000   0.03000   0.03000   0.03000
CO     0.00000   0.00000   0.03000   0.03000   0.03000   0.03000   0.03000   0.03000   0.03000   0.03000
#GRAPHICS ON
DEVICE 1
WINDOW    0.    0.    0. 1279. 1023. 4095.
```

T5118-C.INP:CFAST input file for Test T51.18 (11 cribs)

```
VERSN    3T51-18: 9 Room+Dome+Level 1.4 Connect
TIMES   5500    100    50     0     0
DUMPR T5118-C.HIS
STPMAX  1.00000
TAMB  288.000  101300. 0.000000
EAMB  288.000  101300. 0.000000
HI/F   0.250  0.000  0.000  0.000  0.000 11.100 11.100 11.100 11.100 16.150  0.300
WIDTH  2.950  4.950  4.300  4.330  1.800  7.920  4.300  4.330  9.670 14.370  3.000
DEPTH  3.650  1.800  2.750  2.720  6.350  7.920  2.750  2.720  9.670 14.370  3.000
HEIGH  2.750  2.485 11.100 11.100  3.500  4.600  5.050  5.050  5.050 34.950 13.200
CEILI FIRECEIL YTONG100 CONCR050 CONCR050 CONCR050 CONCR050 CONCR050 CONCR050 CONCR050 CONCR050 CONCR050
WALLS YTONG250 YTONG100 CONCR050 CONCR050 CONCR050 CONCR050 CONCR050 CONCR050 CONCR050 CONCR050 CONCR050
FLOOR FIRE_FLR CONCR100 CONCR050 CONCR050 CONCR050 CONCR050 CONCR050 CONCR050 CONCR050 CONCR050 CONCR050
HVENT  1  2  1  1.010  1.975  0.000
CVENT  1  2  1  1.000  1.000  1.000  1.000  1.000  1.000  1.000  1.000  1.000  1.000  1.000
HVENT  2  3  1  1.800  2.485  0.000
CVENT  2  3  1  1.000  1.000  1.000  1.000  1.000  1.000  1.000  1.000  1.000  1.000  1.000
HVENT  3  4  1  4.300  0.500  0.000
CVENT  3  4  1  1.000  1.000  1.000  1.000  1.000  1.000  1.000  1.000  1.000  1.000  1.000
HVENT  3  5  1  2.000  0.500  0.000
CVENT  3  5  1  1.000  1.000  1.000  1.000  1.000  1.000  1.000  1.000  1.000  1.000  1.000
HVENT  4  5  1  2.700  3.100  1.100
CVENT  4  5  1  1.000  1.000  1.000  1.000  1.000  1.000  1.000  1.000  1.000  1.000  1.000
HVENT  5 11  1  1.800  3.500  0.300
CVENT  5 11  1  1.000  1.000  1.000  1.000  1.000  1.000  1.000  1.000  1.000  1.000  1.000
HVENT  6  7  1  3.000  4.250  0.000
CVENT  6  7  1  1.000  1.000  1.000  1.000  1.000  1.000  1.000  1.000  1.000  1.000  1.000
HVENT  6  8  1  3.000  4.250  0.000
CVENT  6  8  1  1.000  1.000  1.000  1.000  1.000  1.000  1.000  1.000  1.000  1.000  1.000
HVENT  6  9  1  3.000  4.250  0.000
CVENT  6  9  1  1.000  1.000  1.000  1.000  1.000  1.000  1.000  1.000  1.000  1.000  1.000
HVENT  7  8  1  3.000  4.250  0.000
CVENT  7  8  1  1.000  1.000  1.000  1.000  1.000  1.000  1.000  1.000  1.000  1.000  1.000
HVENT 11 12  1  0.030  9.800  3.300
CVENT 11 12  1  1.000  0.000  0.000  0.000  0.000  0.000  0.000  0.000  0.000  0.000  0.000
HVENT  6 11  1  3.000  2.400  0.000
CVENT  6 11  1  1.000  1.000  1.000  1.000  1.000  1.000  1.000  1.000  1.000  1.000  1.000
VVENT  7  3  4.54000  2
VVENT  8  4  5.75000  2
VVENT 10  7  4.54000  2
VVENT 10  8  6.97000  2
VVENT 10  9  5.28000  2
CHEMI  13.800  0.000  0.000  2.721E+007  293.000  493.000 0.200
LFBO 1
LFBT 2
CJET OFF
FPOS   1.475  1.825  0.000
FTIME   220.00    700.00   1060.00   1300.00   1600.00   1900.00   2500.00   3700.00   4900.00   5500.00
FHIGH  0.00000   0.00000   0.28100   0.28100   0.28100   0.28100   0.28100   0.28100   0.28100   0.28100   0.00000
FAREA  0.00000   0.00000   1.84300   1.84300   1.84300   1.84300   1.84300   1.84300   1.84300   1.84300   0.00000
FMASS  0.00000   0.00000   0.01389   0.08567   0.06715   0.04862   0.00926   0.00463   0.00232   0.00116   0.00000
FQDOT  0.00000   0.00000   378000.  2331000.  1827000.  1323000.   252000.   126000.   63000.0   31500.0   0.00000
HCR    0.00000   0.00000   0.21050   0.21050   0.21050   0.21050   0.21050   0.21050   0.21050   0.21050   0.00000
OD     0.00000   0.00000   0.03000   0.03000   0.03000   0.03000   0.03000   0.03000   0.03000   0.03000   0.03000
CO     0.00000   0.00000   0.03000   0.03000   0.03000   0.03000   0.03000   0.03000   0.03000   0.03000   0.03000
#GRAPHICS ON
DEVICE 1
WINDOW    0.    0.    0. 1279. 1023. 4095.
```

APPENDIX B: CFAST O_2 CARD

This appendix discusses the difficulties encountered when using the CFAST O2 card. The input file for T51.16 was modified to add the O2 card. These modifications consisted of respecfying the heat of combustion and pyrolysis rate back to their unmodified values. The modified T51.16 input file is shown below:

```
VERSN    3T51-16: 9 Room+Dome+Level 1.4 Connect
TIMES   5500    100     50      0      0
DUMPR T5116-D.HIS
STPMAX  1.00000
TAMB  288.000  101300. 0.000000
EAMB  288.000  101300. 0.000000
HI/F   0.250  0.000  0.000  0.000  0.000 11.100 11.100 11.100 11.100 16.150  0.300
WIDTH  2.950  4.950  4.300  4.330  1.800  7.920  4.300  4.330  9.670 14.370  3.000
DEPTH  3.650  1.800  2.750  2.720  6.350  7.920  2.750  2.720  9.670 14.370  3.000
HEIGH  2.750  2.485 11.100 11.100  3.500  4.600  5.050  5.050  5.050 34.950 13.200
CEILI FIRECEIL YTONG100 CONCR050 CONCR050 CONCR050 CONCR050 CONCR050 CONCR050 CONCR050 CONCR050 CONCR050
WALLS YTONG250 YTONG100 CONCR050 CONCR050 CONCR050 CONCR050 CONCR050 CONCR050 CONCR050 CONCR050 CONCR050
FLOOR FIRE_FLR CONCR100 CONCR050 CONCR050 CONCR050 CONCR050 CONCR050 CONCR050 CONCR050 CONCR050 CONCR050
HVENT  1  2  1  1.010  1.975  0.000
CVENT  1  2  1  1.000  1.000  1.000  1.000  1.000  1.000  1.000  1.000  1.000  1.000  1.000
HVENT  2  3  1  1.800  2.485  0.000
CVENT  2  3  1  1.000  1.000  1.000  1.000  1.000  1.000  1.000  1.000  1.000  1.000  1.000
HVENT  3  4  1  4.300  0.500  0.000
CVENT  3  4  1  1.000  1.000  1.000  1.000  1.000  1.000  1.000  1.000  1.000  1.000  1.000
HVENT  3  5  1  2.000  0.500  0.000
CVENT  3  5  1  1.000  1.000  1.000  1.000  1.000  1.000  1.000  1.000  1.000  1.000  1.000
HVENT  4  5  1  2.700  3.100  1.100
CVENT  4  5  1  1.000  1.000  1.000  1.000  1.000  1.000  1.000  1.000  1.000  1.000  1.000
HVENT  5 11  1  1.800  3.500  0.300
CVENT  5 11  1  1.000  1.000  1.000  1.000  1.000  1.000  1.000  1.000  1.000  1.000  1.000
HVENT  6  7  1  3.000  4.250  0.000
CVENT  6  7  1  1.000  1.000  1.000  1.000  1.000  1.000  1.000  1.000  1.000  1.000  1.000
HVENT  6  8  1  3.000  4.250  0.000
CVENT  6  8  1  1.000  1.000  1.000  1.000  1.000  1.000  1.000  1.000  1.000  1.000  1.000
HVENT  6  9  1  3.000  4.250  0.000
CVENT  6  9  1  1.000  1.000  1.000  1.000  1.000  1.000  1.000  1.000  1.000  1.000  1.000
HVENT  7  8  1  3.000  4.250  0.000
CVENT  7  8  1  1.000  1.000  1.000  1.000  1.000  1.000  1.000  1.000  1.000  1.000  1.000
HVENT 11 12  1  0.030  9.800  3.300
CVENT 11 12  1  1.000  0.000  0.000  0.000  0.000  0.000  0.000  0.000  0.000  0.000  0.000
HVENT  6 11  1  3.000  2.400  0.000
CVENT  6 11  1  1.000  1.000  1.000  1.000  1.000  1.000  1.000  1.000  1.000  1.000  1.000
VVENT  7  3  4.54000  2
VVENT  8  4  5.75000  2
VVENT 10  7  4.54000  2
VVENT 10  8  6.97000  2
VVENT 10  9  5.28000  2
CHEMI  29.800 20.000  0.000  1.262E+007  293.000  493.000 0.200
LFBO 1
LFBT 2
CJET OFF
FPOS   1.475  1.825  0.000
FTIME   100.00    700.00   1000.00   1126.00   1306.00   1480.00   1720.00   2260.00   3100.00   4900.00
FHIGH  0.00000   0.00000   0.28100   0.28100   0.28100   0.28100   0.28100   0.28100   0.28100   0.28100   0.00000
FAREA  0.00000   0.00000   0.70900   0.70900   0.70900   0.70900   0.70900   0.70900   0.70900   0.70900   0.00000
FMASS  0.00000   0.00000   0.02000   0.09200   0.08000   0.03900   0.05300   0.02500   0.00500   0.00250   0.00000
FQDOT  0.00000   0.00000   252000.  1159200.  1008000.   491400.   667800.   315000.   63000.0   31500.0   0.00000
HCR    0.00000   0.00000   0.21050   0.21050   0.21050   0.21050   0.21050   0.21050   0.21050   0.21050   0.00000
O2     0.00000   0.00000   1.40400   1.40400   1.40400   1.40400   1.40400   1.40400   1.40400   1.40400   0.00000
OD     0.00000   0.00000   0.03000   0.03000   0.03000   0.03000   0.03000   0.03000   0.03000   0.03000   0.03000
CO     0.00000   0.00000   0.03000   0.03000   0.03000   0.03000   0.03000   0.03000   0.03000   0.03000   0.03000
#GRAPHICS ON
DEVICE 1
WINDOW    0.    0.    0. 1279. 1023. 4095.
```

The three figures below, Figures B.1 through B.3, show the calculated fire power, upper layer temperatures in the fire room, and the upper layer velocity from the fire room to the hallway.

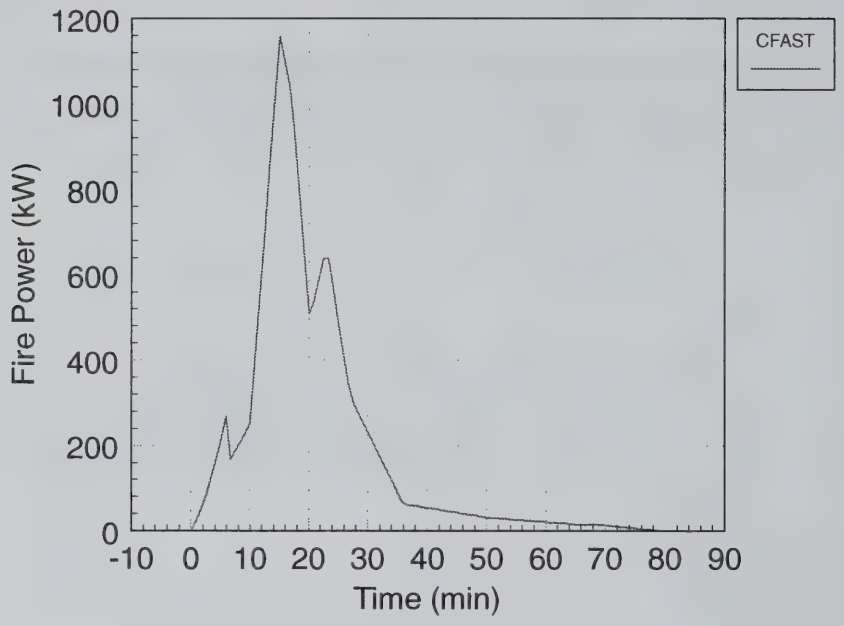

Figure B.1: Fire Power

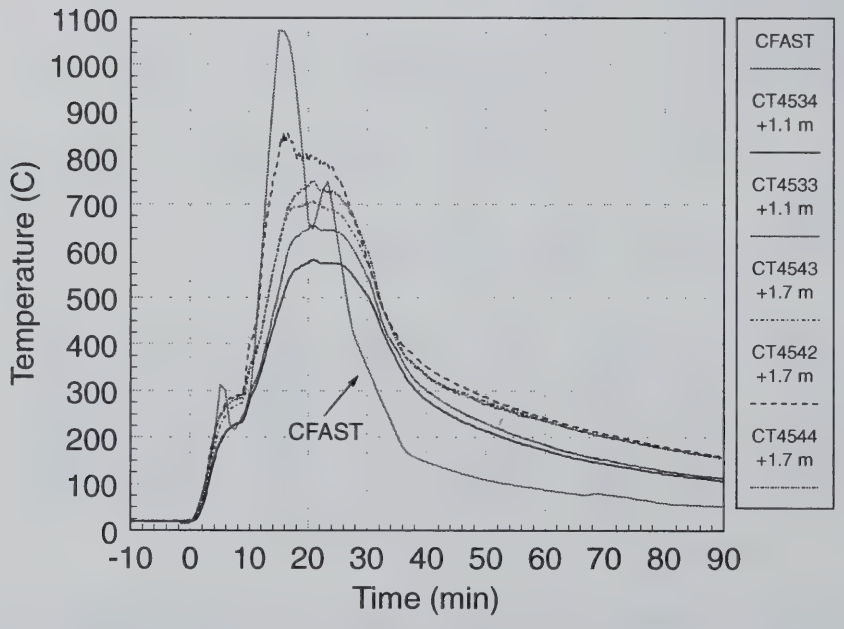

Figure B.2: Fire Room Upper Layer Temperature

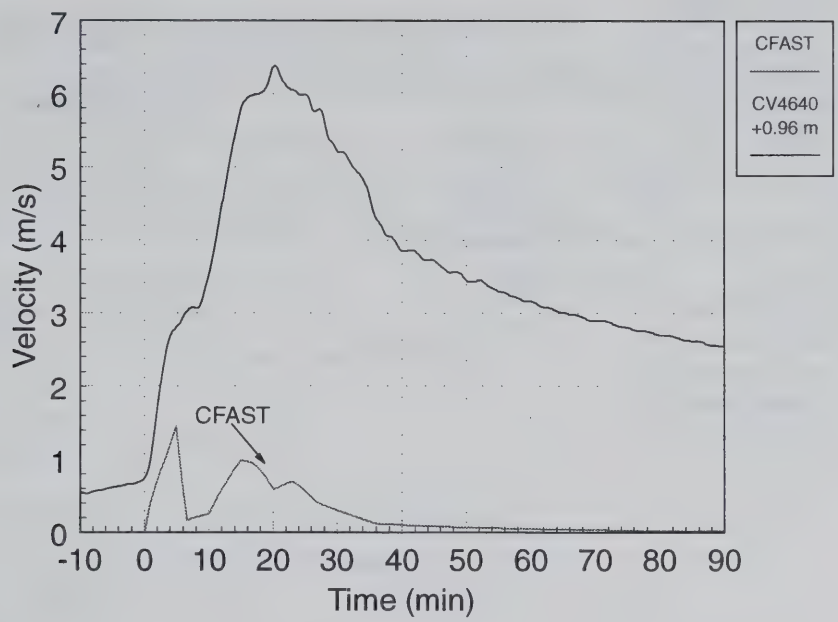

Figure B.3: Fire Room Upper Layer Velocity

Figure B.1 and B.3 show that with the O2 card activated the fire generates the same power and mass flow rate as with the O2 card deactivated. Since fire power and exit mass flow from the fire room determines the heat input into the fire room, if they are equivalent between the two cases, one would expect the fire room temperatures to also be equivalent. Figure B.2 shows that this is not the case. With the O2 card turned on, the upper layer temperature in the fire room is over 200 °C higher than with the O2 card turned off.

The next two figures, Figures B.4 and B.5, show the upper layer O_2 and CO_2 concentrations in the fire room. Since the empirical formula of wood is $C_{0.95}H_{2.4}O$, each mole of wood empirical formula requires an additional 0.55 moles of O_2 for complete combustion. Therefore, one would expect a decrease in the fire room O_2 concentration to be calculated by CFAST. CFAST, however, calculates a slight increase in the O_2 concentration. Further more, since the same amount of carbon is being combusted, one would expect to see similar CO_2 concentrations between the O2 card and the no O2 card predictions. With the O2 card activated, CFAST calculates almost no CO_2 production.

It is clear from these few comparisons that with the O2 card enabled difficulties arise due to its implementation and its use should be avoided if CFAST is to calculate reasonable results. Based one these observations it was decided to remove the oxygen from the wood when specifying the fuel in CFAST.

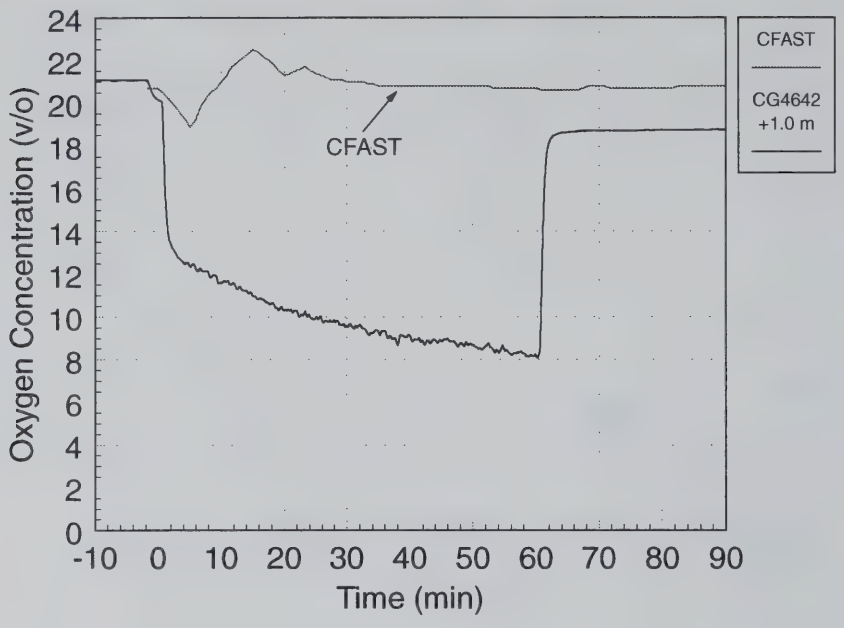

Figure B.4: Fire Room Upper Layer O_2 Concentration

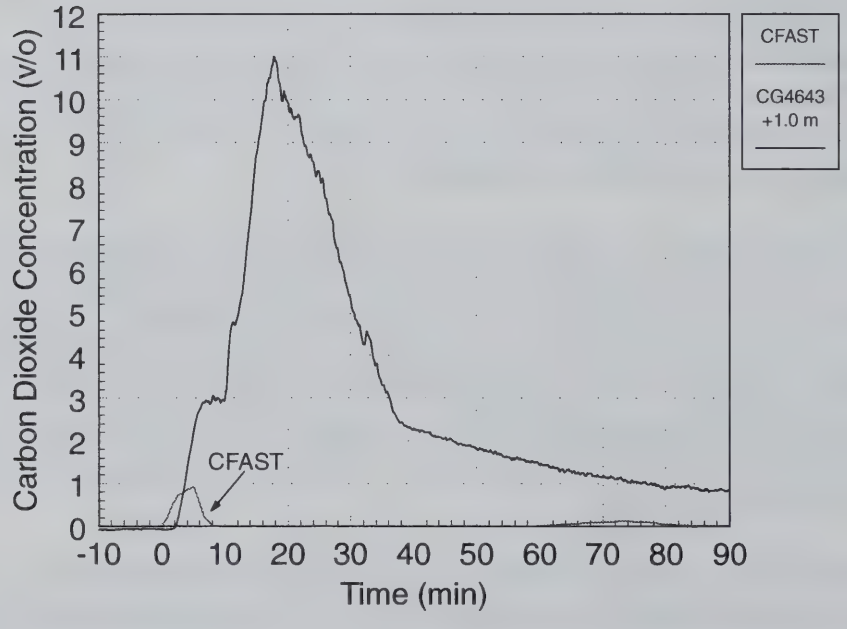

Figure B.5: Fire Room Upper Layer CO_2 Concentration

NIST-114
(REV. 11-94)
ADMAN 4.09

U.S. DEPARTMENT OF COMMERCE
NATIONAL INSTITUTE OF STANDARDS AND TECHNOLOGY

MANUSCRIPT REVIEW AND APPROVAL

(ERB USE ONLY)
ERB CONTROL NUMBER | DIVISION
PUBLICATION REPORT NUMBER | CATEGORY CODE
NIST GCR 99-778

INSTRUCTIONS: ATTACH ORIGINAL OF THIS FORM TO ONE (1) COPY OF MANUSCRIPT AND SEND TO THE SECRETARY, APPROPRIATE EDITORIAL REVIEW BOARD.

PUBLICATION DATE: September 1999
NUMBER PRINTED PAGES:

TITLE AND SUBTITLE (CITE IN FULL)
Evaluation of the HDR Fire Test Data and Accompanying Computational Activities with Conclusions from Present Code Capabilities. Volume 3: Test Series Description and CFAST Validation for HDR T51 Wood Crib Fire Test Series

CONTRACT OR GRANT NUMBER: Contract 60NANB6D0127
TYPE OF REPORT AND/OR PERIOD COVERED: July 1998

AUTHOR(S) (LAST NAME, FIRST INITIAL, SECOND INITIAL)
Floyd, J. and Wolf, L.
Department of Materials and Nuclear Engineering
University of Maryland
College Park, MD 20742

PERFORMING ORGANIZATION (CHECK (X) ONE BLOCK)
- [ ] NIST/GAITHERSBURG
- [ ] NIST/BOULDER
- [ ] JILA/BOULDER

LABORATORY AND DIVISION NAMES (FIRST NIST AUTHOR ONLY)

SPONSORING ORGANIZATION NAME AND COMPLETE ADDRESS (STREET, CITY, STATE, ZIP)
U.S. Department of Commerce
National Institute of Standards and Technology
Gaithersburg, MD 20899

PROPOSED FOR NIST PUBLICATION
- [ ] JOURNAL OF RESEARCH (NIST JRES)
- [ ] J. PHYS. & CHEM. REF. DATA (JPCRD)
- [ ] HANDBOOK (NIST HB)
- [ ] SPECIAL PUBLICATION (NIST SP)
- [ ] TECHNICAL NOTE (NIST TN)
- [ ] MONOGRAPH (NIST MN)
- [ ] NATL. STD. REF. DATA SERIES (NIST NSRDS)
- [ ] FEDERAL INF. PROCESS. STDS. (NIST FIPS)
- [ ] LIST OF PUBLICATIONS (NIST LP)
- [ ] NIST INTERAGENCY/INTERNAL REPORT (NISTIR)
- [ ] LETTER CIRCULAR
- [ ] BUILDING SCIENCE SERIES
- [ ] PRODUCT STANDARDS
- [ ] OTHER NIST GCR

PROPOSED FOR NON-NIST PUBLICATION (CITE FULLY) [ ] U.S. [ ] FOREIGN

PUBLISHING MEDIUM
- [X] PAPER
- [ ] CD-ROM
- [ ] DISKETTE (SPECIFY)
- [ ] OTHER (SPECIFY)

SUPPLEMENTARY NOTES

ABSTRACT (A 2000-CHARACTER OR LESS FACTUAL SUMMARY OF MOST SIGNIFICANT INFORMATION. IF DOCUMENT INCLUDES A SIGNIFICANT BIBLIOGRAPHY OR LITERATURE SURVEY, CITE IT HERE. SPELL OUT ACRONYMS ON FIRST REFERENCE.) (CONTINUE ON SEPARATE PAGE, IF NECESSARY.)

Between 1984 and 1992 four major test series were performed in the HDR containment encompassing various fuels and three different axial positions in the high-rise, multi-level, multi-compartment facility. At that time, each HDR fire test series was accompanied by extensive efforts to evaluate the predictive capabilities of a variety of fire models and codes developed in different countries by both blind pre-test and open post-test mputations. A quite large number of open issues remained in the area of fire computer code predictive qualities upon completion of the HDR program. Volume 1: Test Series Description Report for T51 Gas Fire Test Series, NIST GCR 97-727. Volume 2: CFAST Validation for T51 Gas Fire Test Series, NIST GCR 97-731.

KEY WORDS (MAXIMUM OF 9; 28 CHARACTERS AND SPACES EACH; SEPARATE WITH SEMICOLONS; ALPHABETIC ORDER; CAPITALIZE ONLY PROPER NAMES)
combustion products; compartment fires; doors; fire models; large scale fire tests; temperature; validation; vents

AVAILABILITY
- [X] UNLIMITED
- [ ] FOR OFFICIAL DISTRIBUTION - DO NOT RELEASE TO NTIS
- [ ] ORDER FROM SUPERINTENDENT OF DOCUMENTS, U.S. GPO, WASHINGTON, DC 20402
- [X] ORDER FROM NTIS, SPRINGFIELD, VA 22161

NOTE TO AUTHOR(S): IF YOU DO NOT WISH THIS MANUSCRIPT ANNOUNCED BEFORE PUBLICATION, PLEASE CHECK HERE. [ ]